MAGYAR ÁLLAMI
EÖTVÖS LORÁND
GEOFIZIKAI INTÉZET

GEOFIZIKAI
KÖZLEMÉNYEK

ВЕНГЕРСКИЙ
ГЕОФИЗИЧЕСКИЙ
ИНСТИТУТ
ИМ Л. ЭТВЕША

ГЕОФИЗИЧЕСКИЙ
БЮЛЛЕТЕНЬ

BUDAPEST

GEOPHYSICAL

TRANSACTIONS

EÖTVÖS LÓRÁND GEOPHISYCAL INSTITUTE OF HUNGARY

CONTENTS

VOL. 37. NO. 1. FEBR. 1992. (ISSN 0016-7177)

TARTALOMJEGYZÉK

СОДЕРЖАНИЕ

Licensed to cruise at super seismic speeds

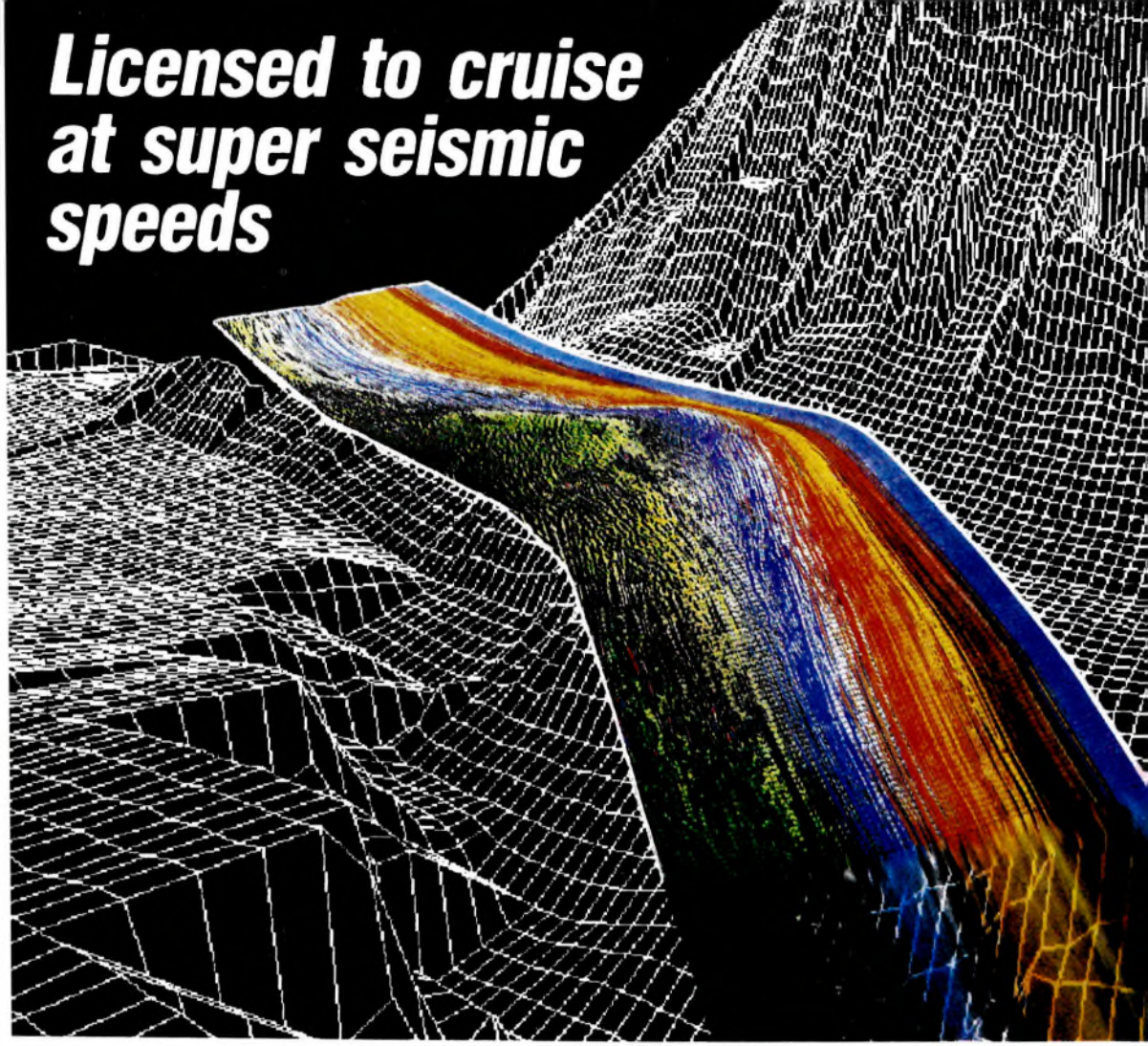

If your seismic data processing gets stuck in first gear when entering complex geological zones, consider licensing seismic processing software from Western Geophysical.

Western software is being used to process data from geologic provinces throughout the world. In fact, more miles of seismic data are processed with Western software, at the highest efficiency level, than any other software.

Western seismic processing software operates on vector supercomputers as well as scalar mainframes and departmental minicomputers. Every user has access to Western's comprehensive program library designed for effective and efficient processing of 2-D and 3-D surveys on land, at sea, and across shallow-water transition zones.

The latest software enhancements, released on a continuous basis by Western's R&D and Computer Science departments, are available through the Software Subscription Service. If you run into a problem, our Rapid Response teams are on alert to clear any processing flightpaths.

Whether you need a basic processing package or full facility management, call Western Geophysical and shift your seismic center into high gear.

Western Atlas International
A Litton/Dresser Company

WESTERN GEOPHYSICAL

Wesgeco House
PO Box 18
455 London Road
Isleworth, Middlesex
England TW7 5AB
(081) 560-3160
Fax (081) 847-3131

Houston	(713) 789-9600
Denver	(303) 770-8660
Calgary	(403) 291-8100
Singapore	65-258-3455
Caracas	58-2-262-0272
Bogota	57-1-267-6199
Rio de Janeiro	55-21-541-1599

EÖTVÖS L. GEOPHYSICAL INSTITUTE OF HUNGARY

THE OLDEST INSTITUTION FOR APPLIED GEOPHYSICS OFFERS THE LATEST ACHIEVEMENTS FOR GROUND-WATER PROSPECTING and ENVIRONMENTAL PROTECTION

The most often occurring demands:

- local geophysical measurements for the water supply of small communities by a few wells
- regional geophysical mapping to determine hydrological conditions for irrigation, regional agricultural development,
- large-scale exploration for the water supply of towns, extended areas i.e. regional waterworks,
- determination of bank storage of river terraces, planning of bank filtered well systems,
- thermal water exploration for use as an energy source, agricultural use or community utilization,
- cold and warm karst water prospecting,
- water engineering problems, water construction works

The Maxi-Probe electromagnetic sounding and mapping system – produced under licence by Geoprobe Ltd. Canada – is an ideal tool for shallow depths, especially in areas where seismic results are poor or unobtainable

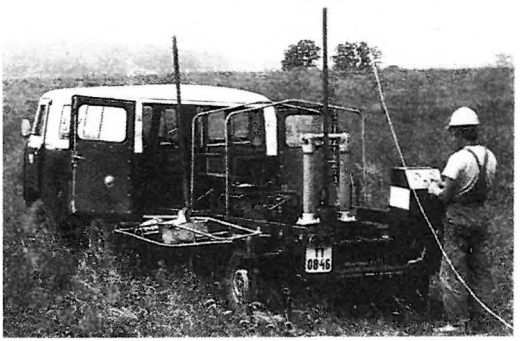

ELGI has a vast experience in solving problems of environmental protection such as control of surface waters, reservoir construction, industrial and communal waste disposal, protection of surface and ground water etc. ELGI's penetrologger provides in-situ information – up to a maximum depth of 30 m – on the strength, sand/shale ratio and density without costly drilling.

Field work with ELGI's 24-channel portable seismograph

ELGI offers contracts with co-operating partners to participate in the whole complex process of exploration–drilling–production.

For further information ask for our booklets on instruments and applications. Let us know your problem and we will select the appropriate method and the best instrument for your purpose.

Our address: ELGI POB 35. Budapest, H–1440. HUNGARY
Telex: 22-6194 elgi h

Editor's note

The most observant readers probably recognized, even in the previous number, that there was a change in the person of the editor. Commencing with this volume we have also changed the front cover of our journal. Both alterations mean that our journal is undergoing renovation. This process started with the publication of advertisements: the main purpose of this being our wish to improve the financial circumstances of Geophysical Transactions. The technical background has changed as well, we have out-grown our computer-based DTP system. It is to be hoped that the introduction of more up-to-date techniques will accelerate the publishing process and will result in a decrease of misprints.

All the above-mentioned changes are connected mainly with external factors, the present editorial staff would like to pay tribute to the sterling work of Mrs. Éva Kilényi, the previous editor. It was through her efforts that this journal was raised to international level. We should very much like to maintain this level and to support it with the appropriate external effects. In this way, there is every chance that our journal will be an up-to-date scientific journal from outside as well as from inside.

Dear present and future authors, we consider it a great honour that you have chosen our journal as the vehicle for publishing your last best paper. There is no need for us to emphasize that we need only a short time for getting it through the press. If you meet all the — not extensive — requirements connected with the submission of papers, it is almost certain that you will see your paper in print within a year. Attention is drawn to the fact that it would be helpful and most appreciated if you would also send us your paper on floppy diskette written in textfile using any of the standard word-processing programs (e.g. WORD5, WordStar, etc.).

Within this note the editorial staff would like to express their appreciation to the numerous referees for assisting the authors with their good advice and for helping the editors in their decision-making. Many of our referees have been working in association with us long periods of time, we should like to thank them for what is often a thankless task and for their goodwill.

Finally, may I wish you every success in finding good ideas for writing papers for Geophysical Transactions and may you prosper and gain greater success through the published articles. For ourselves, my wish is that you keep us in mind when you are about to submit a new paper, and that we may have the opportunity of continuing this work into the distant future. And we wish you a

HAPPY 1992!

Zsuzsanna Hegybíró

and the editorial staff of
Geophysical Transactions

'Beneath our feet stretches the open country of the Hungarian Plain, crowned with hills. Over the years this region has shaped itself naturally, as it wished. I wonder what it was like in former days. What sort of hills have been eroded and what valleys filled with loose deposits before this fertile area of golden grain came into being, this life-giving Hungarian plain? As I walk upon it and eat its bread my mind dwells upon these question which would give me such joy to anser.'

(Eötvös)

Eötvös Loránd 1848 - 1919

ONE HUNDRED YEARS OLD: THE EÖTVÖS TORSION BALANCE

Zoltán SZABÓ

In 1991 we are celebrating the 100th anniversary of the completion of Eötvös' first torsion balance and the first field observations carried out on Ság hill, Transdanubia, Hungary.

The invention of the torsion balance represented an important milestone in the history of applied geophysics: it was the first instrument to be employed in oil exploration. This centenary provides an opportunity to commemorate Loránd Eötvös the man, and Loránd Eötvös the scientist and organizer.

1. Eötvös the Man

Loránd Eötvös was born in Buda in the capital of Hungary on 27th July 1848, the year of the Hungarian revolution and fight for independence. His father, József Eötvös, came from an impoverished noble family. As a writer and politician of great renown, he was one of the leaders of the movement for reform. Because of his eminence in the political field, he was elected minister of religion and education in the first independent government of Hungary after the revolution. As a reformer, Eötvös was appalled by the violent path taken during the struggle for independence, so left the country with his family, returning to Hungary only in 1850. During his period abroad he interested himself primarily in matters of state and philosophy. On returning home he strove to establish peace between Hungary and the ruling Habsburg dynasty, a policy which did not at first gain undivided support. During the fifteen years that followed, those in favour of agreement managed to achieve a compromise. As a result, in the Hungarian government established in 1867, József Eötvös was again appointed minister of religion and education.

In recognition of his literary work, József Eötvös became an associate member of the Academy in 1835, an honorary member in 1839 and in 1866 he was elected president.

From an early age his son, Loránd, was educated by private tutors and he later attended the Piarists' high school, from where he matriculated in 1865. In those days it was assumed that sons of aristocratic families who wished to receive higher education had to enter some branch of the law. The law failed to satisfy Eötvös, but he always managed to find time to attend lectures in the natural sciences.

In March 1866 he wrote the following words to his father: *'I was born with ambition and a sense of duty not only to one nation but towards the whole of humanity. In order to satisfy these urges and to retain my own individual independence, my aim in life will best be achieved, as far as I can see at present, by following a career in science.'* Despite the fact that he had completed his law studies, his dearest wish was *'to study at a university abroad under the guidance of enlightened professors'* in order to fully understand the natural forces at work in the scientific field.

In 1867, with his father's consent, he took the final decision to follow a career in the natural sciences, and to this end he enrolled at Heidelberg

University. There he became a student of Kirchhoff, Bunsen and Helmholtz. First of all he studied physics, maths and chemistry. The following six months he spent at the University of Koenigsberg, but found the lectures too abstract and returned to Heidelberg.

During his university years he kept up a regular correspondance with his father. These letters reveal the depth of understanding and sincerity in the relationship between father and son. Thirsty for adventure, in 1869 the young Eötvös planned to join Petermann the German geographer on his expedition to Spitzbergen. His father disagreed with his son's plans and wrote the following: *'On this occasion, however, I do see the need to warn you of my situation, which demands that economies be made by the whole family, including yourself. For years I've almost always been in a situation in which my expenses exceed my income ... I willingly give whatever is necessary to further your scientific studies ..., but I must ask you to forgo certain luxuries for the sake of us all — and your planned expedition is one of them. I'm not referring to the Transylvanian expedition but the one to the Arctic.'*

At his father's request Loránd Eötvös gave up his plan to travel with Petermann and applied all his energy to preparing for his examinations. In his letter of 8th July, 1870 he says: *'... I've had the results of my doctorate today. And my greatest delight is that this news will bring you pleasure. I passed my finals with first class honours, a distinction envied by many.'*

Shortly after his return home in February 1871, his father died — *'the best and truest friend'*. On his death bed he warned his son that his future happiness depended on his devoting himself to science and keeping out of politics. After his father's death, Eötvös successfully applied for the post of lecturer advertised by the faculty of theoretical physics at Pest University; this university now bears his name. It was characteristic of the social climate of the time that the majority of the students attending his inaugural lecture did so because they were curious to see a real baron giving a lecture on physics at the university.

After a short period of lecturing in 1872 he was publicly honoured by the king, who awarded him the chair of theoretical physics. In 1874 he was asked to give lectures in experimental physics; four years later he became professor in this field. He was then given the task of combining the departments of experimental and theoretical physics, and was appointed director to the newly established Institute of Physics.

In 1873 he became an associate member of the Academy, a full member in 1883, and in 1889 he was elected president. Among his offices he became minister of religion and education for seven months in 1894.

Eötvös was a modest scientist who shunned the limelight. He disliked uproarious ceremonies and did not seek moral or financial reward. In spite of this he was acclaimed and received awards at home and abroad for his scientific work and for his skill as an organizer. The more important honours included the French Legion of Honour, the Franz Joseph award from the Hungarian king, the Saint Sava award from the King of Serbia. He was also elected honorary member of the Prussian Royal Academy of Sciences in Berlin and was given honorary doctorates from Jagello University in Cracow and the Norwegian Royal Frederick University in Oslo (known as Christiania at the time). In addition to the above he received several other awards during his life and was elected president or a leading member of various social and scientific societies.

Eötvös was a well balanced individual. Besides his intensive mental work he always found time for relaxation and sport. He often went riding and regularly made the eleven kilometre journey from his home to the university on horse back. In the summer he often cycled and indulged in his passion for mountaineering . In the classic time of alpinism he ranked among the best. As an enthusiastic photographer, he took hundreds of pictures during his mountaineering expeditions. In his later years his doughters accompanied him on his expeditions, and also became keen alpinists. Eötvös' climbing achievements in the southern Tirol made the Hungarian professor's name so well-known that in 1902 one peak of 2837 m in the Dolomites (Italy) was named after him — el Cima di Eötvös — the Eötvös Peak. In the company of friends he often jokingly said that he was prouder of his mountaineering successes than his discovery of the torsion balance. For many years as president of the Hungarian Touring Society, he did a great deal to popularize tourism in Hungary.

With advancing years, he strove to avoid prestigious appointments in order to devote himself entirely to research. This prompted him to give up his position as president of the Academy in 1905. The last years of his life were clouded by severe illness, but he continued to lecture at the university so long as it was humanly possible.

Up to the last moments of his life he followed torsion balance field work with great interest. Initially he asked his colleagues to inform him of

the daily results of their survey by telegram because he was very anxious to know how far the results of the survey supported his theories. He had never been able to tear himself away from his research, even during his summer trips to the mountains. When on holiday he always kept up a regular correspondence with his co-workers. He continued his scientific work from his sick-bed and sent his last paper to be published only a few days before he died on 8th April 1919.

The international scientific community and the whole of Hungarian society mourned his death. Hungary had said farewell to one of the last great representatives of classical physics and to the country's greatest natural scientist. Through his work, however, his name will live forever in the history of physics and geophysics.

2. Eötvös the Scientist

In his scientific research Loránd Eötvös was not interested in those topics that were fashionable at that time, and that would have brought him immediate public acclaim. Instead, he was concerned with capillarity, gravitation and magnetism, phenomena so taken for granted that a superficial observer would fail to see the mysterious powers at work within them.

He was still a university student when he began to concern himself with capillarity under the guidance of F. Neumann. This force governs the shape of the surface of water in a glass; due to its effect drops of water are rounded and water is caused to rise in capillary tubes. Eötvös worked out a new way of determining surface tension called the reflection method. This method made it possible to determine the exact surface tension of different liquids. During his experiments Eötvös found that there was a relationship between the surface tensions of liquids and their molar weight.

Based on this perception the rule, later to become known as the Eötvös rule, could be concluded which states that the rate of change of molar surface energy with temperature is a constant for all liquids. For liquids this constant is as fundamental as is the universal gas constant for gases.

After studying capillarity Eötvös turned his attention to gravitation and magnetism. From then onwards for the nearly forty years until his death, he was concerned with these two fields. In his research on the spatial changes in gravitation, he used a modified version of Coulomb's balance.

His research method was based on two fundamentals: one was the strict theoretical physical aspect of the process; the other was the construction of an unbelievably sensitive instrument.

Eötvös built two different types of torsion balance for carrying out his gravitational investigations. The first type was a light horizontal beam suspended on a torsion wire with platinum masses attached to each end so that the masses were at the same level (curvature variometer). This type was identical in form with the instrument used by Cavendish. The curvature variometer measures the 'curvature' values which give the deviation of equipotential surfaces of gravity from spherical shape, and give the directions of minimum curvature.

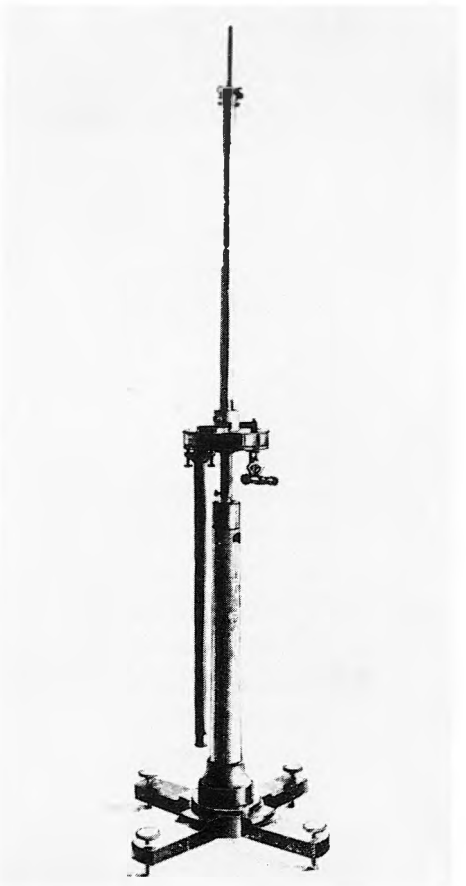

The first Eötvös torsion balance

The second type has a platinum mass attached to one end of a horizontal beam, while on the other end a platinum cylinder hangs on a wire so that this cylindrical mass is at a lower level than the mass at the other end (horizontal variometer). In both cases the beam turns around the torsion wire in a horizontal plane and is deflected from the torsion-free position of the wire by the horizontal components of the forces of gravity. This seemingly insignificant modification was Eötvös' most important invention, in fact this second version is known as the Eötvös Torsion Balance.

The horizontal variometer gives the 'gradient' of gravity which is defined as the rate of change of gravity over a horizontal distance of 1 centimetre. The horizontal variometer also furnishes the curvature values if the instrument is set up in at least five azimuths. The unit of gradient and curvature are named after Eötvös. 1 EU = 10^{-6} mGal/cm; that is, if the horizontal gradient is 1 EU the gravity acceleration at two neighbouring points 1 cm apart difference 10^{-12}g.

Of his instrument Eötvös himself said the following: *'It is as simple as Hamlet's flute, if you know how to play it. Just as the musician can coax entrancing melodies from his instrument, so the physicist, with equal delight, can measure the finest variation in gravity. In this way we can investigate the Earth's crust at depths that the eye cannot penetrate and the drilling rig cannot reach.'*

The mechanical parts of the instruments were designed and built in 1890 under the guidance of Eötvös in cooperation with N. Suess in Suess' Mechanical Workshop. Calibration of the instruments were carried out in Eötvös' Laboratory and the first instrument was completed in 1891. In the same year the first observations were carried out.

A modified version of the horizontal variometer specially designed for field work, was completed in 1898. It was shown and awarded a prize at the Expo of Paris in 1900.

In order to increase the efficiency of field work, Eötvös constructed a double instrument with two balances in antiparallel arrangement (1902).

At the beginning Eötvös experimented with his instruments in the laboratory of the university, then later in the garden of his summer house. He carried out his first field measurements on Ság hill in Transdanubia in 1891, where he proved that errors had been made in the relative pendulum measurements carried out by Sterneck; Sterneck was an Austrian geodetic surveyor who had carried out measurements in the same area seven years

earlier. Eötvös' first report on gravitation was written in 1888 for the Academy. In 1896 he published his fundamental paper entitled Studies in the Field of Gravitation and Magnetism, in which he gave a theoretical and practical summary of his experiments to date.

The first experiments on a larger area using the Eötvös balance took place in the winter of 1901 on the frozen surface of Lake Balaton. Eötvös chose the mirror-like frozen surface of the lake to carry out his measurements so that he would not have to concern himself with the disturbing effect of topographic masses. He continued his survey work in the winter of 1903, completing measurements at altogether forty different stations. From the results of his torsion balance survey it was established that parallel to the axis of the lake ran a tectonic line. This was the first geological conclusion based on torsion balance measurements.

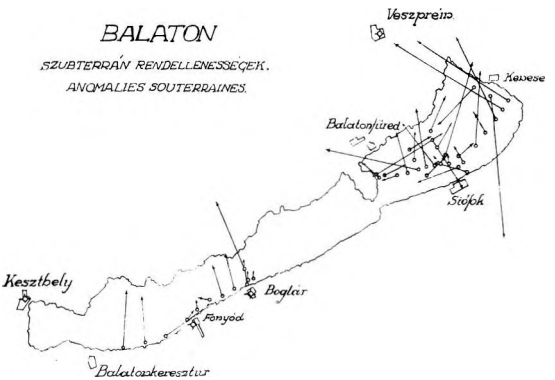

The first gradient map, obtained on the frozen lake Balaton (1901-03)

As a results of his success when he presented his results in Paris in 1900, Eötvös' gravitational experiments became the focus of international attention. The high degree of sensitivity of his instrument was doubted by some. And it was not until the XV Congress of the Internationale Erdmessung held in Budapest in 1906 at which he spoke about his latest experiments that Eötvös' claims received general recognition. He also made it possible for interested foreign scientists to observe his torsion balance measurements carried out in the field — in the Arad region. The participants of the conference found Eötvös' research so significant that they petitioned the Hungarian government requesting that increased financial help be given

for gravitational research. The Hungarian government agreed to the suggestion and from 1907 onwards a separate fund was allocated for Eötvös' gravitational studies. From this time onwards geophysical research was recognized in Hungary as a separate field of science in its own right.

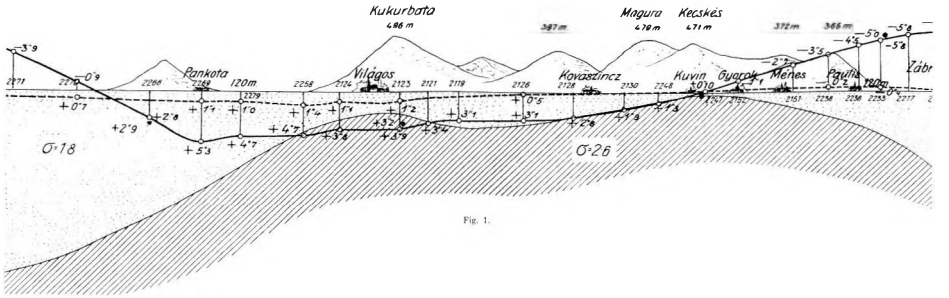

Fig. 1.

Lotabweichungen nach Osten längs des Breitenkreises von Menes (z = 46°8').

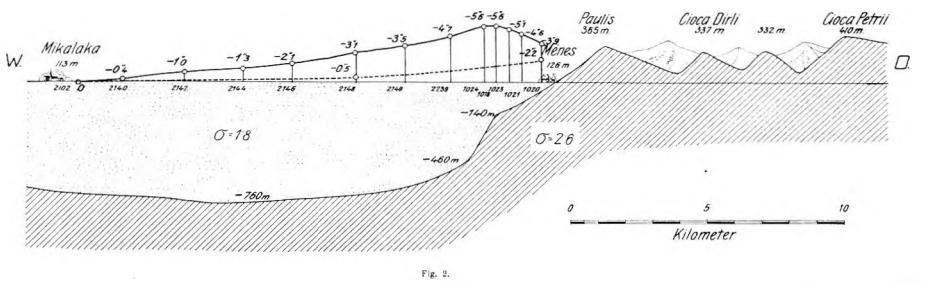

Fig. 2.

Geological interpretation of the torsion balance survey carried out in the region of Arad (1906)

At first Eötvös' gravitational measurements were carried out for geodetical purposes, but from the very beginning Eötvös had wondered what geological conclusions could be deduced from the results of his work. At the XVII Congress of the Internationale Erdmessung held in Hamburg in 1912 Eötvös wrote the following in his report of the practical application of the torsion balance: *'Geologists seem to agree that the most substantial discharges of gas occur in the immediate vicinity of gas-bearing anticlines, and overlying sediments. Experience gained in America (Ohio) and observations in Transsylvania, where the subsurface geological structures could be determined from superficial indications, further endorse these assumptions. Such geological indications, however, are absent in the sand and humus covered surface of the Great Hungarian Plain. He who searches for*

gas-bearing anticlines in this or similar areas should not fail to take note of conclusions drawn from torsion balance observations.'

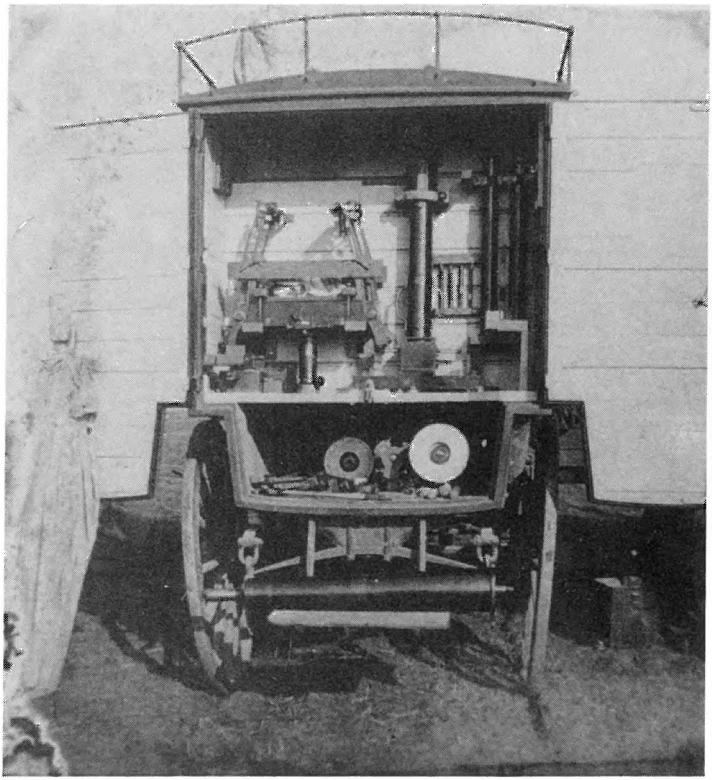

The Eötvös torsion balance packed in a horse cart used for transportation in the filed (1907)

In 1916, on the initiative of Hugo Böckh, an eminent Hungarian geologist, torsion balance measurements were carried out in the region of Egbell, where oil was produced from a recognized anticlinal structure. The aim of these measurements was to establish the extent to which the effect of the oil-bearing anticline is reflected in the results of torsion balance measurements. On the basis of the survey carried out at 92 stations the contours of the anticlinal oil field were clearly ascertained. These results proved the efficacy of the torsion balance in oil exploration and paved the way towards world renown for Eötvös and his balance. After his death, in the 1920s and 1930s, hundreds of oil fields were discovered throughout the world with the help of Eötvös' ingenious instrument.

Siesta in the camp, Eötvös is sitting before the tent

Among Eötvös' gravitational instruments, his gravity compensator is also worthy of mention. This instrument is strictly speaking a curvature variometer provided at both ends with sector-shaped deflectors, whose position can be changed by rotation about a horizontal axis. If the deflectors are in a vertical position their attraction to the balance is zero, in a horizontal position their effect is maximum. If the beam of the balance is in the centre of its case, the attraction of the deflectors is zero because of the symmetrical disposition but if the beam is not in the central position because of deflection by some outside mass, the deflectors become effective since they are now not symmetrically positioned with respect to the beam (astatization). If the position of the deflectors is changed with respect to the horizontal direction, the sensitivity of the gravity compensator can be further increased up to the point of instability.

Although best known for his torsion balance, Eötvös also developed a gravimeter. It was completed in 1901, and was based on the bifilar principle. The experimental measurements carried out with this instrument, however, failed to meet his expectations, so he did not publicize his activities in this field. His gravimeter still exists today, an indication of the extent of his love for experimentation.

In 1890 Eötvös worked out a method, the dynamic method, for measuring the gravitational constant. The dynamic method was based on the concept that the period of oscillation of a pendulum placed between two parallel lead walls was depending on whether it oscillated parallel or perpendicular to the walls. If one measures the periods of oscillation in both positions and determines the exact mass of the attracting walls the gravitational constant can be calculated.

In physics, mass can be defined in two ways, viz. inertial and gravitational. The inertial mass of a body determines the acceleration given by an applied force (Newton's second law); the gravitational mass of the body determines the force it experiences due to the gravitational attraction of another body. Eötvös became concerned with the question of the ratio of proportionality of the inertial and gravitational mass as early as 1880. In order to examine this phenomenon, he used his sensitive torsion balance. He examined the state of equilibrium of the balance by attaching masses of different composition to each end of the arm of the balance. If the quantity of gravitational force depended on the composition of the mass, when placing bodies of different composition on to the balance, the state of equilibrium should change in each case. This phenomenon did not occur. In 1908 Eötvös and his colleagues, Jenő Fekete and Dezső Pekár, perfected their measurements to such an extent that they were able to establish that the difference between the inertial and gravitational mass was at most 1/20,000,000. Their paper on the subject won them the Benecke award at Göttingen University. The experiments carried out by Eötvös and his colleagues on the proportionality of the inertial and gravitational mass supports Einstein's theory of relativity. The reexamination of the results published in their paper recently led E. Fischbach to the debated hypothesis of the existence of a 'fifth force'.

Eötvös was also interested in the question of gravitational absorption. His method was the following: the beam of a horizontal variometer is placed perpendicularly to the direction of the rising or setting sun. Let us suppose

that two straight lines are drawn from a fixed point on the sun, one directed to the upper weight on the balancing rod, and one to the lower. If the sun is just below the horizon, the parts of the two straight lines passing through the earth will differ in length. For example, if the straight line drawn to the upper weight just touches the earth, then the line directed to the weight which is one metre below will pass through the earth for seven kilometres. If this layer of the earth could change the attraction of the sun, deflection would be indicated by the variometer. The instrument did not show any definite deflection at sunrise or sunset. The degree of sensitivity of this instrument was such that Eötvös could state that if the upper layer of the earth changes the sun's attraction the effect was less than 1:100,000,000.

In the last years of his life, Eötvös carried out experiments which showed that the weight of moving bodies on the earth's surface changed depending on the direction and speed at which they were proceeding. A clear explanation of this change can be given on the basis of the mechanics of Galileo and Newton. The gravitational force of the earth is the resultant of two forces: the principal one caused by attraction according to Newton's law, the second one the centrifugal force caused by the earth's rotation. Since the distribution of the masses in the earth and the speed at which the earth rotates are constant, the weight of objects on the earth's surface is also constant. The situation is different, however, in the case of moving objects. As the earth rotates from west to east, the centrifugal force on a moving object is greater if its motion on earth is towards the east than towards the west. As a result of this phenomenon the weight of a body moving eastwards will decrease, while that moving westwards will increase.

It is interesting to note the circumstances that initiated Eötvös' research on this topic. O. Hecker, an eminent research worker at the Institute of Geodesy in Potsdam, led a team to the Atlantic Ocean in 1901 and then in 1904-1905 to the Indian and Pacific Oceans, to carry out gravity measurements on moving boats. While studying Hecker's results in the published report, Eötvös noticed that no consideration had been given to the forces developed by the motion of the boat. In a letter to Hecker, Eötvös pointed out his error, but Hecker at first refused to give credence to this criticism. His colleagues, however, persuaded him that Eötvös was right and so in 1908 new measurements were carried out in the Black Sea to prove this phenomenon. Observations were made in two boats, one moving towards the east and one towards the west. The results substantiated Eötvös' claim.

The international scientific world recognizes this phenomenon as the Eötvös Effect. The Eötvös Effect has special importance nowadays in the field of sea- and air-borne gravimetry.

In 1915 Eötvös constructed a special instrument to demonstrate this phenomenon. The device is basically a balance with a horizontal axis, with weights attached to the ends of the arm. The balance stands on a tripod, which rotates evenly. When the balance is rotated the weight moving towards the west will become heavier, the one moving towards the east lighter. The balance will, therefore, deflect from its state of equilibrium. If rotation period equals the period of oscillation resonance gradually increases its amplitude.

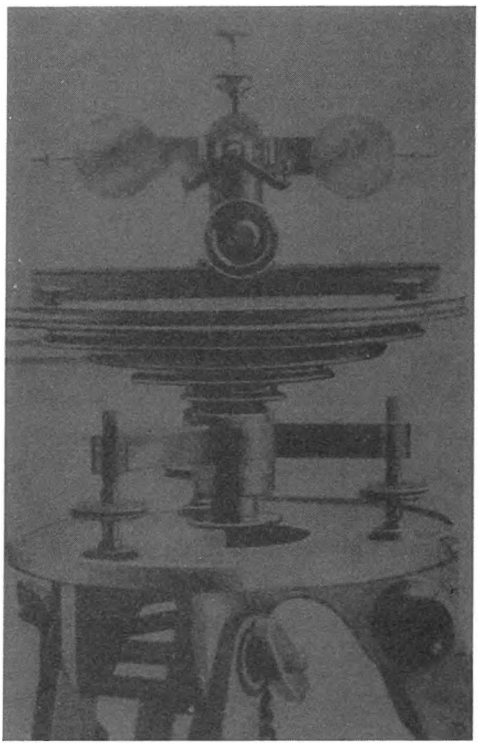

Instrument to demonstrate the Eötvös effect (1915)

This experiment is yet further proof of the earth's rotation, and has even greater significance than Foucault's famous pendulum experiment carried out in the Pantheon in Paris.

Parallel with their field work utilizing the torsion balance, Eötvös and his colleagues determined the horizontal component and the declination and inclination of the earth's magnetic field at every observation point. The extensive observational data available enabled them to give an integrated geological interpretation of the measurements.

In order to study the characteristics of the earth's magnetic field, Eötvös designed an instrument on the analogy of his torsion balance, called a magnetic translatometer. It differed from the torsion balance in that the lower weight was replaced by a magnetic needle. The needle could be rotated around its horizontal axis and could thus be positioned in the direction of the earth's magnetic field. The suspending wire of the magnet became the centre of the rotation axis of the instrument. Because of the instrument's high sensitivity Eötvös was able to determine the magnetic moment of rocks and other bodies exhibiting weak magnetism. He carried out similar measurements on old bricks and clay pots. During the baking and cooling of the bricks and pots, several hundred years earlier, they had acquired a remanent magnetization in the direction of the ambient magnetic field. Since it was easy to recognize the sides of the bricks and the bottoms of the pots on which they had rested during baking, it was possible to position them in the same way. After having determined the direction of their magnetization, the inclination of the magnetic field at the time of their cooling could be defined. In 1900 Eötvös gave a lecture on his studies in this subject, entitled 'Magnetic Inclination in the Past'.

3. Eötvös the Organizer

In addition to activities as a research worker and lecturer, Eötvös played an important role in organizational work, thus promoting the development of the natural sciences in Hungary.

In 1885, in the company of other university lecturers, he took part in discussions on the latest scientific results. This group later became known as the Mathematical Society, in which physicists played an ever increasing role. As a result, in 1891 the Mathematical and Physical Society was formed, with Eötvös as its president. The society's journal was entitled the Mathematical and Physical Papers. The society was split in the year 1949, the Physical Society took the name of Loránd Eötvös and the Mathematical

Society was called after one of Hungary's great mathematicians, János Bólyai. In 1894, not long after Eötvös was appointed minister, the Physical Society gave their president a festive welcome, and to honour the occasion they announced a mathematical and physical competition for secondary school children, the winners of which would receive an Eötvös award.

During his career as a teacher Eötvös quickly realized that a great number of talented and hard working students were forced to stop their studies, due to lack of financial support. He wished to help solve this problem and so during the time he was minister, he established a residental college, which was named the József Eötvös College — after his father. Within the framework of the college future secondary school teachers received excellent tuition and took part in special tutorials to promote and develop individual scientific work. In order to assist the poorest students no fees were required for thirty of the one hundred places.

The financial situation of some of the students is characterized by the following story. In 1918, on the seventieth birthday of the now seriously ill Eötvös, the leaders of the college and six of the students visited him on his sick bed. During the conversation Eötvös asked how the six representatives of the students had been chosen. One of the students gave this explanation: 'Honourable sir, it was a question of jackets. It was only those with proper jackets who came.' The Eötvös College trained numerous excellent research workers and teachers in the following decades.

To promote the natural sciences Eötvös convinced Andor Semsey, a great Hungarian patron of the sciences to establish a scholarship which was to be awarded to young graduates who wished to devote themselves to scientific studies.

Eötvös kept in close touch with several international scientific organizations. The foremost of these was the Internationale Erdmessung, precursor of the international Union of Geodesy and Geophysics (IUGG). Eötvös regularly attended the general meetings of this organization and on each occasion reported on his research. As already mentioned, the 1906 general meeting of the Internationale Erdmessung held in Budapest played an important role in the further development of geophysical research in Hungary.

From 1907 onwards Eötvös' torsion balance project was financed by a special fund. After his death geophysical research became financially independent of the University Institute of Physics, under the name of

Eötvös Loránd Geophysical Institute (ELGI). This group of scientists, which, during Eötvös' lifetime consisted of a few members, has developed into a research establishment of about five hundred members, all striving in his name to further develop the science of geophysics.

GEOPHYSICAL TRANSACTIONS 1991
Vol. 37. No. 1. pp. 25-38

SUBSURFACE ELECTROMAGNETIC PARAMETERS IN TERMS OF THE DISTRIBUTION OF CURRENT

László SZARKA* and Gaston FISCHER**

Electric and magnetic fields below the horizontal surface of a conducting structure have been derived in terms of the subsurface currents. The formulae obtained are valid for any subsurface electromagnetic problems, e.g. for sea-bottom magnetotellurics or mining electromagnetics. The simplifications of these general three-dimensional formulae to one-dimensional and to the basic two-dimensional situations yield a clear physical meaning to the depth-dependence of the impedance and consequently to the apparent resistivity and the phase: in all instances the impedance at a given depth and location is entirely determined by the complex mean depth of the currents flowing beneath the actual measuring point.These results are extensions of similar ones published recently for electromagnetic parameters at the surface.

Keywords: electromagnetic parameters, current distribution, magnetotellurics

1. Introduction

All electromagnetic sounding methods relying on natural or artificially-generated fields try to determine the subsurface conductivity structures by means of some interpretational parameters (e.g. impedance,

* Geodetic and Geophysical Research Institute of the Hungarian Academy of Sciences, H-9401 Sopron, POB 5, Hungary
** Observatoire Cantonal, CH - 2000 Neuchatel, Rue de l'Observatoire 58, Switzerland

Manuscript received: 29 November, 1989

apparent resistivity, phase), which are derived from the distribution and/or period-dependence of the field components at the surface.

Even after the basic geo-electromagnetic induction studies in the frequency domain [e.g. CAGNIARD 1953, WEIDELT 1972, PRICE 1973] and other papers dealing with different interpretational parameters (e.g. FISCHER 1985 on the 2-D magnetotelluric phase; SPIES and EGGERS1986 on the apparent resistivity, etc.) the physical meaning of the geophysical interpretational parameters in the frequency domain has not always become clear.

In the paper by SZARKA and FISCHER [1989] the surface impedance and some corresponding parameters are interpreted in a novel way, based on the distribution of the subsurface currents. The formulae derived provide clear physical meanings for the impedance, the apparent resistivity and the phase. For example, the imaginary part of the surface impedance derives directly from the depth to the centre of gravity of the currents which are in phase with the surface magnetic field; the real part, on the other hand, is determined by the mean depth of the out-of-phase currents. The apparent resistivity — depending on how it is defined — is always related to the period-dependence of some function of the real and/or imaginary part of the complex depth of the current system; the phase tangent, in turn, is the ratio of the mean depths of in-phase and out-of-phase currents.

In this paper the subsurface impedance formulae will be given in analogous fashion to the expressions derived for the surface values by SZARKA and FISCHER [1989]. Similarly to this latter paper, all fields are taken to be functions of x, y, and z, and μ and ε are assumed constant, independent of space and time. Maxwell's equations, in which displacement currents are neglected, can then be written:

$$\oint \boldsymbol{H}\,\mathrm{d}\boldsymbol{l} = \iint_S \boldsymbol{j}\,\mathrm{d}\boldsymbol{S}\,, \tag{1}$$

$$\oint \boldsymbol{E}\,\mathrm{d}\boldsymbol{l} = -\,\mathrm{i}\omega\mu \iint_S \boldsymbol{H}\,\mathrm{d}\boldsymbol{S}\,, \tag{2}$$

$$\oint \boldsymbol{H}\,\mathrm{d}\boldsymbol{l} = 0\,, \tag{3}$$

$$\oint \boldsymbol{E}\,\mathrm{d}\boldsymbol{l} = Q\,. \tag{4}$$

For the horizontal electromagnetic components the resulting equations derived by SZARKA and FISCHER [1989] are the following

$$H_x(x,y,0) = -\int_0^\infty \left(j_y + \frac{\partial H_z}{\partial x} \right) dz , \tag{5}$$

$$H_y(x,y,0) = \int_0^\infty \left(j_x - \frac{\partial H_z}{\partial y} \right) dz , \tag{6}$$

$$E_x(x,y,0) = i\omega\mu \int_0^\infty z \left(j_x - \frac{\partial H_z}{\partial y} \right) dz - \int_0^\infty \frac{\partial E_z}{\partial x} dz , \tag{7}$$

$$E_y(x,y,0) = i\omega\mu \int_0^\infty z \left(j_y + \frac{\partial H_z}{\partial x} \right) dz - \int_0^\infty \frac{\partial E_z}{\partial y} dz . \tag{8}$$

It will be shown that very similar equations can be derived for the subsurface electromagnetic components.

2. Depth-dependence of subsurface electromagnetic components

In *Fig. 1* a closed line-integral is shown for a domain extending from an arbitrary depth z to infinity. The horizontal electric and magnetic fields can be obtained by integration over the domain from z to infinity.

$$H_x(x,y,z) = -\int_z^\infty \left[j_y(y,x,z') + \frac{\partial H_z(x,y,z')}{\partial x} \right] dz' \tag{9}$$

$$H_y(x,y,z) = \int_z^\infty \left[j_x(x,y,z') - \frac{\partial H_z(x,y,z')}{\partial y} \right] dz' \tag{10}$$

$$E_x(x,y,z) = i\omega\mu \int_z^\infty H_y(x,y,z')\, dz' - \int_z^\infty \frac{\partial E_z(x,y,z')}{\partial x} dz' \tag{11}$$

$$E_y(x,y,z) = i\omega\mu \int_z^\infty - H_x(x,y,z')\, dz' - \int_z^\infty \frac{\partial E_z(x,y,z')}{\partial y} dz' \tag{12}$$

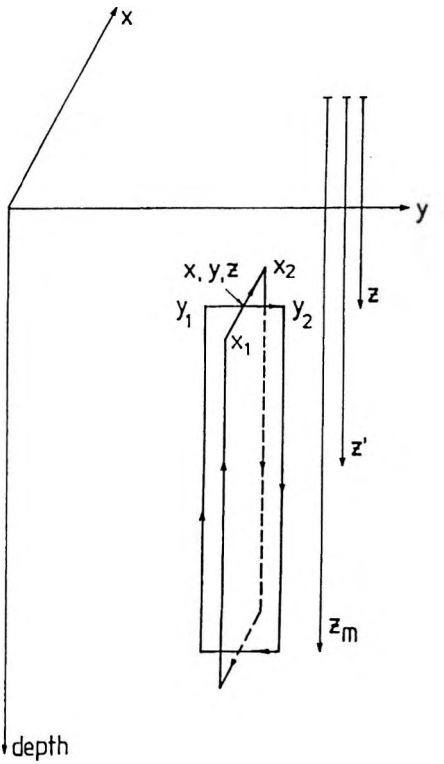

Fig. 1. Closed rectangular lines for integration between depths z and z_m

1. ábra. A z és z_m mélységek közötti integrálás zárt derékszögű útjai

Рис. 1. Замкнутые прямоугольные пути интегрирования между глубинами z и z_m

The form given to eqs (7) and (8) for the surface electric fields derives from the use of partial integrations, as shown below for the case of the E_x component:

$$\int_0^\infty H_y(x,y,z)\,dz = [\,z\,H_y]_0^\infty - \int_0^\infty z\,\frac{\partial H_y(x,y,z,)}{\partial z}\,dz = \\ = -\int_0^\infty z\,\frac{\partial H_y(x,y,z)}{\partial z}\,dz = \int_0^\infty z\,(j_x - \frac{\partial H_z}{\partial y})\,dz \qquad (13)$$

However, if we integrate from $z \neq 0$ to infinity the term zH_y does not disappear, and we obtain

$$\begin{aligned}
&\int_z^\infty H_y(x,y,z')\,dz' = [\,z\,H_y]_z^\infty - \int_z^\infty \frac{\partial H_y(x,y,z')}{\partial z'}\,dz' = \\
&= -z\,H_y(x,y,z) - \int_z^\infty z'\,\frac{\partial H_y(x,y,z')}{\partial z'}\,dz' = \\
&= \int_z^\infty z'\,[j_x(x,y,z') - \frac{\partial H_z(x,y,z')}{\partial y}]\,dz' - z\,H_y(x,y,z) = \\
&= \int_z^\infty (z'-z)\left[j_x(x,y,z') - \frac{\partial H_z(x,y,z')}{\partial y'}\right]dz'
\end{aligned} \tag{14}$$

On the basis of eq. (14) the following expressions can therefore be derived for the horizontal electric components:

$$E_x(x,y,z) = i\omega\mu \int_z^\infty (z'-z)\left[j_x(x,y,z') - \frac{\partial H_z(x,y,z')}{\partial y}\right]dz' - \int_z^\infty \frac{\partial E_z(x,y,z')}{\partial x}\,dz' \tag{15}$$

$$E_y(x,y,z) = i\omega\mu \int_z^\infty (z'-z)\left[j_y(x,y,z') + \frac{\partial H_z(x,y,z')}{\partial x}\right]dz' - \int_z^\infty \frac{\partial E_z(x,y,z')}{\partial y}\,dz' \tag{16}$$

We would mention here the similarity between expressions (5-8), valid at the top surface, and eqs (9, 10) and (15, 16) which apply at depth. This means that here too, the magnetic field at depth is given in large part by the depth integral of the current density beneath the measuring point, while the subsurface electric field strongly depends on the first moment of this current density.

The perfectly analogous structures of the two sets of equations (5-8) for the surface fields and (9, 10, 15, 16) for the fields at an interior point, clearly demonstrate that these equations are not restricted to uniform primary inducing fields. This can best be seen if we first consider a system of uniform primary inducing fields at the upper surface of a conductor bound by a plane of surface $z=0$. Then, for a given period T, each of the four equations, eqs (5-8), can be factored into amplitude and structural factors. The structural factor would depend only on the conductive struc-

ture and on the period, and would therefore entirely determine the impedance tensor Z at the surface. Equations (9, 10, 15, 16), on the other hand, cannot similarly be factored because the fields at an interior point $z > 0$ depend on the structure above that point. For example, if we imagine a structure stable below a certain depth z_0, covered with an overburden at $z < z_0$ which we assume arbitrarily variable, then the fields at the $z=z_0$ surface will depend on this superior structure. Unless the structure for $z<z_0$ is 1-D and the primary fields are uniform, the primary field at $z=z_0$ will not be uniform. The structural features above a given depth z_0 can therefore be looked upon as producing non-uniform primary fields at the z_0 level. Since the z_0 level is arbitrary, it follows that eqs (9, 10, 15, 16) remain valid at the surface as well as inside any conducting structure, including situations where the surface of the conductor is not bound by a plane surface and where the primary inducing field is not uniform. Formulae (9, 10, 15, 16) are therefore of quite general validity; in particular they remain unchanged if the surface of the conductor exhibits complicated topography and if the primary inducing field is not uniform, as for example in the immediate vicinity of an antenna.

3. 1-D and 2-D formulae at arbitrary depths

In one-dimensional (1-D) geometry the following relations can be derived from eqs. (9, 10, 15, 16):

(a) when current flow is along the x axis:

$$E_x(z) = i\omega\mu \int_z^\infty (z' - z)\, j_x(z')\, dz' \tag{17}$$

$$H_y(z) = \int_z^\infty j_x(z')\, dz' \tag{18}$$

(b) when current flow is along the y axis:

$$E_y(z) = i\omega\mu \int_z^\infty (z' - z)\, j_y(z')\, dz' \tag{19}$$

$$H_x(z) = -\int_z^\infty j_y(z')\, dz' \tag{20}$$

With two-dimensional (2-D) structures we must distinguish between *E*- and *H*-polarization configurations and we take the strike to be in the direction of the *x* axis.

(a) In *E*-polarization:

$$E_x(y,z) = i\omega\mu \int_z^\infty (z' - z) \left[j_x(y,z') - \frac{\partial H_z(y,z')}{\partial y} \right] dz' \tag{21}$$

$$H_y(y,z) = \int_z^\infty \left[j_x(y,z') - \frac{\partial H_z(y,z')}{\partial y} \right] dz' \tag{22}$$

(b) In *H*-polarization:

$$E_y(y,z) = i\omega\mu \int_z^\infty (z' - z)\, j_y(y,z')\, dz' - \int_z^\infty \frac{\partial E_z(y,z')}{\partial y} dz' \tag{23}$$

$$H_x(y,z) = - \int_z^\infty j_y(y,z')\, dz' \tag{24}$$

4. Impedance formulae at arbitrary depth

The impedance tensor is given in terms of ratios of horizontal electric and magnetic components. In the one-dimensional geometry the tensor component $Z_{xy}(z)$ takes the simple form:

$$Z_{xy}(z) = - i\omega\mu \left[\frac{\int_z^\infty z'\, j_x(z')\, dz'}{\int_z^\infty j_x(z')dz'} - z \right] = - i\omega\mu\, (z^*_{1\text{-}D} - z) \tag{25}$$

Ignoring the factor ($- i\omega\mu$) we see that the 1-D impedance Z_{xy} is given in terms of quantities with the dimensions of depths: the 1-D impedance is simply proportional to the complex mean depth below the observation point of the currents flowing beneath depth z. We saw earlier that the amplitude of this current distribution is, naturally, determined by currents flowing above the measuring point, but this does not appear explicitly in eq. (25).

The well-known constancy of the impedance in the lowest layer follows directly from eq. (25) since in this lowest, or n-th layer, where the current density at the top is j_{no} and $k_n^2 = -i\omega\mu\,\sigma_n$, we find

$$Z_{xy}(z) = -i\omega\mu \frac{\int_z^\infty z' j_{no} e^{-k_n z'} dz'}{\int_z^\infty j_{no} e^{-k_n z'} dz'} + i\omega\mu z = \tag{26}$$

$$= -i\omega\mu (z + 1/k_n) + i\omega\mu z = -\frac{i\omega\mu}{k_n}$$

Obviously, according to eq. (26), $Z_{xy}(z)$ in the bottom layer does not depend on depth.

In 2-D E-polarization we find

$$Z_{xy}(x,z) = -i\omega\mu \left\{ \frac{\int_z^\infty z' \left[j_x(y,z') - \frac{\partial H_z(y,z')}{\partial y} \right] dz'}{\int_z^\infty \left[j_x(y,z') - \frac{\partial H_z(y,z')}{\partial y} \right] dz'} - z \right\} = \tag{27}$$

$$= -i\omega\mu (z_E^* - z)$$

and in H-polarization

$$Z_{xy}(y,z) = -i\omega\mu \left[\frac{\int_z^\infty z' j_y(y,z')\, dz'}{\int_z^\infty j_y(y,z')\, dz'} - z \right] + \frac{\int_z^\infty \frac{\partial E_z(y,z')}{\partial y} dz'}{\int_z^\infty j_y(y,z')\, dz'} = \tag{28}$$

$$= -i\omega\mu (z_H^* - z) + f(E_z)$$

Finally, in the general three-dimensional situation the component $Z_{xy}(x,y,z)$ can be written as follows:

$$Z_{xy}(x,y,z) = -\frac{E_x}{H_y} = -\,i\omega\mu\,\frac{\int_z^\infty z'\left[j_x(x,y,z') - \dfrac{\partial H_z(x,y,z')}{\partial y}\right]dz'}{\int_z^\infty \left[j_x(x,y,z') - \dfrac{\partial H_z(x,y,z')}{\partial y}\right]dz'} + \tag{29}$$

$$+\,\frac{\int_z^\infty \dfrac{\partial E_z(x,y,z')}{\partial x}\,dz'}{\int_z^\infty \left[j(x,y,z') - \dfrac{\partial H_z(x,y,z')}{\partial y}\right]dz'} + i\omega\mu\, z = -\,i\omega\mu\,(z^*_{3\text{-}D_z} - z) + f_{3\text{-}D}(E_z)$$

where

$$z^*_{3\text{-}D_z} = \frac{\int_z^\infty z'\left[j_x(x,y,z) - \dfrac{\partial H_z(x,y,z)}{\partial y}\right]dz'}{\int_z^\infty \left[j_x(x,y,z') - \dfrac{\partial H_z(x,y,z')}{\partial y}\right]dz'}$$

and

$$f_{3\text{-}D}(E_z) = \frac{\int_z^\infty \dfrac{\partial E_z(x,y,z')}{\partial x}\,dz'}{\int_z^\infty \left[j_x(x,y,z') - \dfrac{\partial H_z(x,y,z')}{\partial y}\right]dz'}$$

Equation (29) is clearly more complicated than eqs. (25-28), but on the basis of its one- and two-dimensional limiting behaviour all three dimensional features can easily be understood. The other impedance components can similarly be derived.

5. New way of looking at an old example

In *Fig. 2* we show the magnetotelluric phase distribution inside the upper layer of a two-layered half-space, with $\sigma_2/\sigma_1 = 100$. For the two logarithmic axes we have, respectively, the relative depth z/h (where h is the thickness of the first layer) and a normalized wavelength $\lambda_1/h_1 \sim \sqrt{T}$

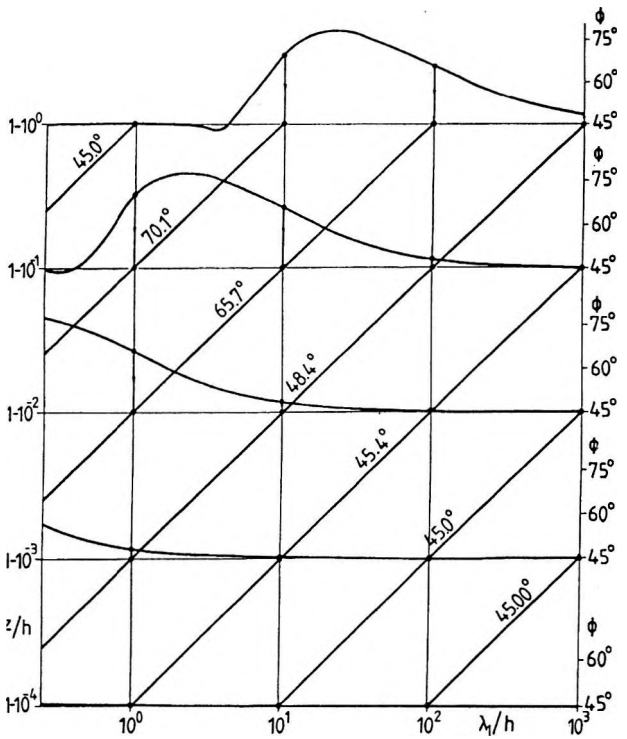

Fig. 2. Magnetotelluric phase Φ inside the first layer of a two-layer half-space (σ_1,σ_2, h), when $\sigma_2/\sigma_1 = 100$n as a function of the relative wavelength λ_1/h in the upper layer and for various relative depths z/h inside this layer. In addition to the five phase curves for $z/h = 0, 0.9, 0.99, 0.999$ and 0.9999, several straight lines connecting points of constant phase are shown

2. ábra. Magnetotellurikus fázis (Φ) kétréteges féltér első rétegében (σ_1,σ_2, h) $\sigma_2/\sigma_1 = 100$ esetre, a felső rétegbeli relatív hullámszám (λ_1/h) függvényében, különböző relatív mélységekre *(z/h)*. A z/h = 0, 0,9, 0,99, 0,999 és 0,9999 értékekre kiszámolt öt fázisdiagramon kívül az állandó fázisokat összekötő egyenes vonalakat is ábrázoltuk.

Рис. 2. Магнитотеллурическая фаза (Φ) в первом слое двуслойного полупространства (σ_1,σ_2, h) для случая $\sigma_2/\sigma_1 = 100$ как функция относительного волнового числа (λ_1/h) в верхнем слое, при различных относительных глубинах *(z/h)*. Помимо пяти фазовых диаграмм, рассчитанных для z/h = 0, 0,9, 0,99, 0,999 и 0,9999 показаны также и прямые, соединяющие постоянные фазы

(where λ_1 is the wavelength in the first layer, $\lambda_1 = 2\pi s$, where s is the skindepth).

The phase plots shown are not new but nevertheless they seem to be somewhat surprising: at depths which are increasing by exponentially decreasing amounts we find the same phase behaviour as on the top surface, but at smaller and smaller $\lambda_1/h \sim \sqrt{T}$ values. Expressed mathematically we find identical phase values at all those subsurface sites for which the normalized local wavelength $\lambda_1/(h-z)$ is the same. In other words, the geometrical set of subsurface observation sites having identical phases is given by the equation:

$$\lambda_1(0)/h = \lambda_1(z)/(h-z) \tag{30}$$

As a practical consequence of eq. (30) we find that any surface phase value measured at period $T(0)$ will be obtained at depth z at another period $T(z)$, which (since λ_1 is proportional to $\sqrt{T}$) is given by

$$T(z) = T(0)\ (1 - z/h)^2 \tag{31}$$

This relation is valid only inside the first layer, i.e. for $0 \leq z \leq h$. According to eq. (31) a surface field parameter measured at a period of, say 1000 s can be obtained at a depth z=0.9 h at 10 s . Furthermore what happens at the surface in the period range 10-1000 s occurs in the 0.1-10 s range at the depth z=0.9 h .

The self-repetition of the phase anomaly in Fig. 2 means that

(a) the shape of the phase anomaly is determined exclusively by the resistivity contrast and

(b) the shift of the phase anomaly along the λ_1/h axis is determined by the thickness of layer 1 between the measuring site and the layer boundary.

Points (a) and (b) clearly indicate that the phase anomaly at any depth can be described entirely by what happens below the measuring site. In other words: the phase anomaly at any depth is completely determined by the currents flowing below the observation site.

Of course, the phase anomaly at depth can also be derived starting from the surface anomaly and taking into account the current distribution between the surface and the observation site. In this section we have pointed

out the importance of the first, alternative approach in a simple two-layered case.

We believe that a careful consideration of current and charge distribution below the observation site any 2-D or 3-D problem could help at least in the intuitive understanding of the problem. Such an approach might have direct bearings on sea-bottom magnetotellurics [e.g. FILLOUX 1977] or in mining electromagnetics [e.g. TAKÁCS 1989].

6. Conclusion and significance of the results

The above equations do not give direct solutions for any particular 3-D, 2-D or 1-D problem, but give closer insight into the behaviour of the impedance tensor calculated from horizontal electric and magnetic components at an arbitrary depth. The impedance in any subsurface electromagnetic problem is directly related to the complex mean depth of the currents flowing below the observation point.

The equations derived are simple extensions of the results of SZARKA and FISCHER [1989] and can be obtained directly by replacing the lower integration limit of zero by the arbitrary limit $z>0$ in the original formulae. In other words, the apparent resistivity and the phase are given by the same expressions for points inside or at the surface of a conducting structure.

As we have shown this straightforward extension implies that the formulae we have derived are of very general validity: they remain true even when the surfaces of the conductor exhibits a complicated topography and when the primary inducing fields are not uniform.

The formulae derived in this paper are valid for any subsurface electromagnetic problem, e.g., for sea-bottom magnetotellurics or mining electromagnetics, where interpretational problems have sometimes been especially difficult. The simple connection they establish between the commonly-used impedance parameters at depth and the current distribution beneath this depth should render them useful in applications of subsurface electromagnetic exploration methods.

REFERENCES

CAGNIARD L. 1953: Basic theory of the magnetotelluric method of geophysical prospecting. Geophysics **18**, 3, pp. 605-635.

FILLOUX J. H. 1977: Ocean-floor magnetotelluric sounding over North Central Pacific. Nature **269**, 5626, pp. 297-301.

FISCHER G. 1985: Some remarks on the behavior of the magnetotelluric phase. Geophysical Prospecting **33**, 5, pp.716-722.

FISCHER G., SZARKA L., ÁDÁM A. and WEAWER J. 1991: The magnetotelluric phase over two- and three-dimensional structures. Geophysical Journal International (in press)

SPIES B. R. and EGGERS D. E. 1986: The use and misuse of apparent resistivity in electromagnetic methods. Geophysics **51**, 7, pp. 1462-1471.

SZARKA L. and FISCHER G. 1990: Electromagnetic parameters at the surface of a conductive halfspace in terms of the subsurface current distribution. Geophysical Transactions **35**, 3, pp. 157-172

TAKÁCS E. 1989: In-mine frequency sounding with a buried grounded dipole source. Geophysical Transactions **34**, 4, pp. 343-359.

WEIDELT P. 1972: The inverse problem of geomagnetic induction. Zeitschrift für Geophysik **38**, 2, pp. 257-289.

FELSZÍNALATTI ELEKTROMÁGNESES PARAMÉTEREK A MÉLYBELI ÁRAMELOSZLÁS FÜGGVÉNYÉBEN

SZARKA László és Gaston FISCHER

Az inhomogén vezető közeg horizontális felszíne alatti elektromos és mágneses teret a mélybeli árameloszlás függvényében tárgyaljuk. A levezetett formulák bármely felszínalatti elektromágneses problémára (pl. tengerfenék-magnetotellurikára vagy bányászati geofizikára) alkalmazhatók. Az általános háromdimenziós összefüggéseknek egydimenziós és az alapvető kétdimenziós esetekre történő leegyszerűsítése az impedancia mélységfüggésére, következésképpen a látszólagos fajlagos ellenállásra és a fázisra világos fizikai értelmezést nyújt: bármely tetszőleges felszínalatti pontban az impedanciát az illető pont alatti áramok komplex átlagmélysége határozza meg. Az eredmények a felszíni elektromágneses paraméterekre vonatkozó korábbi eredmények kiterjesztésének tekinthetők.

ПОДПОВЕРХНОСТНЫЕ ЭЛЕКТРОМАГНИТНЫЕ ПАРАМЕТРЫ КАК ФУНКЦИЯ ГЛУБИННОГО РАСПРЕДЕЛЕНИЯ ТОКА

Л. САРКА, Г. ФИШЕР

Электрическое и магнитное поле под горизонтальной поверхностью неоднородной проводящей среды рассматривается как функция глубинного распределения тока. Выведенные формулы могут применяться в решении любых подповерхностных электромагнитных проблем, например, в магнитотеллурике морского дна или в подземной геофизике.

Упрощенное сведение общего трехмерного случая к одномерному и основным двумерным дает ясную физическую интерпретацию зависимости импеданса от глубины и, следовательно, кажущихся удельных сопротивлений и фаз: импеданс в произвольной точке под некоторой поверхностью определяется комплексной средней глубиной токов ниже данной точки.

Результаты могут рассматриваться в качестве расширения выводов, полученных ранее по поверхностным электромагнитным параметрам.

GEOPHYSICAL TRANSACTIONS 1991
Vol. 37. No. 1. pp. 39-55

EFFECT OF LATERAL INHOMOGENEITIES ON THE FREQUENCY SOUNDING CURVES OBTAINED FROM THE VERTICAL ELECTRIC COMPONENT OF A BURIED VERTICAL CURRENT DIPOLE

Ernő TAKÁCS*

The paper discusses how the effect of lateral inhomogeneities manifests itself in underground frequency soundings carried out using vertical electric transmitter and receiver dipoles in an equatorial array.

The simplified models are:

— a vertically infinite interface and sheet perpendicular and parallel to the axis connecting the transmitter and receiver dipoles;

— a break in the horizontal high resistivity layer perpendicular to the axis connecting the transmitter and receiver dipoles.

The former case was studied numerically, the latter one by physical modelling.

Keywords: frequency, electrical sounding, dipole, lateral inhomogeneity, in-mine geoelectric methods, models

1. Introduction

In an earlier paper [TAKÁCS et al. 1986] the characteristics of a vertical electric field of a buried vertical electric dipole in horizontally layered medium were analysed. Survey tasks solved by applying underground transmitter and receiver are, however, rather associated with detection of

* Miskolci Egyetem, Geofizikai Tanszék, Miskolc-Egyetemváros, H-1535

Manuscript received: 10 December, 1990

lateral inhomogeneities either between the transmitter and receiver or in their vicinity. It is essential to study the nature of the effect of such inhomogeneities because observed deviations from the response of horizontally layered models suggest the presence of inhomogeneities.

The approved methods for studying lateral inhomogeneities are seismic and electromagnetic tomography or dc reconstruction. These types of measurements can be carried out only if the relative position of transmitter and receiver can be changed in a sufficiently wide range to obtain as many crossing transilluminating radii as possible. It may happen, however, that this kind of measurement is unaccomplishable and the space between or in the vicinity of the dipoles can only be studied using a given fixed array. The question arises whether frequency sounding might have a role in detecting lateral inhomogeneities in such cases.

To deal with the problem I have carried out physical and numerical modelling for a variety of situations. The models chosen are simplified; they are, however, suitable for recognizing, as a first step, the basic characteristics. The conclusions obtained can be used as a basis for extending the study to more complicated cases.

In every discussed case vertical electric (grounded) transmitter and receiver dipoles in an equatorial array are considered.

The complex shape of frequency sounding curves — quasi-stationary part, possibly a maximum, then a steeply descending branch — makes the visual recognition of the effects of both horizontal stratification and lateral inhomogeneities difficult. The introduction of an apparent resistivity that at any frequency is equal to the resistivity of that homogeneous space which substitutes the inhomogeneous space considering its effect is of help. This apparent resistivity — $\rho_a^*(f)$— can be obtained from measurement of amplitude, phase or in-phase or out-of-phase components. To derive it the dependence of the quantity in question on the induction number — transmitter-receiver separation normalized to the skin depth — in a homogeneous medium should be known. In addition, values of the actual transmitter-receiver separation — R — and frequency will be used. Thus, $\rho_a^*(f)$ can be derived not from the actual field strength value but from the position of characteristic points on the frequency sounding curve along the frequency axis [TAKÁCS et al. 1986].

The other parameter used later is the effective resistivity (ρ_{eff}^*) of the 'rock-slab' containing the transmitter and receiver dipoles. This can be

given knowing the resistivity ρ_a calculated using the factor of the geometric sounding on the quasi-stationary part of the curve and $\rho_a^*(f_{max})$ calculated at the maximum of the amplitude curve. In a continuous layer this is a very good approximation of the actual resistivity. In the case of discontinuity it reflects the degree of discontinuity [TAKÁCS et al. 1986].

In view of the fundamental behaviour of $\rho_a^*(f)$ it can be expected that at lower frequencies the effect of the more distant environment of the dipoles manifests itself as well; then, with increasing frequency, it reflects more and more the resistivity distribution in the closer vicinity of the transmitter.

2. Effect of infinite vertical interface

In one of the cases studied, 20 and 250 Ωm media can be found at two sides of the interface. The measuring array with a constant transmitter-receiver separation — R=100 m — has different positions related to the interface. The direction of R is perpendicular to the interface. The amplitude curves are shown in *Fig. 1,* the phase curves in *Fig. 2.*

Amplitude curves corresponding to the different positions obviously lie between the curves of 20 and 250 Ωm homogeneous space, respectively. As long as the transmitter and receiver are in a medium of the same resistivity the high frequency asymptotes of the curves coincide. It means that an increase in frequency causes a decrease in the effect of the adjacent halfspace. With decreasing frequency, on the other hand, its effect increases. This is the reason why the maximum becomes more enhanced on approaching the low resistivity halfspace from the higher resistivity one. At the same time, the amplitude of the maximum related to the quasi-stationary part of the curve decreases when both the transmitter and receiver are in the halfspace of lower resistivity and they approach the halfspace of higher resistivity.

When the interface lies between the transmitter and receiver, the quasi-stationary field strength remains the same at different positions of the array, and it depends only on the transmitter-receiver separation. In our case it is constant. Location and value level of maxima and descending branches, on the other hand, depend on the effective resistivity of the rock volume determined by the current field developing at the corresponding frequen-

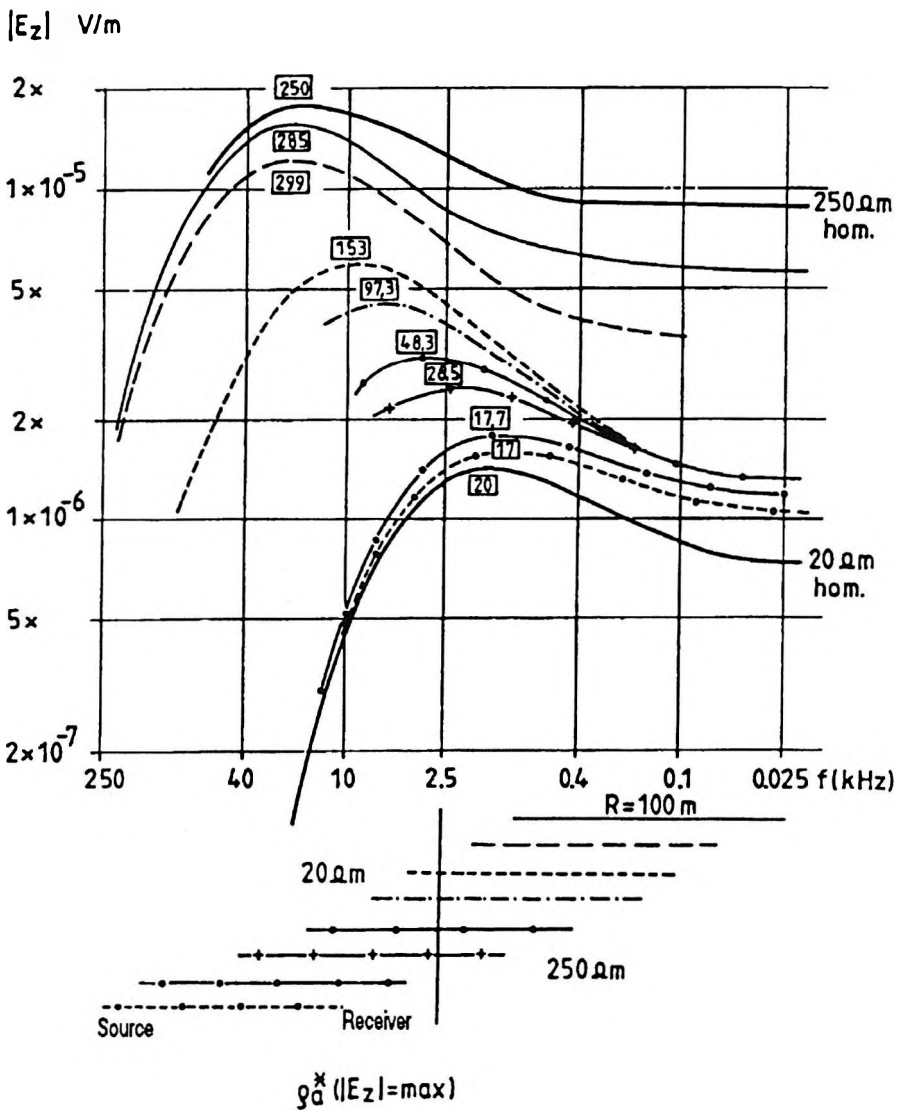

Fig. 1. Amplitude-frequency curves for vertical interface perpendicular to the axis connecting the vertical transmitter and receiver dipoles in an equatorial array, for different positions of the array

1. ábra. Az amplitúdó görbéi az ekvatoriális helyzetű vertikális adó- és vevő-dipólust összekötő tengelyre merőleges vertikális határfelület esetén különböző felállások melett

Рис. 1. Амплитудные кривые частотного зондирования при перемещении установки вертикальных экваториальных диполей вкрест простирания вертикального контакта двух сред

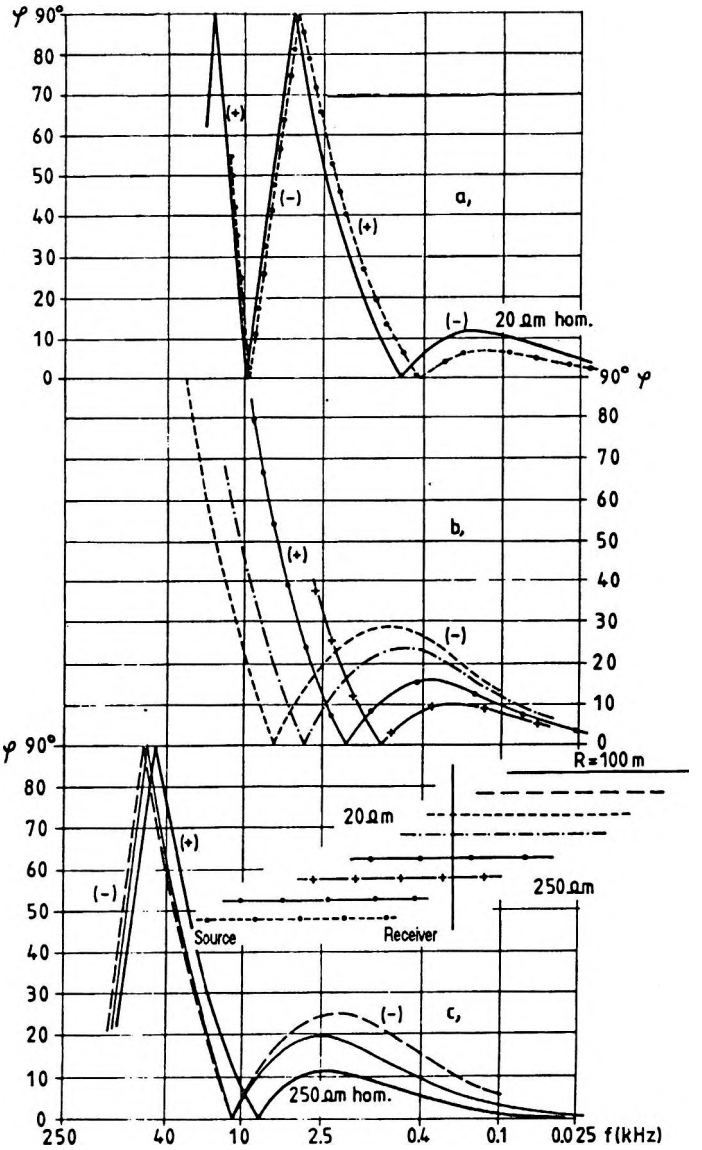

Fig. 2. Phase-frequency curves for vertical interface perpendicular to the axis connecting the transmitter and receiver dipoles in an equatorial array, for different positions of the array

2. ábra. A fázis frekvenciaszondázási görbéi az ekvatoriális helyzetű adó- és vevő-dipólust összekötő tengelyre merőleges vertikális határfelület esetén különböző felállások mellett

Рис. 2. Фазовые кривые частотного зондирования при перемещении установки вертикальных экваториальных диполей вкрест простирания вертикального контакта двух сред

cies. The position of the interface between the transmitter and receiver influences this effective resistivity. The shorter that part of separation R which lies in the lower resistivity halfspace is, the higher the amplitude and the frequency where the maximum can be found will be.

Consequently, frequency sounding curves reflect the position of the dividing, vertical interface between the transmitter and receiver in every case.

The trend of ρ_a^* apparent resistivity values belonging to the maxima — framed numbers in Figure 1 — shows that when the larger part of separation R gets into the halfspace of higher resistivity, sensitivity to the position of vertical interface increases.

The phase curves in Fig. 2 are arranged in three groups according to their position related to the interface; the array lies completely within one of the halfspaces or it intersects the vertical interface. At curves of arrays lying in one or the other halfspace, the curves for the homogeneous space having the resistivity of the corresponding halfspace can also be seen for comparison. In the figure the sign of the phase is indicated at each curve section. In a homogeneous space, in the innermost, low frequency current field the value of the phase minimum — negative phase angles — is independent of resistivity. On the other hand, when the resistivity of the homogeneous space is higher the minimum develops at higher frequencies. With an array further from the interface a curve obviously corresponding to the homogeneous space is obtained. Approaching the vertical interface both value and position of the minimum change; their trend can be seen in the figure. For the same shift changes in phase angle are larger when the array is in the higher resistivity part.

When the vertical interface lies between the transmitter and receiver, the transmitter is in the 20 Ωm halfspace and it gradually moves towards the interface starting from 75 m to 12.5 m the position of the minimum shifts more and more towards higher frequencies as a result of increasing effective resistivity; the amplitude of the minimum also increases. With increasing frequency the potential dipole gets into the second current system of positive phase angles. When the transmitter and receiver are in the same halfspace the phase curves hardly separate in the second current system at different positions of the array. On the other hand, when the interface lies between the transmitter and receiver, the position of charac-

teristic parts and branches of the phase curves along the phase axis is very sensitive to the position of the interface.

In the other case, the vertical interface is parallel to the axis connecting the vertical transmitter and receiver dipoles; the separation between this axis and the interface varies (x=10, 20, 30 and 50 m). Both the transmitter and receiver dipoles are in the halfspace of 250 Ωm. The amplitude curves in *Fig. 3* show that the lateral inhomogeneity causes a deviation from the curve of the homogeneous 250 Ωm space when the frequency decreases; it results in a lower field strength. The closer the interface is to the array the higher the frequency where the deviation begins. Moving from the maximum towards the quasi-stationary section the decrease in amplitude is stronger than for the curve of the 250 Ωm space. The maximum becomes wider with decreasing x.

With increasing frequency, on the other hand, that part of the space which is close to the axis of the array has more and more effect on the field strength. This can primarily be seen from the frequency dependence of resistivity $\rho_a^*(f)$, which was calculated on the basis of phase angle. Its behaviour for the two cases studied up to now is shown in *Fig.4.* For the interface perpendicular to the axis of the array — part b — that part of the transmitter-receiver separation can be seen at the individual curves in parenthesis that falls into the halfspace of resistivity indicated. When the array is in only one of the halfspaces the resistivity of this halfspace and the separation x between the interface and the closest electrodes are indicated. For a vertical interface parallel to the transmitter-receiver axis — part a — the parameter of the curves is the separation x between the interface and the parallel array in the 250 Ωm medium.

When the array is in only one of the halfspaces — parallel array and some perpendicular arrays — the high frequency asymptote is the resistivity of the host medium. At lower frequencies the effect of the other halfspace prevails more and more. At intermediate frequencies, however, 'overshoots' also appear.

3. Effect of vertical infinite sheet

An interesting case in practice is when the transmitter and receiver are situated in the same rock and information on the homogeneity or inhomo-

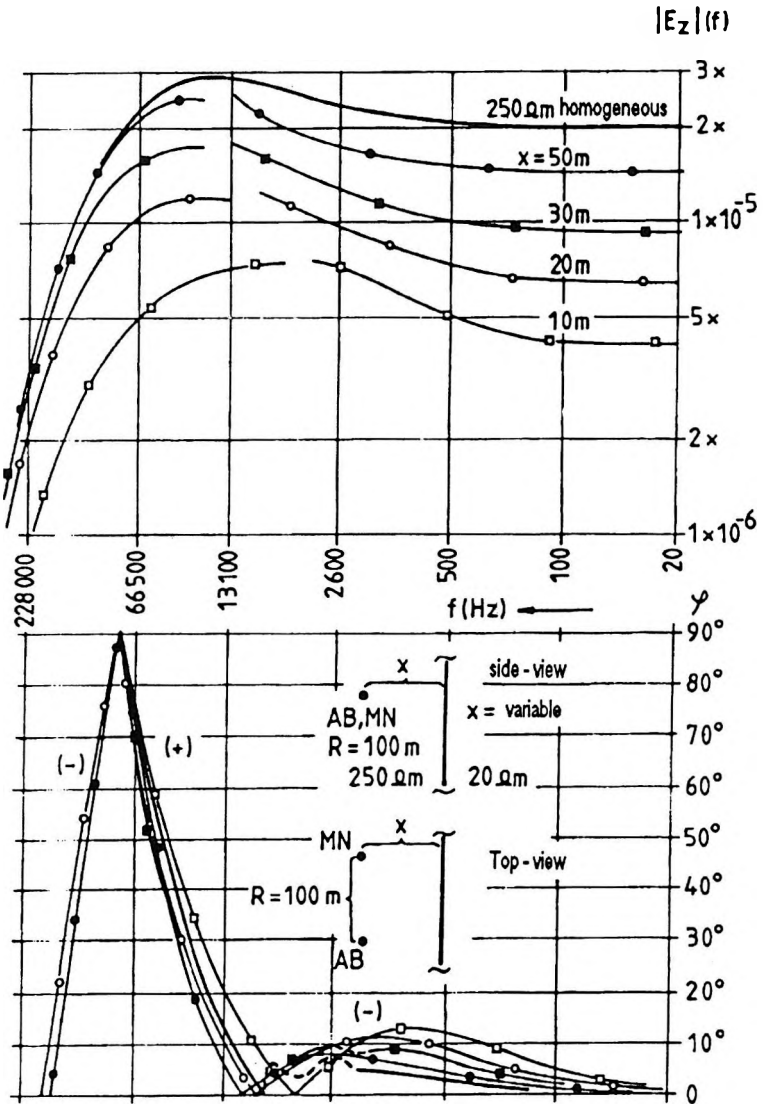

Fig. 3. Amplitude-frequency and phase-frequency curves for interface parallel to the axis connecting the vertical transmitter and receiver dipoles in an equatorial array, for different positions of the array

3. ábra. Az amplitúdó és fázis frekvenciaszondázási görbéi az ekvatoriális helyzetű vertikális adó- és vevő-dipólust összekötő tengellyel párhuzamos határfelület esetén különböző felállások mellett

Рис. 3. Амплитудные и фазовые кривые частотного зондирования при перемещении установки вертикальных экваториальных диполей по простиранию вертикального контакта двух сред

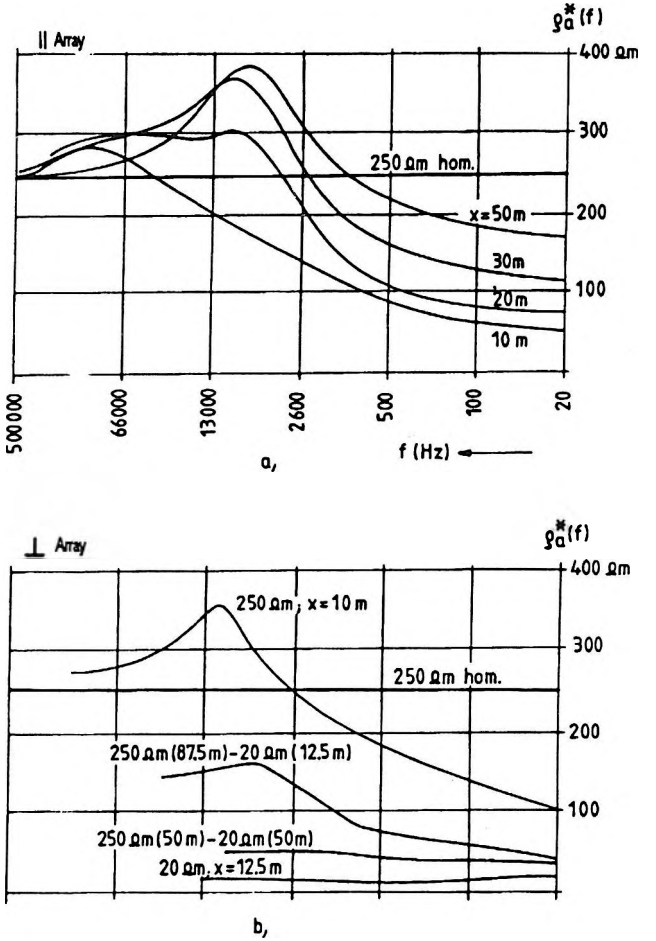

Fig. 4. Curves of apparent resistivity $\rho_a^*(f)$ for an array parallel and perpendicular to the vertical interface (model of Figs.1. and 3)

4. ábra. A $\rho_a^*(f)$ látszólagos fajlagos ellenállás görbéi a vertikális határfelülettel párhuzamos és rá merőleges felállásnál (Az 1. és 3. ábra modellje)

Рис. 4. Кривые кажущихся сопротивлений $\rho_a^*(f)$ для установок, параллельных и перпендикулярных вертикальному контакту двух сред (Модели рис 1. и 3.)

geneity of the space between them needs to be obtained by means of frequency sounding.

To study this potential application a vertically infinite, 20 m wide sheet of 20 Ωm embedded in a homogeneous space of 50 Ωm was considered.

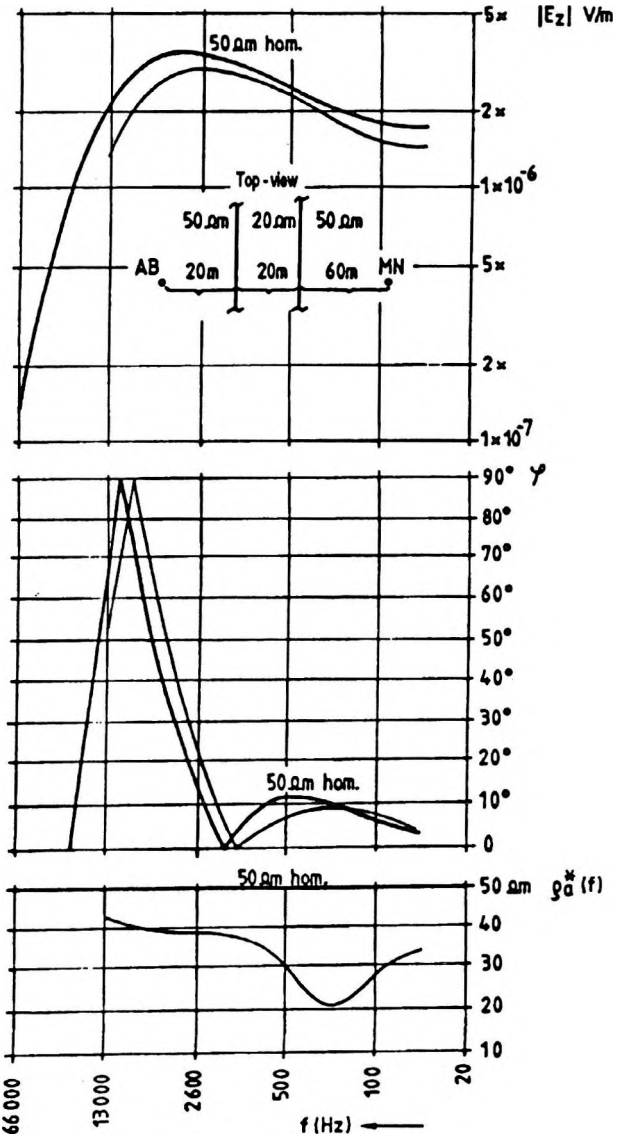

Fig. 5. Amplitude-frequency, phase-frequency and apparent resistivity ($\rho_a^*(f)$)- frequency curves for array passing through the vertical sheet

5. ábra. Az amplitúdó, a fázis és a $\rho_a^*(f)$ látszólagos fajlagos ellenállás frekvenciaszondázási görbéi a vertikális lemezt közrefogó felállásnál

Рис. 5. Кривые кажущихся сопротивлений ($\rho_a^*(f)$), а также амплитудные и фазовые при частотном зондировании для установки, внутри которой находится вертикальная пластина

The transmitter and receiver dipoles are vertical, their separation is 100 m, the array axis is perpendicular to the sheet and its position is asymmetrical to the sheet. The top-view of the geometric arrangement, together with the amplitude and phase curves for the homogeneous and inhomogeneous cases, respectively, can be seen in *Fig. 5.*

It is obvious that because of the lower effective resistivity in the inhomogeneous case the maximum of the corresponding curve is shifted towards lower frequencies. Details, however, should appear in the shape of the curves. To enhance them, from the phases apparent resistivities $\rho_a^*(f)$ were calculated which are shown in the lower part of the figure. For the homogeneous 50 Ωm space $\rho_a^*(f)$ = 50 Ωm = const. On the other hand, the effect of the embedded 20 Ωm sheed, can clearly be seen on the apparent resistivity curve at frequencies between 100 and 500 Hz. This example is remarkable from the aspect of investigation of inhomogeneities located between the transmitter and receiver. Of course, other models that more closely approximate reality should also be studied.

The lateral zone, which has an effect on the underground measurements can be investigated when a 60 m wide, 250 Ωm vertical slab is embedded into a medium of 20 Ωm; and the array of 100 m transmitter-receiver separation is in a horizontal plane, in the middle of the slab. The amplitude curves for the 250 Ωm homogeneous medium, and for the inhomogeneous model are shown in *Fig. 6.* At the highest frequencies the curves for homogeneous and inhomogeneous cases coincide or lie close to each other because, as a result of the lateral contraction of the current system, the low resistivity part of the space has no effect on the field strength. In practice, at frequencies higher than about 200 kHz the electromagnetic field concentrates in the higher resistivity slab. At a given frequency the width of the lateral zone having an effect on the measurement becomes wider with increasing transmitter-receiver separation and slab resistivity.

In the model of *Fig. 7* the 10 m wide vertical sheet of 5 Ωm is parallel to the axis of the dipole equatorial array located in the 50 Ωm homogeneous space.

The distance from the sheet and the transmitter-receiver separation are also taken as variables. The lower resistivity sheet causes a distortion in the amplitude curves at the maximum and at the beginning of the descending branch of the curves — which may not occur in horizontally

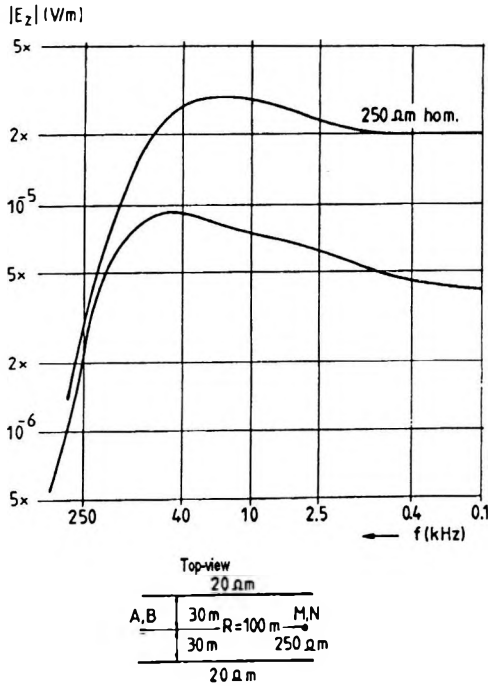

Fig. 6. Amplitude-frequency curves for vertical transmitter and receiver dipoles in an equatorial array within the vertical slab

6. ábra. Az amplitúdó frekvencia-szondázási görbéi a vertikális lemezen belüli ekvatoriális helyzetű vertikális adó- és vevő-dipólus esetében

Рис. 6. Амплитудные кривые частотного зондирования при положении установки вертикальных экваториальных диполей внутри вертикальной пластины

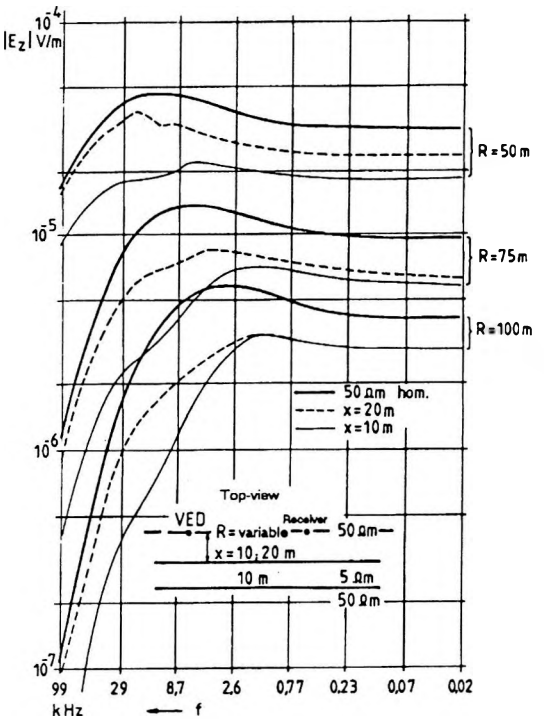

Fig. 7. Amplitude-frequency curves for a lower resistivity vertical sheet parallel to the axis connecting the vertical transmitter and receiver dipoles in an equatorial array

7. ábra. Az amplitúdó frekvenciaszondázási görbéi az ekvatoriális helyzetű vertikális adó- és vevődipólust összekötő tengellyel párhuzamos kisebb fajlagos ellenállású vertikális lemez esetén

Рис. 7. Амплитудные кривые частотного зондирования при наличии вертикальной пластины пониженного сопротивления параллельно установки вертикальных экваториальных диполей

layered models. The presence of a relative minimum between the frequencies 2.6 and 29 kHz is connected with the phenomenon that the current system contracting towards the transmitter and receiver gradually leaves the 50 Ωm medium on the other side of the sheet; and the effect of the sheet gradually ceases to exist above 29 kHz.

In *Fig. 8* frequency dependence of apparent resistivity $\rho_a^*(f)$ calculated from the curves of amplitude, phase, in-phase and out-of-phase components is plotted together with the curve of geometric sounding. $\rho_a^*(f)$ has a value

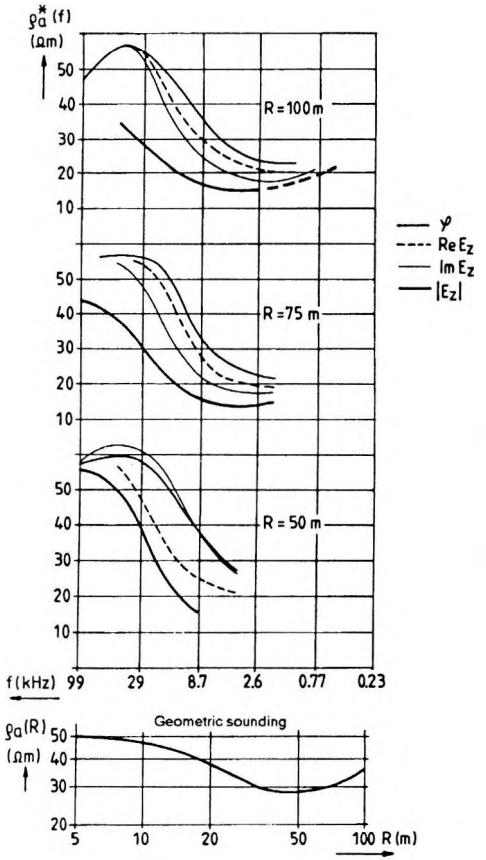

Fig. 8. Frequency dependence of apparent resistivity $\rho_a^*(f)$ calculated from in-phase, out-of-phase components, phase and amplitude for a vertical sheet parallel to the array

8. ábra. A valós és képzetes összetevőből, a fázisból és amplitúdóból számított $\rho_a^*(f)$ látszólagos fajlagos ellenállás frekvenciaszondázási görbéi a terítéssel párhuzamos vertikális lemez esetében

Рис. 8. Кривые кажущихся сопротивлений $\rho_a^*(f)$ частотного зондирования, рассчитанные по реальной и мнимой компонентам, а также по фазе и амплитудам для установки, параллельной вертикальной пластине

close to 50 Ωm at the highest frequency for each R, and it decreases towards lower frequencies. The effect of the 50 Ωm part of the space on the other side of the sheet begins to appear only at R=75 and 100 m, and rather in the out-of-phase component. This figure demonstrates the fact — that can be observed in other cases too — that in-phase and out-of-phase compo-

nents of the field strength reflect geologic conditions of different surroundings of the transmitter dipole. Both of them are transferred into the summarized geologic information of amplitude and phase.

4. Effect of a break in the high resistivity horizontal layer

At our request the effect of a break in the high resistivity plate was studied by physical modelling in the Geodetic and Geophysical Research Institute of the Hungarian Academy of Sciences. The structure of the model, its data and the frequency sounding curves can be seen in *Fig. 9.* Moving

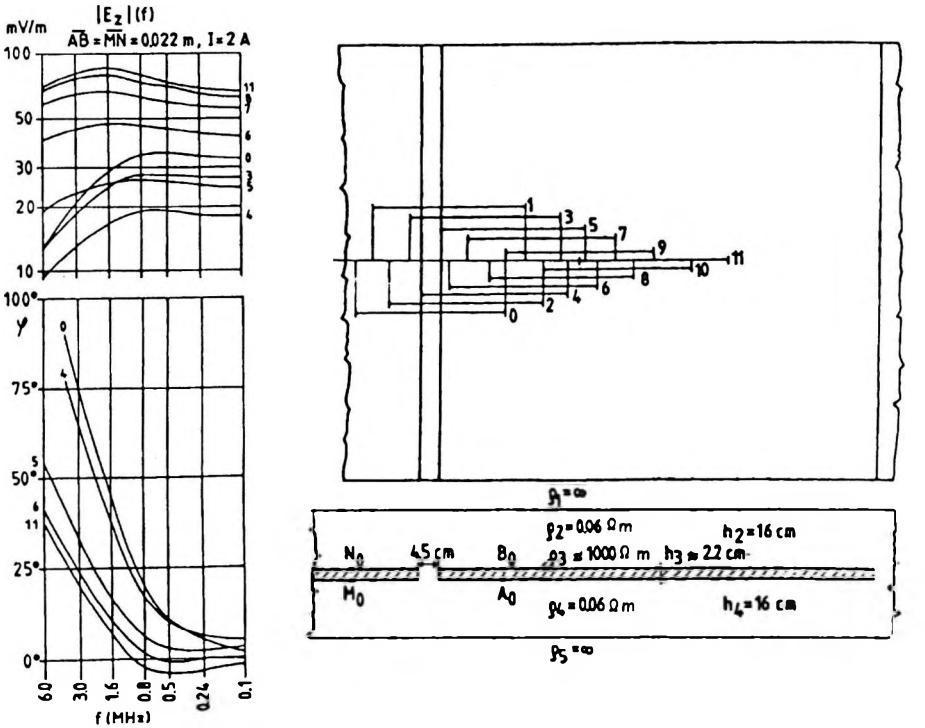

Fig. 9. Amplitude and phase curves obtained by physical modelling using constant vertical transmitter-receiver dipole separation for a break in the high resistivity plate

9. ábra. Konstans távolságú vertikális adó- és vevő-dipólussal végzett fizikai modellezéssel kapott amplitúdó- és fázisgörbék a nagy fajlagos ellnállású lemez megszakadása esetén

from the middle of the plate — station 11— towards the break a strong decrease in the field strength can be observed starting from station 8. A definite change in the position of maximum along the frequency axis takes place only if one of the electrode pairs — either transmitter or receiver dipole — gets into contact with the break.

For arrays passing through the break — stations 4 to 0 — the maximum gets to lower frequencies because of the reduced effective resistivity. The field strength is lowest at station 4 when one of the electrode pairs falls into the break. On crossing the break the field strength increases.

A break in the high resistivity plate has a drastic effect on the phase as well, particularly at high frequencies. Phase curves reflect location better than amplitude curves. Their shape and position depend less on the place of break in the case of an array passing through the break.

Profile curves belonging to a constant frequency are informative too. Profiles for the lowest and highest frequencies are shown in *Fig. 10.* In the

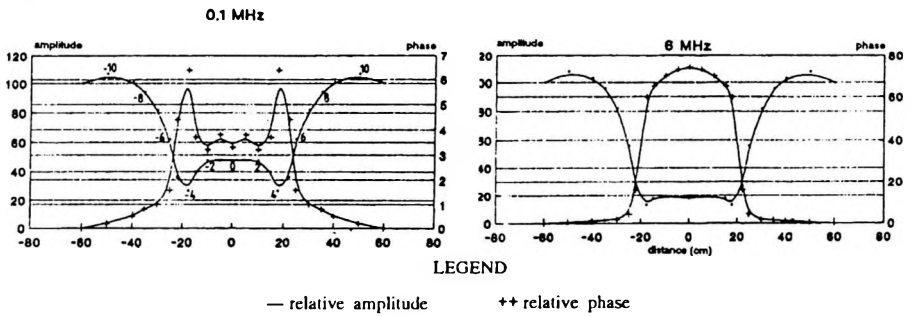

Fig.10. Amplitude and phase profiles for highest and lowest frequencies used in physical modelling

10.ábra. Az amplitúdó és fázis szelvény menti alakulása a fizikai modellezésnél használt legkisebb és legnagyobb frekvencián

Рис. 10. Амплитудные и фазовые кривые при наименьших и наибольших частотах, использовавшихся при физическом моделировании

Рис. 9. Амплитудные и фазовые кривые, полученные при физическом моделировании с постоянным расстоянием между вертикальными передающим и приемным диполями при разрыве в пластине высокого сопротивления

curve for 0.1 MHz reference points of the plotted values are indicated as well. It can be seen that changes caused by the break are larger both in amplitude and phase at high frequency. At the same time the lateral effect is smaller than at lower frequency. For arrays passing through the break, the shape of the curves is different too.

REFERENCES

TAKÁCS E., NAGY J., MÁDAI F. 1986 : Field of vertical alternating current, electric elementary dipole in a layered medium. Geophysical Transactions **32**, 1, pp. 43-56

TAKÁCS E. 1988: In-mine sounding with a buried grounded dipole source. Geophysical Transactions **34**, 4, pp. 343-359

LATERÁLIS INHOMOGENITÁSOK HATÁSA A FELSZÍN ALATTI VERTIKÁLIS ÁRAMDIPÓLUS VERTIKÁLIS ELEKTROMOS ÖSSZETEVŐJÉNEK FREKVENCIASZONDÁZÁSI GÖRBÉIRE

TAKÁCS Ernő

A tanulmány azt mutatja be, hogy az ekvatoriális elrendezésű vertikális elektromos adó- és vevő-dipólussal végzett földalatti frekvenciaszondázásnál hogyan jelentkezik a laterális inhomogenitások hatása.

Az egyszerűsített modellek az alábbiak:

— az adó- és vevő-dipólust összekötő tengelyre merőleges és vele párhuzamos vertikálisan végtelen kiterjedésű réteghatár és lemez,

— a nagy fajlagos ellenállású vízszintes réteg megszakadása az adó- és vevő-dipólust összekötő tengelyre merőlegesen.

Az előbbi esetet numerikus, az utóbbit fizikai modellezéssel vizsgáljuk.

ВЛИЯНИЕ ЛАТЕРАЛЬНЫХ НЕОДНОРОДНОСТЕЙ НА КРИВЫЕ ЧАСТОТНОГО ЗОНДИРОВАНИЯ, ПОЛУЧЕННЫХ ПО ВЕРТИКАЛЬНОЙ ЭЛЕКТРИЧЕСКОЙ КОМПОНЕНТЕ ПОДЗЕМНОГО ВЕРТИКАЛЬНОГО ТОКОВОГО ДИПОЛЯ

Эрнё ТАКАЧ

В работе рассматривается эффект от латеральных неоднородностей в подземном частотном зондировании, выполненном вертикальными экваториальными диполями.

Упрощенными моделями являлись следующие:

— установка направлена вкрест простирания и по простиранию бесконечного вертикального контакта двух сред и такой же пластины,

— разрыв в горизонтальной пластине высокого сопротивления перпендикулярно оси установки.

Первый случай исследуется путем численного, а второй — физического моделирования.

GEOPHYSICAL TRANSACTIONS 1991
Vol. 37. No. 1. pp. 57-73

LITHOPROBE, VANCOUVER ISLAND INTERVAL VELOCITY CASE STUDY

István KÉSMÁRKY* and Zoltán HAJNAL**

A seismic interval velocity study was carried out in the central part of Vancouver Island Line No.1 of the LITHOPROBE project. Independently of other methods, we concentrated on a more accurate estimation of the 'high velocity region', which is probably the most interesting part of the subduction zone.

The main point of our effort was to carry out a series of high precision stacking velocity analyses along the line (including several neighbouring CDPs, similarly to applying 'vertical stacking' prior to velocity analysis), by taking into consideration the dips and curvatures observable on the time section. The interval velocity calculations were based on a 2-D model containing plane and curved dipping interfaces.

Besides interval velocity calculation, the reliability (standard deviation) of the estimates was also strictly controlled. Taking into account the arrival time uncertainties of the individual traces (standard deviation of the remaining trim statics, not decomposable into shot and receiver components), the reliability of the estimated parameters could be calculated via the error propagation law. This theoretical model showed that in spite of the relatively small normal moveouts, the interval velocities could be estimated with appropriate accuracy if 50-150 neighbouring CDPs were considered simultaneously.

The model studies carried out parallely with the data processing clearly showed the practical limits of the accuracy of the interpretation and the achievable lateral resolution.

Keywords: velocity, case studies, LITHOPROBE

* Geophysical Exploration Co., 1065 Budapest, Gorkij fasor 42, Hungary
** University of Saskatchewan, Dept. of Geological Sci, Saskatoon SK, Canada S7N OWO
Manuscript received: 11 October, 1990

1. Introduction

LITHOPROBE, a multidisciplinary earth science research program, is investigating fundamental questions concerning the structure of the lithosphere in Canada [CLOWES et al. 1984]. A part of the program was the Vancouver Island Seismic Project conducted in 1980 to study the subducting oceanic plate and the overriding continental America plate. The principal refraction and reflection lines were shot perpendicular to the continental margin *(Fig. 1)*.

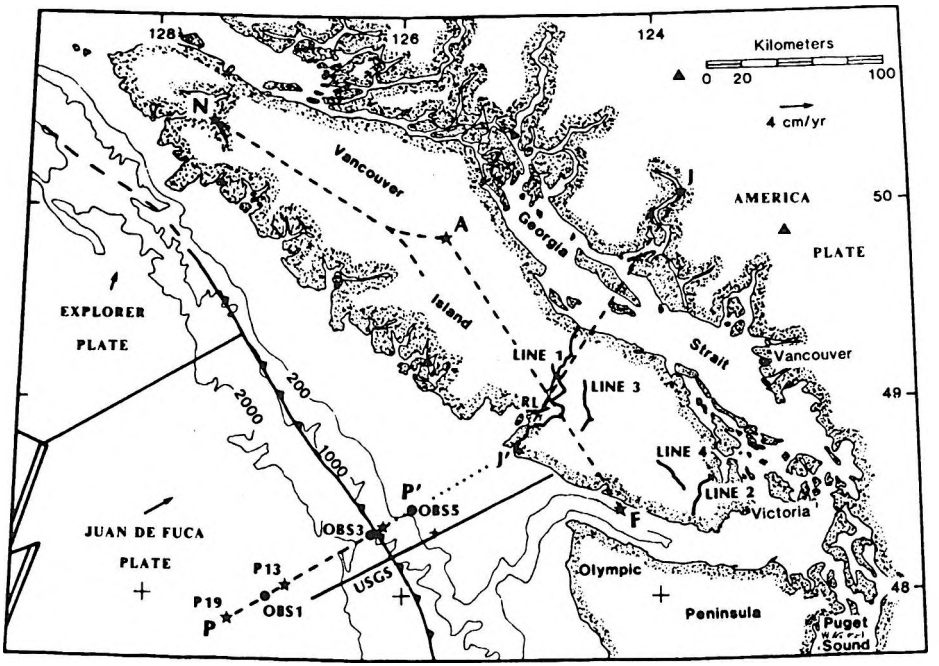

Fig. 1. Map of offshore-onshore study area, with the major survey lines. N-A-F, 'USGS' and P-P'-J'-J are refraction lines (ocean bottom seismographs were applied in the P-J' interval). Lines 1-4 are onshore reflection seismic lines [CLOWES et al. 1984]

1. ábra. A tengeri és szárazföldi kutatási terület térképe a fontosabb vonalakkal. Az N-A-F, USGS és a P-P'- J'-J vonalakon refrakciós mérések történtek (a P-J' szakaszon óceánfenékre helyezett szeizmográfokkal). Az 1-4 vonalakon szárazföldi mérések történtek [CLOWES et al. 1984]

Рис. 1. Карта наземных и морских исследований с основными профилями. По профилям N-A-F, USGS и P-P' - J'-J были выполнены измерения МПВ (на отрезке профиля P-J' - с сейсмоприемниками на дне океана). По профилям 1- 4 выполнены наземные измерения [CLOWES et al. 1984]

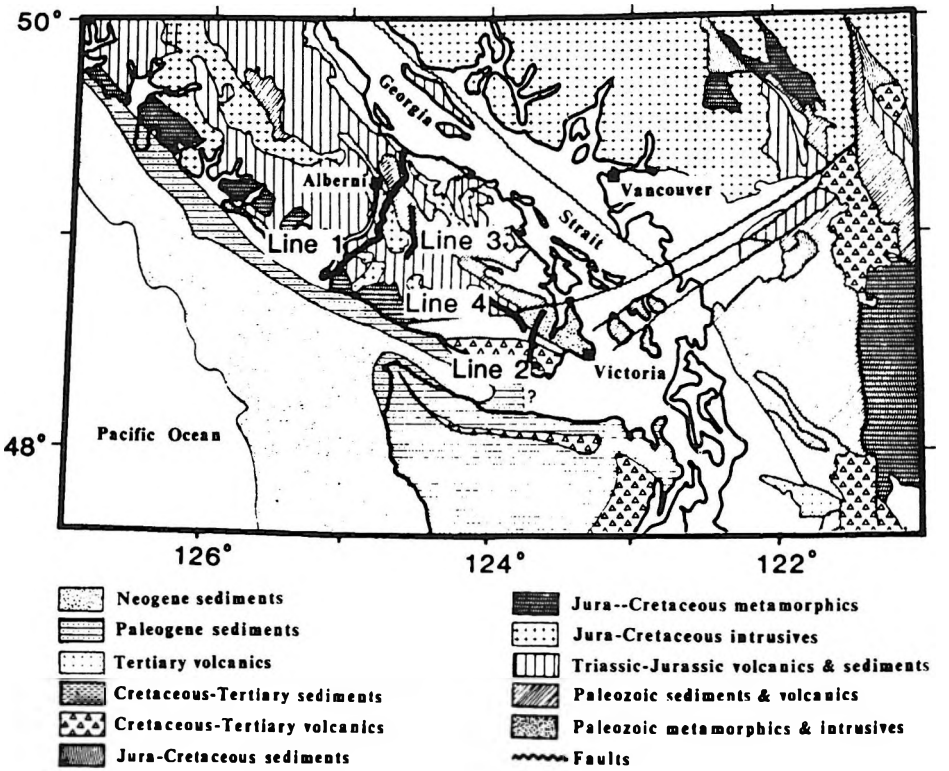

Fig. 2. Map of Vancouver Island survey area describing onshore reflection seismic lines 1-4 [CLOWES et al. 1984]

2. ábra. A kutatási terület Vancouver szigeti részének térképe az 1-4 szárazföldi vonalakkal [CLOWES et al. 1984]

Рис. 2. Карта участка исследований на о-ве Ванкувер с наземными профилями 1-4 [CLOWES et al. 1984]

To study the subduction zone, a special 30-fold VIBROSEIS* section was recorded along Line No. 1 across Vancouver Island using 10.8 km long spread lengths *(Fig. 2).* Additional details of the survey procedures were described by CLOWES [1987].

* Trademark of Continental Oil Co.

A combined interpretation of the region using the described data and additional geophysical information was attempted by SPENCE et al. [1985]. A very high density and velocity (7.7 km/s) rock mass was placed above the subducting plate as a consequence of a gravity high and anomalous refraction arrival times observed along a segment of Vancouver Island *(Fig. 3)*.

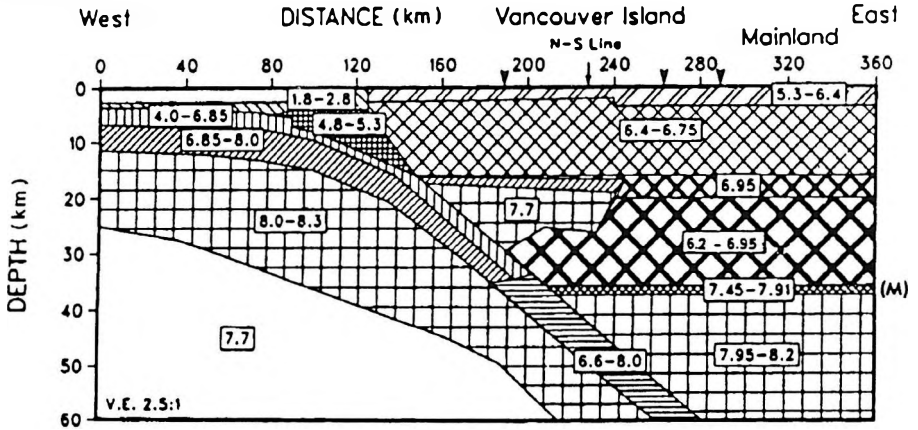

Fig. 3. Structural cross section and regional velocity segments according to SPENCE et al. [1985]

3. ábra. SPENCE és munkatársai által 1985-ben publikált szerkezeti szelvény a feltételezett intervallumsebességekkel

Рис. 3. Структурный разрез, опубликованный Спенсом с сотрудниками SPENCE et al. [1985] с предполагаемыми поинтервальными скоростями

The reflection portion of the data set became available to institutions for reprocessing and interpretation. At the seismic laboratories of the University of Saskatchewan, an interval velocity study was undertaken on a portion of this information covering the central segment of Line 1. This investigation concentrated on establishing a more accurate estimate of the acoustic properties of the high velocity region.

2. Theoretical background

The main point in establishing the reliability of the estimated velocities is quite simple. Assuming identical waveforms roughly positioned along a nearly hyperbolic reflection arrival time curve, the arrival times of these

wavelets can be treated as random variables [AL-CHALABI 1974] due to the effect of noise and some deterministic but unknown effects. The zero offset arrival time t_0 and the stacking velocity v_s can be estimated as the parameters of a hyperbola, fitted to these random arrival times by the least squares method. It is important to note that even the arsenal of the more advanced and more general information theory gives almost the same result as this simple heuristic least squares approach [KÉSMÁRKY 1985].

In the case of hyperbolic arrival times, this statistical model would provide absolutely correct results for noise free traces. In other words this would mean infinite resolving power and complete discrimination between any possible velocities. In practical cases however, the possible effects of the above mentioned 'noise' must be taken into consideration.

Using the data acquisition parameters (cable length, geophone and shot spacing, coverage number, etc.) and the standard deviation of the random arrival time shifts, the standard deviations of the resultant t_0 and v_s parameters can be calculated via the error propagation law [HAJNAL and SERADA 1983 and KÉSMÁRKY 1985]. The results confirm the well known rule of thumb that, in general, the reliability of the stacking velocity quickly deteriorates for depths greater than the cable length. (The relevant formulae can be found in the above mentioned references.)

Neglecting the non-hyperbolic components of the reflection arrival times, the most straightforward way to improve the reliability of stacking velocities would be the application of longer and longer cables. The designer of the LITHOPROBE Vancouver Island survey [CLOWES 1987] employed a cable length (10.8 km) significantly longer than the usual lengths deployed in oil exploration. Once the data acquisition parameters had been fixed, the only way to further improve the reliability of the estimated velocities was to increase the signal to noise ratio by including numerous neighbouring CDPs into the computations or in other words to increase the quantity of input data considered. For example, a conventional velocity spectrum calculated from a single CDP set may show uninterpretable results. A commonly applied practice is the vertical stacking of a group of neighbouring CDP sets, prior to the velocity analysis, which means an averaging of data along the common offset profiles. This process profoundly influences the reliabilities of the estimates. The noise suppression ability of this method and the exact semblance is discussed in the Appendix. The more stable exact semblance function has been used in the following

investigation. Of course, these methods need special care in the case of dipping reflections as will be discussed later.

After obtaining the estimates of the stacking velocity and its standard deviation, the interval velocities and their standard deviations could be calculated [KÉSMÁRKY 1985]. The estimated interval velocities are even more sensitive to the random time shifts. In the case of thin layers the interval velocity estimates become very unreliable and highly correlated. Fortunately the 'high velocity zone' to be examined has significant dimensions. It has roughly a 3000 ms interval in the time section between 4200 and 8800 ms.

Two cases for random time shifts have to be considered:

— The random time shifts have a 'static' nature or, in other words, for a given trace the random shifts are the same for each horizon. Because of these correlated shifts, the hyperbolae fitted to the different arrivals will have the same residual NMO values. This situation influences the estimated interval velocities in a special way: the interval velocity errors of all layers due to this uniform residual NMO will have the same sign. The magnitude of the interval velocity errors will increase with depth since this ambiguous residual NMO becomes larger and larger relative to the NMO itself. There will be a positive correlation between all estimated interval velocities.

— The case of totally random time shifts is more problematic and generally results in much larger interval velocity errors. In this case the random time shifts and the resultant residual NMOs are independent for each horizon. The residual NMO of a given horizon will influence only the two interval velocity estimates below and above the given interface, but a strong negative correlation will exist between them.

An analysis was carried out to find out which extreme case outlined previously is closer to the real situation. First, the trim statics of the upper and lower boundary of the 'high velocity region' were determined. The correlation between the trim statics of the two horizons was quite low, so the hypothesis of the random model was accepted. If these statics were decomposed into shot and receiver components separately, and the resultant components were subtracted from the original trim statics, the residual could be considered as representing the random time shift of the original

reflection arrival model. The estimated standard deviation of the trim statics was 8-10 ms (rather high) for both the upper and lower boundaries. Using only a single 30-fold CDP set, the standard deviation of the interval velocity of the 'high velocity layer' is about 205 m/s standard deviation. The vertical stacking of more and more neighbouring CDP sets is equivalent with the existence of fewer and fewer random time shifts due to the effect of noise suppression. The deviation is inversely proportional to the square root of the number of neighbouring CDP-s involved in the vertical stacking. Consequently, the vertical stacking of 100 neighbouring CDP-s results in ten times smaller deviations. Smaller deviations mean better resolving power and more reliable discrimination between two different hypothetical interval velocities.

3. Data processing

Three zones of Line No. 1 were selected for velocity analysis, shot-points 1323-1438, 1169-1263 and 835-901. These correspond to CDP intervals 50-250, 350-501 and 919-1040 with widths of 8955, 6750 and 3600 meters respectively *(Fig. 4)*.

The velocity analysis using the semblance function (Appendix) was carried out along the dipping horizons *D1* and *E1* of time section 1, interpreted as the top and bottom reflectors of the underplated 'high velocity' layer.

The survey fold is high (86) in zone 1, due to the special acquisition process adopted at the west end of the line. The fold in the central and east zones reached the range of 30-40. The reprocessing of the data set was extended to the time section generation. The top and bottom horizons of the 'high velocity region' were carefully picked. The dips and parabolic curvatures of both horizons were compensated (flattened) by applying appropiate bulk static corrections to the unstacked traces. An iterative process was applied to make certain that each selected dip and curvature resulted in the largest semblance peak in the velocity spectra. Significant curvature was detected only at zone 3. This operation resulted in six separate 'super CDP gathers', one for the upper and one for the lower horizon of each zone for the semblance calculation. The six velocity

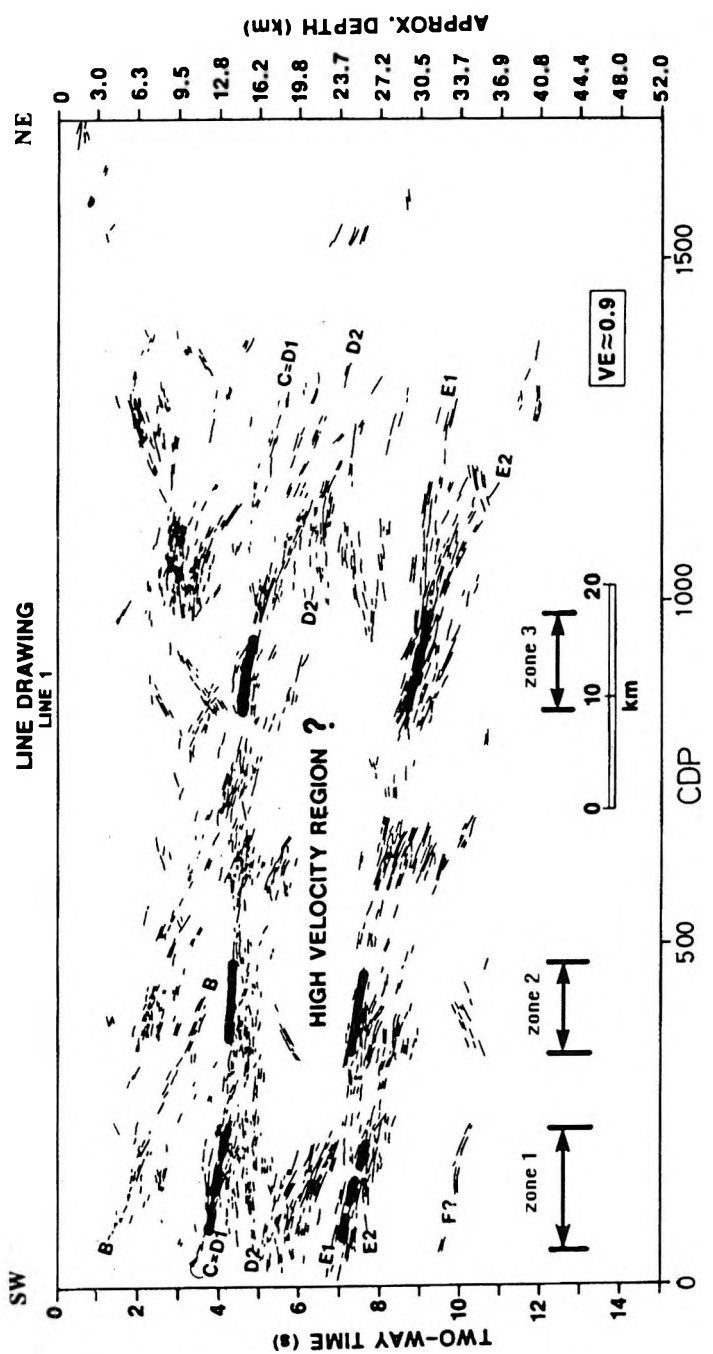

Fig. 4. Simplified time section of Line No.1 [CLOWES 1987]

4. ábra. Az 1-es szeizmikus időszelvény kiértékelhető horizontjainak egyszerűsített képe [CLOWES 1987]

Рис. 4. Упрощенный временный разрез по профилю 1 [CLOWES 1987]

spectra computed from these super gathers were focused to the corresponding six reflection horizon segments.

This manipulation of data introduces errors since the reflection hyperbolae on the neighbouring CDP sets are not identical after compensating for the dip visible on the time section. An analysis examined the errors introduced by this form of data handling, which works similarly to the slant stack, applied to common offset gathers along a certain dip. A simple 2-D model consisting of homogeneous layers divided by dipping and bending interfaces was subjected to the same procedure. The results reveal that these systematic errors are much smaller than a quarter of the dominant wavelength. In this particular case the reflection hyperbolae on the neighbouring CDP profiles were fairly similar. The velocity spectra calculated for the upper and lower horizon of zone 2 and 3 are shown in *Figs. 5* and *6*, respectively.

The unique, well detectable peaks of the velocity spectra of zone 2 are quite convincing in Fig. 5. The velocity spectrum of the upper horizon of zone 3 (in the upper part of Fig. 6) contains a high velocity peak probably related to some uninterpretable interference, so a smaller, more reasonable local maximum has been picked. As zone 1 resulted in uninterpretable stacking velocities, probably due to the more complex subsurface conditions, it was discarded from the case study.

The interval velocity and depth calculations were based on a simple 2-D model containing dipping curved interfaces. The algorithm (recoursive stripping, using iterative calculation of the normal incidence path) is the generalized form of the well-known Dix's formula, described in KREY and HUBRAL [1980]. The curvatures are characterized by a single radius. The input features of the velocity spectra and the time section (t_0 and stacking velocity v_s, the dip and the parabolic term p of the time horizon) and the interpretation results (estimated depth, spatial dip, interval velocity and radius of the reflector) are summarized in *Tables I* and *II*, for zones 2 and 3 respectively.

The t_0 and depth values are related to the center of the zone. The dips and curvatures show characteristic differences in the two zones considered.

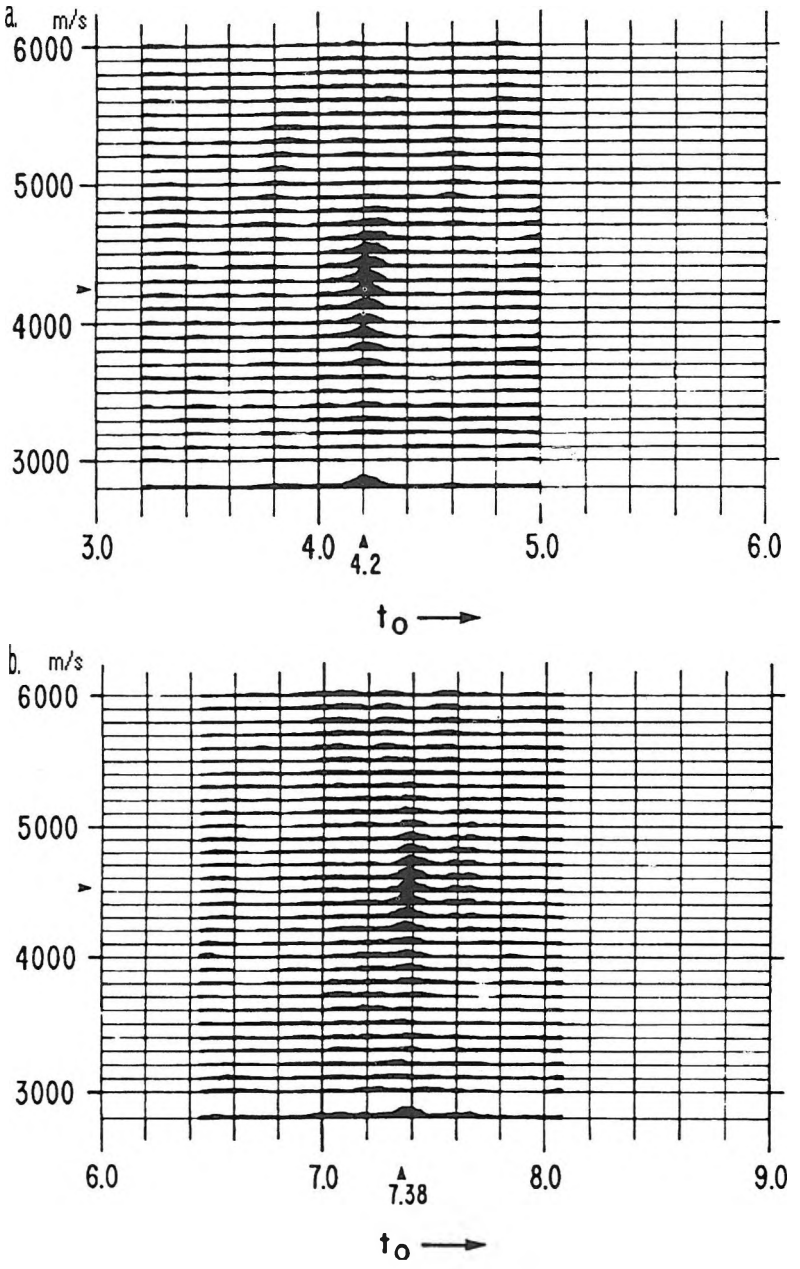

Fig. 5. Upper (a) and lower (b) spectra of zone 2

5.ábra. A 2. zóna felső (a) és alsó (b) horizontjára számított sebességspektrum

Рис. 5. Спектр скоростей для верхнего (a) и нижнего (b) горизонта зоны 2

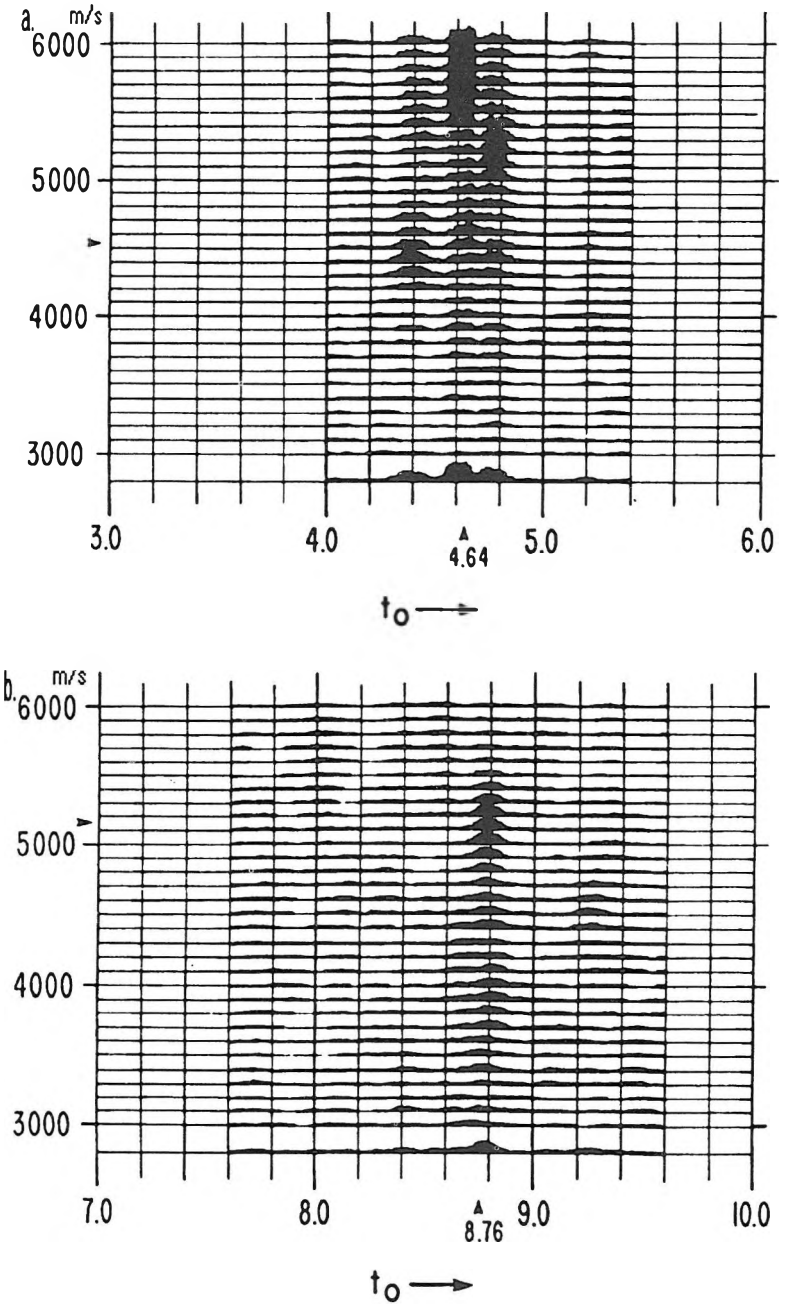

Fig. 6. Upper (a) and lower (b) spectra of zone 3
6. ábra. A 3. zóna felső (a) és alsó (b) horizontjára számított sebességspektrum
Рис. 6. Спектр скоростей для верхнего (a) и нижнего (b) горизонта зоны 3

hor.	input				output			
	t_0	v_s	t_0 dip	term p	depth	v_{int}	dip	curvature
	ms	m/s	ms/m	ms/km^2	m	m/s	degree	1/m
upper	4200	4250	0.0044	0.000	8930	4895*	0.5	0
lower	7380	4550	0.0313	0.000	16750		4.3	0

*Neglecting the dip, the resultant interval velocity would be 4920 m/s.

Table I. Interpretation results for zone 2
I. Táblázat. A 2. zóna kiértékelési eredményei
Табл. I. Результаты интерпретации по зоне 2

hor.	input				output			
	t_0	v_s	t_0 dip	term p	depth	v_{int}	dip	curvature
	ms	m/s	ms/m	ms/km^2	m	m/s	degree	1/m
upper	4640	4550	0.0215	7.472	10600	4905**	10	0.00024
lower	8760	5150	0.0639	1.851	21300		23	0.00006

**Neglecting the curvature, the resultant interval velocity would be 5643 m/s. Neglecting both the dip and curvature, the resultant interval velocity would be 5750 m/s. So, the curvature really gives a significant effect (16-17%)!

Table II. Interpretation results for zone 3
II. Táblázat. A 3. zóna kiértékelési eredményei
Табл. II. Результаты интерпретации по зоне 3

4. Conclusions

The almost identical (~4900 m/s) interval velocities estimated from the reflection seismic data of zones 2 and 3 are much lower than those derived by CLOWES et al. [1984] (7700 m/s). Such a significant difference (2800 m/s) can reliably be detected since the moveout even at the lower horizon is not less than 200 ms and, in principle, the 1-2% relative accuracy of the interval velocity is attainable because of the extensive vertical stacking and the significant thickness of the layer considered. As the standard deviation of the interval velocity estimated by our statistical approach is only about 20 m/s because of the extensive vertical stacking in this particular case, the interval velocity calculated from the velocity

spectrum is in considerable discordance with the prior postulation of a high velocity (7700 m/s) rock mass above the subducting slab. In other words, no reflection seismic evidence of such a high velocity formation at the previously defined depth was found.

Both observational [ODP Leg 110 Scientific Party 1978, PEARCE 1983] and seismic evidence [NELSON et al. 1985a and 1985b] attest that in zones of tectonic convergence, sedimentary strata may be subducted to crustal levels. At these depths, the acoustic properties of these rocks may be highly anomalous, and depend on local effects. Recent drilling investigations [STILLER 1990, KOZLOVSKY 1984] reveal that considerable porosity and fluid content can exist in greater than expected crustal depths. Thus zonal material heterogeneity, with properties comparable to the results of this investigation, can be expected to the considerable depth above the decollment zone of the subducting slab.

The geological ambiguity of this segment of the continental margin is further increased by the reinterpretation by DREW and CLOWES [1990] of the original data set. This new model subdivides the earlier anomalous zone into a four layer structure where two thin low velocity (6350 m/s) and two thick higher velocity layers (7100–7180 m/s) alternate with each other. The average compressional velocity of this complex crustal interval has been significantly reduced although it is still higher than portrayed by the reflection data alone.

The results of this investigation are further supported by the refraction data based model of FOWLER and PANDIT [1990]. This new crustal section explains the relevant refraction arrival time differences by introducing a simple anomalous segment in a portion of the subduction zone itself. The fitting of the existing gravity data to this most recent model of the plate convergence under Vancouver Island requires further investigation.

Acknowledgement

The authors are grateful to Rick Ogloff for his valuable assistance in processing this complex data set.

REFERENCES

AL-CHALABI M. 1974: An analysis of stacking, RMS, average and interval velocities over a horizontally layered ground. Geoph. Prospecting **22**, 3, pp. 458-475

CLOWES R. M., GREEN A. G., YORATH C. J., KANASEWITCH E. R., WEST G. F. and GARLAND G. D. 1984: LITHOPROBE — a National Program for studying the third dimension of geology. Journal of the Canadian Society of Exploration Geophysicists **20**, 1, pp. 23-39

CLOWES R. M. 1987: LITHOPROBE: Exploring the subduction zone of Western Canada. The Leading Edge **6**, 6, pp. 12-19

DREW J. J. and CLOWES R. M. 1990: A reinterpretation of the seismic structure across the active subduction zone of western Canada. G. S. C. Paper 89-13, pp. 115-133

FOWLER C. M. R., PANDIT B. I. 1990: Analysis of CCSS data set I: reflection-refraction data from Vancouver Island continental margin of western Canada. Ed: A. G. Green, Geological Survey of Canada Paper 89-13, pp. 79-91

HAJNAL Z., SERADA I. T. 1983: Maximum uncertainty of interval velocity estimates. Geophysics **50**, p.1790

KÉSMÁRKY I. 1985: High resolution interval velocities. Geophysical Transactions **31**, 1-5, pp. 265-266

KOZLOVSKY Y. A. 1984: The world's deepest well. Scientific American **251**, pp. 98-104

KREY T., HUBRAL P. 1980: Interval velocities from seismic reflection time measurements. (SEG publication)

NELSON K. D., ARNOW J. A., MCBRIDE J. H., WILLEMEN J. H., HUANG J., ZHENG L., OLIVER J. E., BROWN L. D. and KAUFMAN S. 1985a: New COCORP profiling in the southeastern United States. Part I: Late Paleozoic suture and Mesozoic rift basin. Geology **13**, pp. 714-718

NELSON K. D., MCBRIDE J. H., ARNOW J. A., OLIVER J. E., BROWN L. D. and KAUFMAN S. 1985b: New COCORP profiling in the southeastern United States. Part II: Brunswick and east coast magnetic anomalies, opening of the north-central Atlantic Ocean. Geology **13**, pp. 718-721

ODP Leg 110 Scientific Party 1987: Expulsion of fluids from depth along a subduction zone decollment horizon. Nature **326**, pp. 785-799

PEARCE J. A. 1983: Role of the sub-continental lithosphere in magma genesis of active continental margins. *in* C. J. Hawkesworth and M. J. Norry, eds.: Continental basalts and mantle xenoliths. Shiva, Nantwich pp. 230-249

SPENCE G. D., CLOWES R. M., ELLIS R. M. 1985: Seismic structure across the active subduction zone of Western Canada. Journal of Geophysical Research **90**, B8, pp. 6754-6772

STILLER M. 1990: 3-D Vertical incidence seismic reflection survey at the KTB location, Oberpfalz: Planning acquisition and preliminary results. Paper presented at the Fourth International Conference on Deep Seismic Reflection Profiling, Bayreuth, FRG, September 4-7.

APPENDIX

Noise suppression properties of the correct semblance and the semblance after vertical stacking in the common offset domain

The semblance function has the following, well-known form:

$$S = \frac{\sum_{i}^{I}\left(\sum_{j}^{J}\sum_{k}^{K} x_{ijk}\right)^2}{JK\sum_{i}^{I}\sum_{j}^{J}\sum_{k}^{K} x_{ijk}^2} \qquad \text{(A1)}$$

where x_{ijk} represents a sample of a given seismic trace (after NMO correction), index i runs from 1 to I along a time window, offset index j runs from 1 to the coverage number J, and CDP index k runs from 1 to K. Our ultimate aim is to improve the resultant spectra by using a larger number of CDPs.

The following formula is generally used if vertical stacking is carried out in the 'common offset' domain prior to the calculation of the semblane:

$$S' = \frac{\sum_{i}^{I}\left(\sum_{j}^{J}\sum_{k}^{K} x_{ijk}\right)^2}{J\sum_{i}^{I}\sum_{j}^{J}\left(\sum_{k}^{K} x_{ijk}\right)^2} \qquad \text{(A2)}$$

Since the numerators are the same in both cases, it is enough to deal with the denominators to show the difference. The behaviour of the two functions is compared when the input traces x_{ijk} contain only pure uncorrelated 'white' noise n of zero mean with standard deviation σ:

$$x_{ijk} = n_{ijk} \qquad \text{(A3)}$$

The expected value of the denominator of eq. (A1) is:

$$E(\text{denominator of } S) = IJ^2K^2\sigma^2 \quad \text{(A4)}$$

$$E(\text{denominator of } S') = IJ^2K\sigma^2 \quad \text{(A5)}$$

In contrast with (A4), the expected value of the denominator of eq. (A2) is:

It could easily be demonstrated that in the case of pure signal $x_{ijk}=s_i$, the two functions S and S' have identical unit values. Since in the previous case of pure noise the denominator of S is K times larger than that of S', it can be concluded, that the noise suppression characteristics of S is more favourable than that of S'. Unfortunately, the calculation of S needs significantly more computation time.

LITHOPROBE, INTERVALLUM SEBESSÉG MEGHATÁROZÁSI ESETTANULMÁNY VANCOUVER SZIGETÉN

KÉSMÁRKY István és HAJNAL Zoltán

A LITHOPROBE projekt (kanadai multidiszciplináris litoszférakutatási program) keretében intervallumsebesség meghatározást végeztünk a Vancouver-szigeti 1-es számú szeizmikus vonal középső szakaszán. Elsődleges célunk a feltételezett "nagysebességű összlet" minél pontosabb, más módszerektől független megismerése volt, mely a szubdukciós zóna modelljének legérdekesebb, legvitatottabb része.

A feladatmegoldás lényege, hogy nagypontosságú szeizmikus sebességanalízisek sorozatát készítettük el a vonal mentén a vertikális stackinghez hasonlóan számos (a szokásosnál jóval több) szomszédos CDP csatorna csoport bevonásával, figyelembe véve az időszelvényen is látható horizontok görbületét és dőlését. Az intervallumsebesség becslést dőlt és görbült réteghatárokat tartalmazó kétdimenziós modell alapján végeztük.

Az intervallumsebesség számítása mellett a becslések megbízhatóságának (szórásának) meghatározását is elvégeztük. Az egyes csatornákon mért beérkezési idők hibáinak (a számított maradék statikus tolások geofonponti és robbantóponti komponensre nem bontható részének) szórásából, a hibaterjedési törvény alapján számítottuk a becsült intervallumsebességek szórását. Az elméleti modell alapján a viszonylag kis moveout-ok ellenére is megfelelő pontosság volt elérhető 100-150 szomszédos CDP figyelembe vétele esetén. Eredményeink nem támasztották alá a "nagysebességű összlet" létezését.

Az adatfeldolgozással párhuzamosan elvégzett modellezés világosan mutatta a kiértékelés pontosságának és az oldalirányú felbontás elvi határait.

ОПРЕДЕЛНИЕ ПОИНТЕРВАЛБНЫХ СКОРОСТЕЙ НА О-ВЕ ВАНКУВЕР, ПРОЕКТ ЛИТОПРОБ

Иштван КЕШМАРКИ, Золтан ХАЙНАЛ

В рамках проекта ЛИТОПРОБ (канадская междисциплинарная программа по исследованию литосферы) были выполнены определения поинтервальных скоростей на среднем отрезке сеймического профиля 1 на о-ве Ванкувер. Первичная цель заключалась в как можно более точном, не зависимом от других методов, изучении предполагаемой "толщи высоких скоростей", представляющей наиболее интересную и наиболее спорную часть модели зоны субдукции.

Сущность решения задачи заключалась в том, что была выполнена серия высокоточных анализов сейсмических скоростей вдоль профиля, подобно стэкингу, с объединением многочисленных (намного больше обычного) соседних трасс CDP, учитывая кривизну и наклон горизонтов, наблюдаемых на временных разрезах. Оценка поинтервальных скоростей была проведена на основании двумерной модели с наклонными и искривленными горизонтами.

Помимо расчета поинтервальных скоростей была также выполнена оценка надежности (дисперсии) полученных данных. По разбросу ошибок вступлений по конкретным трассам (той части расчетных остаточных статических смещений, которые не могут быть разложены на компоненты при взрывпункте и сейсмоприемнике) на основании закона распространения ошибок были определены дисперсии полученных поинтервальных скоростей. На основании теоретической модели, несмотря на сравнительно малые значения moveout -ов при объединении 100-150 соседних CDP можно было достичь надлежащей точности. Полученными нами результатами не подтверждается наличие "толщи высоких скоростей".

При моделировании, выполненном одновременно с обработкой данных, четко были выявлены принципиальные пределы точности интерпретации и латеральной разрешающей способности.

GEOPHYSICAL TRANSACTIONS 1991
Vol. 37 . No. 1. pp. 75-89

THE INFLUENCE OF SEA-LEVEL CHANGES ON RESERVOIR DEVELOPMENT ALONG PASSIVE MARGINS

Tom I. KILÉNYI*

In passive margin settings the development of reservoirs is governed largely by the combination of sea-level changes and sediment supply. Three cases are compared, where the overall setting is similar, i.e. a thick sequence of seaward prograding sediments yet the development of the reservoirs is very different. The late Tertiary Nile Delta was exposed to subaerial erosion during the Messinian Salinity Crisis and a system of braided river channels developed on the delta front and its seaward extension. The sands filling these channels are important reservoirs today. In the Duala-basin, Cameroon, two periods of massive sea-level falls in the late Cretaceous and Oligocene initiated turbidites and the associated channel fills and fans act as resevoirs. In the offshore Tarfaya Basin, Marocco, during Jurassic times relatively stable sea levels resulted in a prograding sediment prism. A carbonate fringe developed along the outer margin of the shelf which acted as a reservoir trapping the hydrocarbons derived from Cretaceous sediments further offshore.

Keywords: sea-level, reservoirs, offshore, seismic surveys, Africa, hydrocarbons

1. Introduction

In the last two or three decades hydrocarbon exploration has shifted increasingly towards offshore areas, principally towards the margins of continents, or rather towards the accretionary sediment prisms that extend seawards from these margins . While the accepted plate tectonic classifica-

* GECO - PRAKLA, The GECO Centre, Knoll Rise, Orpington, Kent BR6 0XG England
Manuscript received: 16 November, 1990

tions are undoubtedly useful in recognizing and classifying hydrocarbon habitats it seems that sea level changes have a decisive influence on the development of reservoirs and the resulting plays. In essence we will be considering passive margins which are, on the whole, characterized by thick, seaward prograding sediment prisms, usually very little disturbed by tectonism, unless salt tectonics is involved. In this context deltas and shelves are very similar, the difference is in the concentration of the sediment supply and direction of growth. Along the west coast of Africa, for example, in many places it is possible to look at individual seismic sections extending seawards from the shore; these sections look exactly like a longitudinal section of a typical delta and yet sections on either side will show an identical picture for tens or hundreds of kilometres. Furthermore in some inland rift related basins, or other basinal depressions, similar accretionary sediment prisms can be seen and the similarity is not related to the nature of the plate margin (if any) underlying it, but to factors such as paleotopography, sediment supply, sea level changes, etc.

In this paper we will attempt to show the influence of sea level changes in the development of accretionary sediment prisms and their implications for hydrocarbon exploration. Since changes in sea level and sediment supply have a major influence on coarser detrital sediments, it is the development of reservoirs that will mainly be influenced by these factors. In the following pages three examples will be examined in some detail, in each case the behaviour of sea level relative to the seafloor is different.

2. Rapid sea-level drop — the Messinian of the Nile Delta

The Nile Delta is a large, northwards prograding sediment pile dating from the late Eocene; it is still actively depositing sediments along its rim in the Mediterranean (*Fig. 1*). The delta did not remain static during the Tertiary: it seems that in early Tertiary times it entered the Mediterranean far west of its present delta cone. In recent years gas has been discovered in significant quantities both on and offshore in the upper Miocene Abu Madi Formation and, consequently, this formation has received a lot of attention. In spite of this the interpretation of the formation both on the seismic and in the wells is fraught with problems.

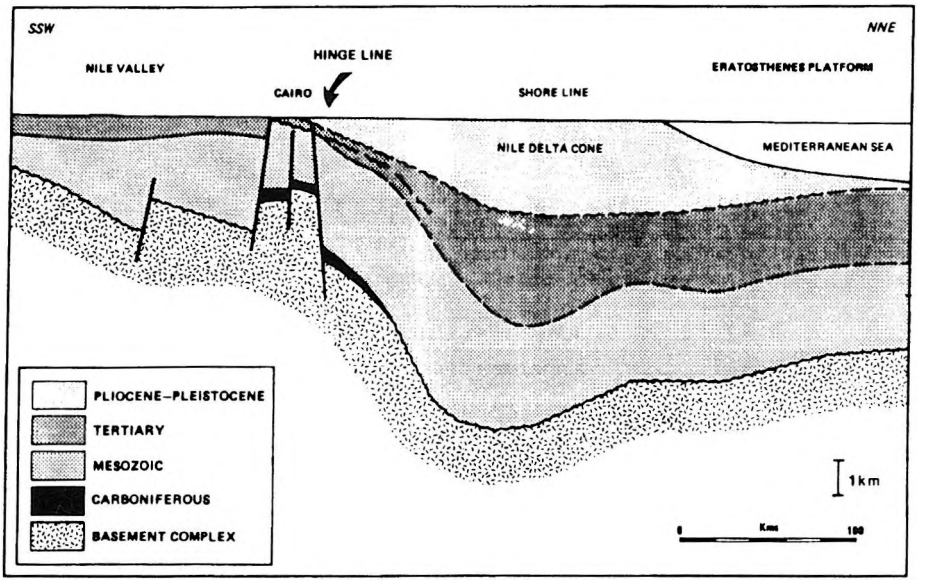

Fig. 1. Schematic longitudinal section along the Nile Delta
1. ábra. Vázlatos hosszanti szelvény a Nílus-delta mentén
Рис. 1. Схематический разрез вдоль дельты Нила

The late Tertiary (Miocene to recent) stratigraphy of the Nile Delta can be seen in *Fig. 2.* The Sidi Salim Formation (Middle Miocene) consists of marine shales and subordinate sandstones up to 1500 m thick; the shale is overpressured and produces intensive diapirs in places. The Upper Miocene Messinian rests with erosional unconformity on the underlying Sidi Salim shales. Three formations are recognized, the Girst being the Qawasim Formation at the base, up to 1200 m thick, consisting of a complex succession of sandstones, conglomerates and interbedded shales. The lithological characteristics point to an alluvial fan type of depositional environment. Next in the succession is the thin Rosetta Formation consisting of anhydrite and salt followed by the Abu Madi Formation, up to 460 m thick, but generally only half of this figure. Lithologically, sandstone and conglomerates dominate the Formation with some subordinate mudstones. The post-Miocene sequence is dominated by marine shales and sands. The Messinian section has been described as having been deposited either in a deep-sea turbidite/fan environment or in a sub-aerial sabkha type setting.

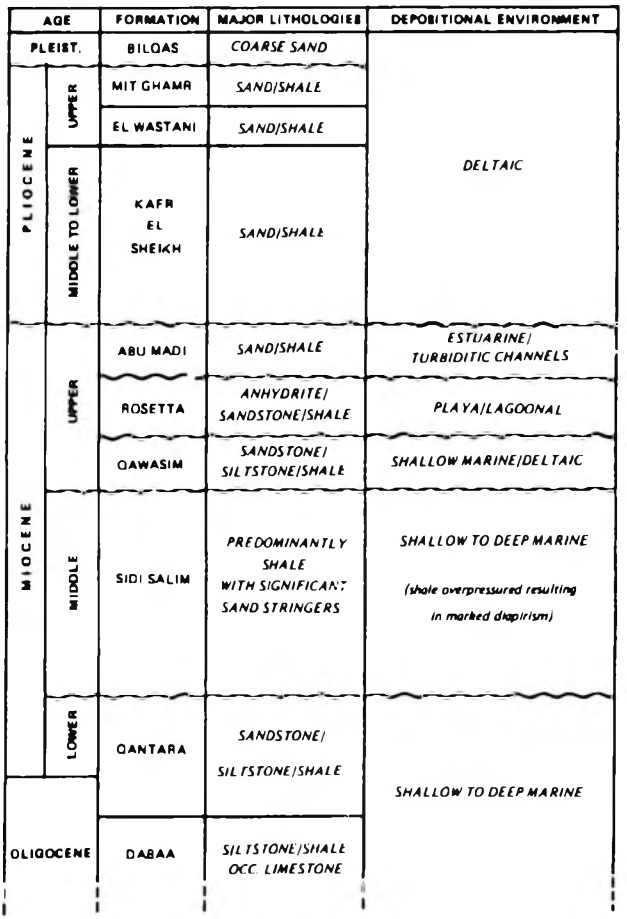

Fig. 2. The stratigraphy of the Nile Delta

2. ábra. A Nílus-delta sztratigráfiája

Рис. 2. Стратиграфия дельты Нила

We believe the seismic evidence supports the Sabkha type environment of deposition.

The three consistent formations of the Messinian are widely distributed over the Delta. Their contacts — either with each other, or with the underlying sequence — are erosive (*Fig. 3*). Channelling is very widespread in the Qawasim and Abu Madi formations but the amplitude (width) of the channels seems to be small and there are numerous, often parallel channels which are seen to be meandering, splitting and uniting when plotted on a map. Furthermore the channels can be grouped together according to their trend (*Fig.4*) and these groups of channels overlap each other indicating their different relative ages. Both the Qawasim and the Abu Madi Formations show this pattern.

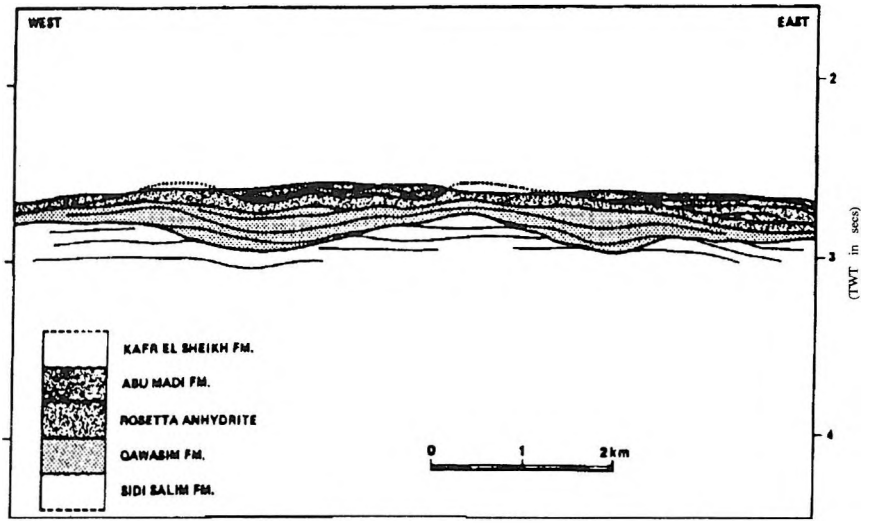

Fig. 3. Geoseismic section of the Messinian of the Nile Delta

3. ábra. A Nílus-delta messiniai emeletet képviselő szakaszának szeizmikus időszelvényét jellemző vázlat

Рис. 3. Геосейсмический разрез мессиния в дельте Нила

The environmental interpretation is, in our view, unequivocal. During the Messinian Salinity Crisis the Mediterranean became separated from its source of supply, the Atlantic Ocean, and the inland sea rapidly lost most of its water due to the high rate of evaporation. As a consequence a very deep depression developed, the floor of which contained hypersaline lakes, while alluvial fans and braided river systems supplied clastic sediments. The proto-Nile was probably the largest source of sediment of the Messinian Mediterranean depression and as a consequence a vast amount of coarse detrital sediments accumulated in this interval in the Nile delta area.

Similar sand rich deposits can therefore be expected in the Messinian not only in the Mediterranean, but also in the other associated inland sea remnants of Tethys, such as the Black Sea, the Caspian Sea, etc.

3. Moderate sea-level drop — Offshore Cameroon , West Africa

While in the previous example the drastic sea-level drop resulted in a complete change in the enviroment of deposition from relatively deep water

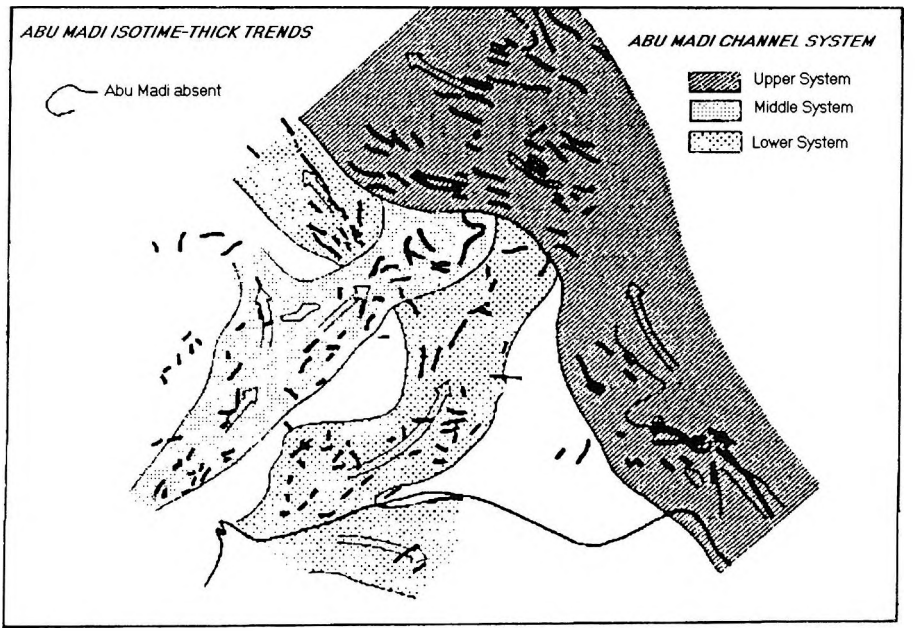

Fig. 4. Channel systems within the Abu Madi Formation, Messinian, Nile Delta
4. ábra. A messiniai Abu Madi formáción belüli csatorna-rendszer, Nílus-delta
Рис. 4. Система каналов в свите Абу Мади, мессиний, дельта Нила

marine to fluvial/sabkha type, in the following case the sea level drop did not result in a change to sub-aerial conditions, it simply rejuvenated the sediment supply in the area resulting in the development of turbidite channels and fans.

The offshore part of Cameroon (*Fig. 5.*) is the northern extension of the West African Salt Basin and is a typical marginal salt basin with up to 6000 m of Cretaceous and Tertiary sediment. The development of the westward prograding sediment prisms began in the early Cretaceous rifting phase with non-marine, lacustrine, fluvial and hypersaline deposits (Mundeck Formation, *Fig.6).* With the beginning of the opening of the south Atlantic ocean drifting commenced in the Cenomanian and from this period to the present day a dominantly clastic sediment prism has gradually been prograding westwards. During the evolution of this sequence of sediments the combination of global sea-level changes and local subsidence rates resulted in two main periods of marked sea-level drops, one in the late

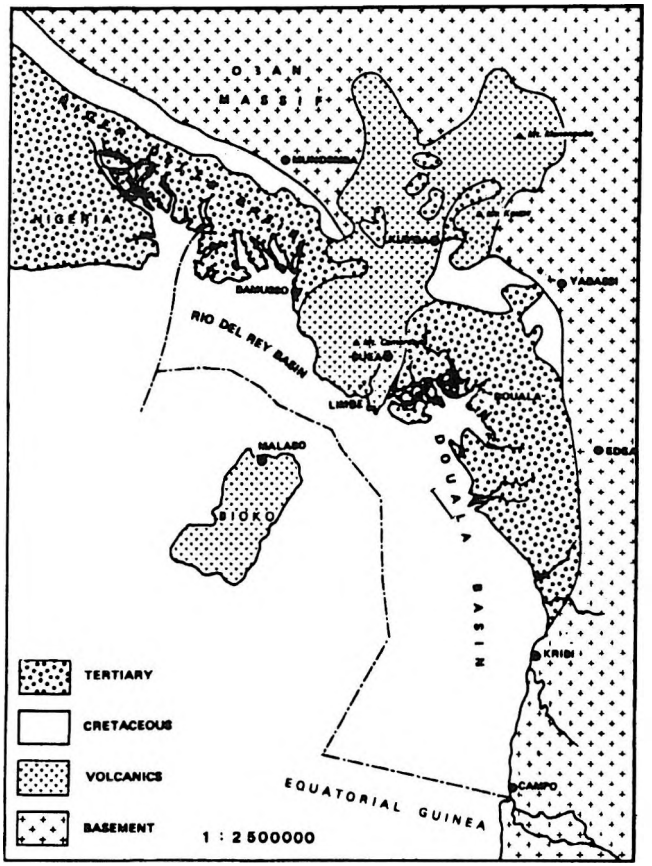

Fig. 5. Sketch map of the geology of the Douala Basin, Cameroon

5. ábra. A kameruni Douala-medence földtani felépítésének vázlata

Рис. 5. Схематическая карта геологии бассейна Дуала

Cretaceous (particulary in the Maastrichtian) and one in the Oligocene. As there are significant oil, gas and condensate accumulations associated with the sands accumulated during these sea-level low-stands it is important to discuss their origin.

Both the evidence of the seismic and wells suggest strong turbidite activity during these periods. This is seen on the seismic in a variety of ways: in the late Cretaceous Logbaba Formation a package of high amplitude reflectors marks the sand rich sequence within which obvious channelling and mounds can be seen *(Fig. 7.)*. Interpretation of the channel features presents no problem but the mound like features may be interpreted either as sand lobes, which are less compacted than the shale surrounding them, or the surface of the 'mounds' may be an erosion surface and one is,

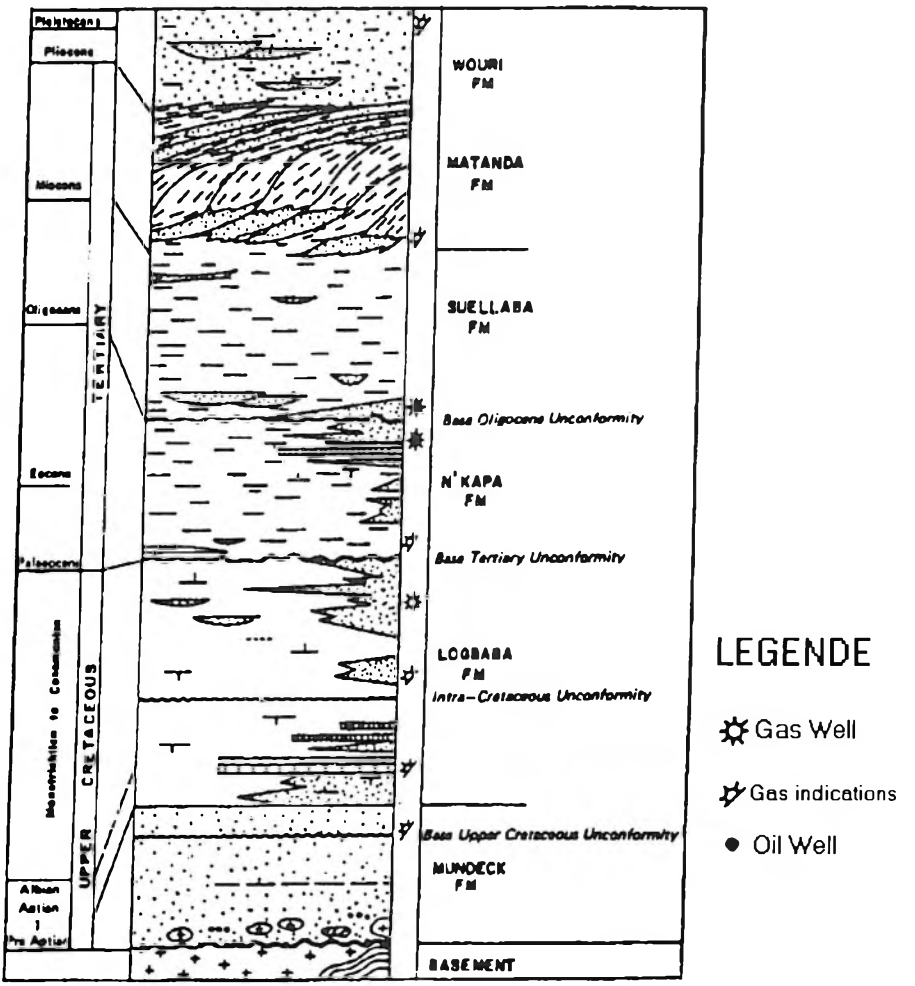

Fig. 6. The stratigraphy of the Douala Basin
6. ábra. A Douala-medence sztratigráfiája
Рис. 6. Стратиграфия бассейна Дуала

in fact, looking at a corrugated surface. We tend to favour the first explanation on the basis of seismic characteristics. During the Oligocene a second marked sea-level low stand occurred. The effect of this is seen in very deep channels cut into the shelf by the turbidity currents and further

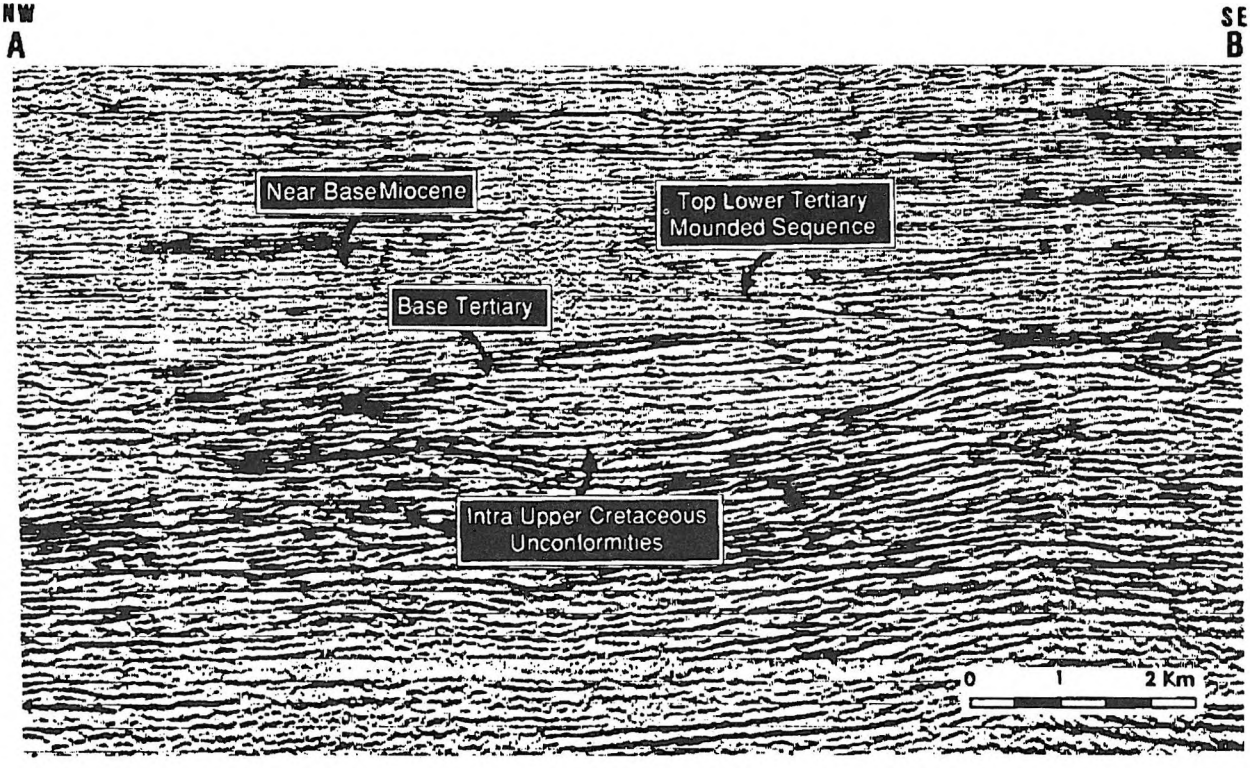

Fig. 7. Seismic section, offshore Douala Basin, showing late Cretaceous and early Tertiary mounded sequences

7. ábra. Szeizmikus szelvény a tengeri Douala-medencéből, felsőkréta és kora harmadkori "buckás" szekvenciával

Рис. 7. Сейсмический профиль, прибрежный бассейн Дуала, с волнистыми верхнемеловой и нижнетретичной толщами

offshore sand lobes forming mounded sequences. It seems that the Oligocene sea-level drop was more drastic than the late Cretaceous one judging by the depth to which, in the case of the Oligocene channels, could reach several hundred metres. The axis of channels in both periods followed more or less the same lines, indicating that the main topography of the basin has remained more or less stable since Cretaceous times.

4. Stable sea-level — Offshore Tarfaya Basin, Morocco

In this particular example only the Jurassic shelf deposits are considered; from the early Cretaceous onwards continuous sea-level low stand produced deep cutting turbidity current channels, very similar to those described in the case of the offshore part of Cameroon.

During Jurassic times the sea level remained remarkably stable or perhaps it is more correct to say that subsidence, sediment accumulation and sea level changes stayed in the same relationship. As a consequence a thick, strongly seaward prograding sediment prism built up, the main accretion direction being lateral rather than vertical (*Fig. 8.*). Even so a total

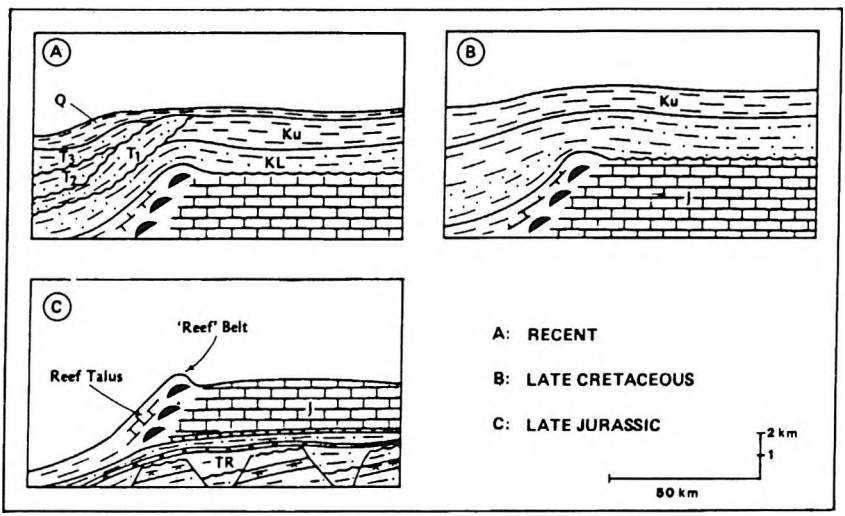

Fig. 8. Schematic geoseismic section across the offshore Tarfaya Basin, Marocco

8. ábra. A tengeri Tarfaya-medencét harántoló szeizmikus időszelvényt jellemző vázlat

Рис. 8. Схематический геосейсмический разрез через прибрежный бассейн Тарфайя, Марокко

thickness of some 3000 metres of Jurassic sediments accumulated consisting of finer grained clastics and some carbonates.

Along the shelf edge a 'carbonate bank' developed which kept pace with both the seaward migration of the shelf edge and also with the vertical accretion of the shelf. On the landward side of the carbonate bank almost 'backreef' like conditions developed, i.e. very shallow water with perhaps increased salinity in which dolomites and occasional anhydrite layers were deposited. On the seaward side the very steeply sloping seafloor was covered with carbonate debris from the bank above. During the early Cretaceous sea level low-stand organic rich shales were deposited off the Jurassic shelf while on the shelf itself little or no sedimentation took place.

From the point of view of hydrocarbon exploration the carbonate banks provide the only acceptable reservoirs, the rest of the Jurassic (and later) sediments being mainly shales.

5. Conclusions

From the three examples given above it seems that relative sea-level movements during the evolution of prograding sediments prisms have a decisive influence on the development of reservoirs.

In the case of the Messinian of the Nile Delta (the first example discussed above) the drastic drop in sea level caused by the dessication of the Mediterranean, resulted in a complete change of the environment of deposition. Braided streams discharging into sabkha plains took the place of deep marine environments. The sands are largely channel fills although sheet sands and alluvial fans can also be expected.

The recognition of sand rich horizons on the seismic is not always easy, although the channel-like features are easy to see (Fig. 3); even so it is by no means certain that these are filled with sand. Sealing of the reservoir may be provided either by locally developed anhydrite or, more regionally, by the deep marine shales that follow the period of basin dessication. This type of situation has so far only been described for the Mediterranean but it could be expected to have occurred in other remnant Tethyan basins such as the Black and Caspian Seas.

The second example discussed in this paper concerned a much more common occurrence: turbidite channels and fans which developed in re-

sponse to periodic sea-level low stands. The effect of these was a periodic rejuvenation of the area of sediment source and consequent increase in sediment supply. The course of the channels/fans tends to remain the same through time as the basic bathymetry of the Atlantic type marginal sag basins tends to remain unchanged. From a hydrocarbon exploration point of view these types of reservoirs are fairly easy to identify on seismic. The sands are either in channel fills or in large scale mounds, and show high amplitude reflections. The main problem seems to be the recognition of the trapping mechanism. If salt tectonics affects the reservoir the structural traps are easy to identify. In most case, however, the traps are stratigraphic and the updip sealing of channel fills or mounds is not easily ascertainable on seismic sections.

The third example, the carbonate bank shelf edge of the Tarfaya Basin, offshore Morocco, is also a widespread setting along passive continental margins. The high porosity carbonate banks could provide excellent reservoirs but there are a number of problems associated with this type of trapping situation. In the Tarfaya Basin the source of the hydrocarbons is the thick early Cretaceous shale sequence which was deposited downslope from the Jurassic shelf edge in deep water. Due to the rapid burial of these shales hydrocarbon generation started in late Cretaceous times and peak generation was reached in the early Tertiary. Strong turbidity flows started eroding into the Jurassic shelf soon after that and the carbonate shelf edge was bared of cover, left with very little seal or even completely eroded away. The trapped oil in many cases migrated away and the presence of heavy or dead oil in these reservoirs supports this view. Only in areas in which a thick cover of sealing shales remained in place can one hope for significant hydrocarbon discoveries.

BIBLIOGRAPHY

BEHRENS M., SIEHL J. 1982: Sedimentation in the Atlas Gulf I: Lower Cretaceous clastics. *in*: Geology of the N. W. African Continental Margin, ed. Von Rad, V., Hinz K., Sarnthein H. and Seibold E., pp. 427-438

BOSSELLINI A. 1984: Postgradational geometrics of carbonate platforms: examples from the Triassic of the Dolomites, Northern Italy. Sedimentology **31**, pp. 1-24

BROWN Jnr. L. F., FISHER W. L. 1977: Seismic stratigraphic interpretation of depositional systems: examples from Brazilian rift and pull-apart basins. A. A. P. G. Memoir **26**, pp. 213-248

BROWN L. F., FISHER W. L. 1980: Interpretation and petroleum exploration. A. A. P. G. Continuing Education Course Note Series 16

BUBB J. N., HATLELID W. G. 1977: Seismic stratigraphy and global changes of sea level. Part 10: Seismic recognition of carbonate buildups. A. A. P. G. Memoir **26**, pp. 185-204

ELLIOT T. 1986: Deltas. *in*: Sedimentary environmemts and facies. Second edition. ed. Reading H. G., Blackwell. Chapter **6**, pp. 113-154

ELLIS P. G., MCLAY K. R. 1988: Listric extensional fault systems—results of analogue model experiments. Basin Research **1**, pp. 55-70

GIBBS A. D. 1984: Structural evolution of extensional basin margins. J. Geol. Soc. London **141**, pp. 609-620

HINZ K., DORSTMANN H., FRITSCH J. 1982: The continental margin of Morocco: Seismic sequences, structural elements and geological development. *in*: Geology of the N. W. African Continental Margin, ed. Von Rad V. Hinz K., Sarnthein H., Seibold E. pp. 34-60

HUBBARD R. J. et al 1987: Depositional sequence mapping to illustrate the evolution of a passive continental margin. *in*: Seismic Stratigraphy II, ed. Berg O. R. and Woolverton D. G., A. A. P. G. Memoir **39**, 93-112

JAMES N. P. 1979: Facies Models II. Reefs. *in*: Facies models, ed. Walker R. G., Geoscience Canada Reprint Series **1**, pp. 121-132

JOHNSON H. D., STEWART D. J. 1982: The role of clastic sedimentology in the exploration and production of oil and gas in the North Sea, Shell U. K. Exploration and Production, London

KINGSTON P. R., DISHROON C. P. and WILLIAMS P. A. 1983: Global basin classification system. A. A. P. G. Bull. **67, 12**, pp. 2175-2193

MACURDA Jnr. D. B. 1987: Listric faults, offshore Morocco. *in*: Atlas of Seismic Stratigraphy Volume 2. ed. Bally A. W., A. A. P. G. Studies in Geology 27

MITCHUM Jnr. R. M. 1977: Seismic stratigraphy and global changes of sea level. Part 11. Glossary of terms used in seismic stratigraphy. A. A. P. G. Memoir **26**, 205-212

MITCHUM Jnr. R. M., VAIL P. R. 1977: Seismic stratigraphy and global changes of sea level. Part 7: Seismic stratigraphic interpretation procedure. A. A. P. G. Memoir **26**, 135-144

MITCHUM Jnr. R. M., VAIL P. R. and SANGREE J. B. 1977: Seismic stratigraphy and global changes of sea level. Part 6: Stratigraphic interpretation of seismic reflection patterns in depositional sequences. A. A. P. G. Memoir **26**, pp. 117-134

MITCHUM Jnr. R. M., VAIL P. R. and THOMPSON S. 1977: Seismic stratigraphy and global changes of sea level. Part 2: The depositional sequence as a basic unit for stratigraphic analysis. A. A. P. G. Memoir **26**, 53-62

NEIDELL N. S. et al. 1987: Depositional sequence mapping as a technique to establish tectonic and stratigraphic framework and evaluate hydrocarbon potential on a passive continental margin. *in*: Seismic Stratigraphy II, ed. Berg O. R. and Woolverton D. G., A. A. P. G. Memoir **39**, pp. 93-116

RANKE V., VON RAD V., WISSMANN G. 1982: Stratigraphy, facies and tectonic development of the On- and Off-shore Aaiun-Targaya Basin. A review. *in:*

Geology of the N. W. African Continental Margin, ed. Von Rad V., Hinz K. Sarnthein H. and Seibold E., 86 p.

READ J. F. 1985: Carbonate platform facies models. The Am. Assoc. Pet. Geol. Bull. **69**, 1, pp. 1-21

SANGREE J. B. and WIDMIER J. M. 1977: Seismic stratigraphy and global changes of sea level. Part 9: Seismic interpretation of clastic depositional facies. A. A. P. G. Memoir **26**, pp. 165-186

SANGREE J. B. and WIDMIER J. M. 1979: Interpretation of depositional facies from seismic data. Geophysics **44**, 2, pp. 131-160

SARG J. F. 1988: Carbonate sequence stratigraphy. *in*: An integrated approach, SEPM Special Publication **42**, pp. 155-180

SELLY R. C. 1985: Ancient sedimentary environments — Deltas. Chapman and Hall, Third Ed.

SHERIFF R. E. 1987: Interpretation of West Africa Line C. *in*: Atlas of Seismic Stratigraphy Volume 2. ed. Bally A. E., A. A. P. G. Studies in Geology 27.

TODD R. G. and MITCHUM Jnr. R. M. 1977: Seismic stratigraphy and global changes of sea level. Part 8: Identification of Upper Triassic, Jurassic and Lower sequences in Gulf of Mexico and offshore West Africa. A. A. P. G. Memoir 26, pp. 145-164

VAIL P. R. 1987: Seismic stratigraphy interpretation procedure. *in*: Atlas of Seismic Stratigraphy Volume 2. ed. Bally A. W., A. A. P. G. Studies in Geology 27.

VAIL P. R., MITCHUM Jnr. R. M. and THOMPSON S. 1977a: Seismic stratigraphy and global changes of sea level. Part 3: Relative changes of sea level from coastal onlap. A. A. P. G. Memoir **26**, pp. 63-82

VAIL P. R., MITCHUM Jnr. R. M. and THOMPSON S. 1977b: Seismic stratigraphy and global changes of sea level. A. A. P. G. Memoir **26**, pp. 83-98

VAIL P. R., POSAMENTIER H. W. and JERVEY M. T. 1988: Eustatic controls on clastic deposition in sea-level changes — an integrated approach. SEPM Special Publication Number 42.

VAIL P. R., TODD R. G. and SANGREE J. B. 1977: Seismic stratigraphy and global changes of sea level. Part 5: Chronostratigraphic significance of seismic reflections. A. A. P. G. Memoir 26, pp. 99-116

WARD R. F., KENDALL C. G. St. G. and HARRIS P. M. 1986: Upper Permian (Guadalupian) facies and their association with hydrocarbons - Permian Basin, West Texas and New Mexico. A. A. P. G. Bull. **70, 3**, pp. 239-262

WIEDMANN J., BUTT A. and EINSELE G. 1982: Cretaceous stratigraphy, environment and subsidence history at the Moroccan continental margin. *in:* Geology of the N. W. African Continental Margin, ed: Von Rad V., Hinz K., Sarnthein H. and Seibold E. pp. 366-395

WIEMER R. J. and DAVIS T. L. 1977: Stratigraphic and seismic evidence for late Cretaceous growth faulting, Denver Basin, Colorado. A. A. P. G. Memoir **26**, pp. 277-300

WINKER C. D. and EDWARDS M. B. 1983: Unstable progradational clastic shelf margins. SEPM Special Pub. **33**, pp. 139-157

WORSTER P. and STETS 1982: Sedimentation in the Atlas Gulf II: Mid-Cretaceous events. *in:* Geology of the N. W. African Continental Margin, ed. Von Rad V., Hinz K., Sarnthein H. and Seibold E. pp. 439-458

TENGERSZINT VÁLTOZÁSOK HATÁSA TÁROLÓK KIALAKULÁSÁRA PASSZÍV LEMEZPEREMEKEN

Tom I. KILÉNYI

Passzív lemezperemeken tárolók kialakulását elsősorban két tényező kombinációja határozza meg: a tengerszintváltozás és az üledék-utánpótlás. Három esetet hasonlítunk össze, ahol az alaphelyzet hasonló: a tenger felé progradáló vastag üledéksorozat, mégis a tárolók kifejlődése erősen eltérő. A fiatal harmadkori Nílus delta eróziónak volt kitéve a Földközi tenger messiniai kiszáradása alatt. Az ekkor, a delta fronton és ennek tenger felőli folytatásában kialakult meanderező folyócsatornákat kitöltő homokok fontos tárolók. A kameruni Douala-medencében két erős tengerszint-csökkenési időszak a felsőkrétában ill. az oligocénben turbiditek képződését idézte elő, és az azokkal kapcsolatos csatorna-kitöltések és törmelékkúpok képezik a tárolókat. A marokkói tengeri Tarfaya-medencében a Jurában relative állandó tengerszint mellett vastag üledékprizma alakult ki. A shelf külső szélén karbonát pad fejlődött ki, amely a szárazföldtől még távolabb leülepedett kréta üledékekben kialakult szénhidrogének csapdája lett.

ВЛИЯНИЕ КОЛЕБАНИЙ УРОВНЯ МОРЯ НА РАЗВИТИЕ РЕЗЕРВУАРОВ ВДОЛЬ ПАССИВНЫХ ОКРАИН

Т. И. Киленьи

В обстановке пассивных окраин развитие резервуаров контроллируется в основном сочетанием колебаний уровня моря и привноса осадков. Сопоставлены три случая, в которых общее положение сходно (имеется мощная, наступающая в сторону моря толща осадков), но резервуары тем не менее существенно отличны друг от друга.

В прибрежном бассейне Тарфайя (Марокко) сравнительно стабильный в юре уровень моря привел к возникновению наступающей призмы осадков. Вдоль внешнего края шельфа протягивается полоса карбонатов, образовавшая резервуар углеводородов, происходящих из меловых отложений, расположенных на большем удалении от береговой линии.

В бассейне Дуала (Камерун) в позднем мелу и олигоцене произошли два крупных спада уровня моря, которые привели к возвикновению турбидитов и сопряженных с ними выполнений каналов и конусов, являющихся резервуарами.Позднетретичная дельта Нила размывалась во время мессинского солевого кризиса, и система ветвящихся речных русел развивалась на фронте дельты и на ее морском продолжении. Пески, выполняющие эти каналы, ныне представляют собой важные резервуары.

GEOPHYSICAL TRANSACTIONS 1991
Vol. 37. No.1. pp. 91-107

DETAILED STUDIES OF SEA FLOOR SEISMICITY AND BENTHIC CURRENTS*

S. L. SOLOVIEV**

After grouping the instruments and basic methods of submarine earthquakes, an account is given of sea-floor seismological studies carried out and new instruments developed by the Laboratory of Seismology. It is stated, that observations by land-based stations do not record a significant number of submarine earthquakes. As some of the ocean bottom stations can, besides seismographs, be equipped with other sensors, such as current-and temperature meter, benthic currents and temperature in the boundary layer were also investigated and the results are presented here.

Keywords: seismicity, seismographs, sea floor, benthic currents

1. Introduction

Although 90% of all earthquakes occur under oceans or seas, most seismic stations are concentrated on land, which comprises less than 1/3 of the Earth's surface. As seismic stations are positioned relative to submarine seismic sources in a one-sided way and are often far apart, no detailed and reliable data on seismicity in underwater areas can be obtained. In the past research showed that observations by land-based stations may even give

* Work of the Laboratory of Seismology, Institute of Oceanology, the USSR Academy of Sciences, Moscow

** Laboratory of Seismology, Institute of Oceanology, Krasikova 23, 117218 Moscow, USSR

Manuscript received:14 August, 1991

an incomplete or distorted view of seismicity under seas and oceans. Up-to-date knowledge of submarine seismicity is essential for working out correct concepts of the contemporary evolution of the Earth, for a detailed seismic regionalization of construction sites for offshore oil and gas platforms, for revealing patterns of seismic process in tsunami source areas, and for other theoretical and practical problems.

Although the first attempts at recording earthquakes on sea and ocean bottom date back to the pre-war period, marine seismology and seismometry began to develop during the 1960s, with the Vela-Uniform and other projects aimed at improving the monitoring of underground nuclear tests.

There are three basic methods of recording submarine earthquakes: (1) by means of permanent seismographs linked to a shore station by submarine cable through which the seismograph receives electric power and the bottom-based instruments transmit seismic signals to the shore, (2) by means of temporary expedition-type ocean bottom stations, (3) by means of seismic radio buoys.

Cable-linked seismographs are very costly, and buoys are mainly of use in studying seismic shocks concentrated in space (swarms or aftershocks of strong earthquakes). Temporary expedition-type stations have been found most useful in supplying information about sea-floor seismicity.

The Laboratory of Seismology, established in late 1978, has been engaged in developing ocean bottom seismographs and applying them to studying seismicity under seas and oceans and processes in the near-bottom boundary layer of the hydrosphere.

2. Principal equipment

The Laboratory of Seismology has a large number of instruments designed for studying submarine seismicity. Arbitrarily, such instruments may be divided into anchored and pop-up types. Pop-up seismographs seem the most promising and are therefore attracting more attention.

The first system developed and tested in the Laboratory was the MADS-6 (1981). This composite pop-up station can carry various sensors which are required to be in close proximity to the ocean bottom. The station is placed on the ocean bottom and popped-up in an original manner. It can

move through the water layer very rapidly. Its geophones make soft contact with the ocean bottom and establish close contact with the ocean bottom sediments. If the station gets buried in mud or sucked into oozy deposits

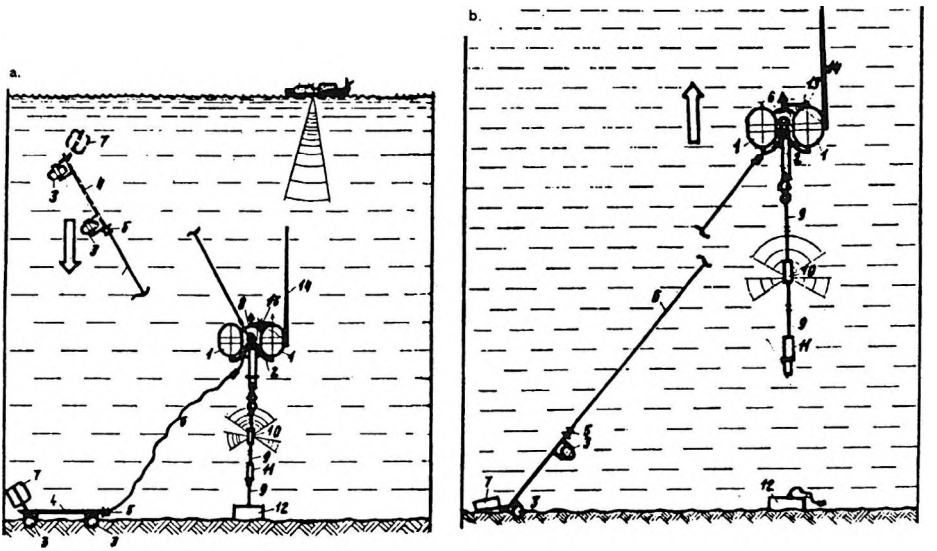

Fig. 1. Sketches showing the MADS-6 self-contained pop-up ocean bottom station (a) in touching the sea bottom (the dotted line showing the position of the cantilever frame with instrumental housings while the station is submerging freely) and (b) in the process of pop-upping:
1 — float module; 2 — supporting frame; 3 — instrument housing; 4 — cantilever boom; 5 — connecting wires drum; 6 — connecting wire; 7 — hydrofoil; 8 — rigging shackle; 9 — composite halyard; 10 — acoustic beacon; 11 — ballast release mechanism; 12 — ballast; 13 — radio beacon; 14 — radio beacon's antenna

1. ábra. A MADS-6 független, automatikusan felmerülő tengerfenéki szeizmográf vázlata (a) lehorgonyozva (a szaggatott vonalak a konzolkeret és a műszerház helyzetét mutatják szabad süllyedés közben) (b) felmerülés közben
1 — lebegő egység; 2 — tartókeret; 3 — műszerház; 4 — konzol; 5 — kábeldob; 6 — összekötő kábel; 7 — siklófelület; 8 — rögzítőgyűrű; 9 — kombinált felhúzókötél; 10 — akusztikus jeladó; 11 — ballasztkioldó szerkezet; 12 — ballaszt; 13 — rádiójeladó; 14 — rádiójeladó antennája

Рис. 1. Схема независимого, автоматически всплывающего придонного сейсмографа МАДС-6 (а) в заякоренном состоянии (штриховыми линиями показано положение консольной рамы и приборного отсека во время свободного погружения), (b) во время всплытия
1—свободноплавающй блок; 2—опорная рама; 3—приборный отсек; 4—консоль; 5—кабельная катушка; 6—соединяющий кабель; 7—плоскость соскальзывания; 8—зажимное кольцо; 9—комбинированный подъемный трос; 10—передатчик акустических сигналов; 11—устройство для сбрасывания балласта; 12—балласт; 13—передатчик радиосигналов; 14—антенна передатчика радиосигналов

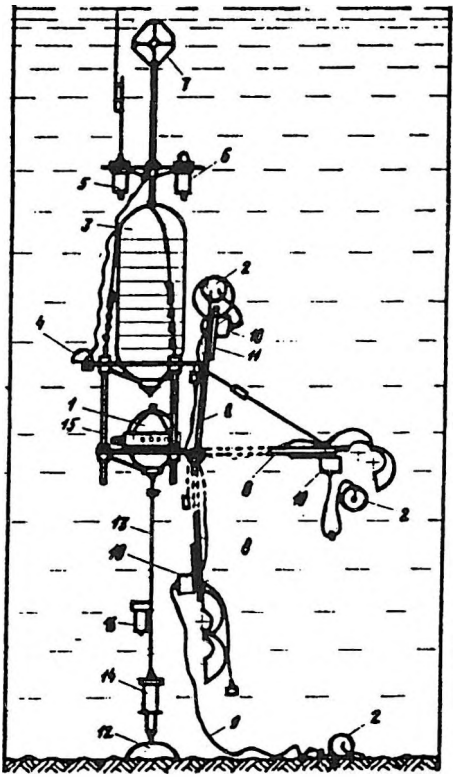

Fig. 2 A sketch showing the ADS-8 self-contained pop-up ocean bottom station
1 — container for tape recorder and time unit; 2 — container for seismic sensors; 3 — deepwater float; 4 — small float of strayline; 5 — radio beacon; 6 — light beacon; 7 — corner reflector; 8 — swing-out boom of seismic sensors package; 9 — cable connecting seismic sensors with recorder; 10 — accumulating cablereel; 11 — hydrofoil; 12 — ballast; 13 — composite halyard; 14 — ballast release mechanism; 15 — framework; 16 — acoustic beacon

2. ábra. Az ADS-8 független, automatikusan felmerülő tengerfenéki szeizmográf vázlata
1 — a mágnesszalagegység és az időjelgenerátor konténere; 2 — szeizmikus szenzorcsoport konténere; 3 — mélyvizi lebegőegység; 4 — hajóútmérő logzsinórra kötött jel lebegő egysége; 5 — rádiójeladó; 6 — fényjeladó; 7 — keretreflektor; 8 — szeizmikus szenzorcsoport kilengő konzola; 9 — a szeizmikus szenzorok és a mágnesszalagegység közti kábelcsatlakozás; 10 — kábeltekercselő dob; 11 — siklófelület; 12 — ballaszt; 13 — kombinált felhúzókötél; 14 — ballasztkioldó szerkezet; 15 — keret; 16 — akusztikus jeladó

Рис. 2. Схема независимого, автоматически всплывающего придонного сейсмографа АДС-8
1—контейнер узла с магнитной лентой и генератора сигнала времени; 2—контейнер группы сейсмических датчиков; 3—глубоководный свободноплавающй блок; 4—свободноплавающй блок, привязанный к тросу измерителя пройденного пути; 5—передатчик радиосигналов; 6—передатчик светосигналов; 7—угловой прожектор; 8—колеблющийся консоль группы сейсмических датчиков; 9—кабельное соединение между сейсмическими датчиками и узлом с магнитной лентой; 10—катушка намотки кабеля; 11—плоскость соскальзывания; 12—балласт; 13—комбинированный подъемный трос; 14—устройство для сбрасывания балласта; 15—опорная рама; 16—передатчик акустических сигналов

its geophones and recorders can easily be torn off the bottom (*Fig. 1*). The usable volume of the MADS-6 instrument housing is 100 dm^3.

The next developments were the ADS-8 (1983), ADS-M (1985), ADS-A (1989) and other pop-up devices. These stations use a burp-out package of seismic sensors to minimize noise from benthic currents (*Fig. 2*). The main instrument housing together with the recorder is attached to the float module and connected to the seismic-sensor package by an electric cable. This spatial layout ensures a higher signal-to-noise ratio during bottom measurements and better seismological information.

Besides seismographs, ADS-series stations equipped with current meters, salinity meters, temperature and pressure meters, sediment traps, etc. lend themselves readily to various measurements in the bottom boundary layer. They are suitable for various measurements and trials (e. g. corrosion tests) even when specimens and instruments are exposed in the bottom boundary layer at abyssal depths for a long time.

3. Sea-floor seismological experiments and their scientific results

The Laboratory of Seismology has been carrying out detailed studies of sea-floor seismicity, mainly with pop-up seismographs, since 1987. It has already accomplished the following experiments:

— in the southern Aegean Sea (Cretan Sea) in April 1987
— in the south-eastern Tyrrhenian Sea in May 1987
— in the central segment of the Hellenic arc south-east of Crete in July 1988
— in the central part of the Azores-Gibraltar fault in August 1988
— in the North-Aegean trough in October 1989
— in the central segment of the Hellenic arc south-east of Crete and in the Cretan Sea in October 1989
— in the Hellenic arc in the Ionian Sea, south-west of the Peloponnese peninsula in November 1989
— in the Gorringe Bank area (the eastern part of the Azores-Gibraltar fault) in December 1989

In addition, some lesser experiments have also yielded valuable results.

The Cretan Sea

In April 1987 five ocean bottom seismographs were placed some 25 km apart at depths of 1000–1800 m north-east of Crete. Working for a week, they recorded 420 local and distant quakes of magnitude M_L from -0.5 to 4 and identified hypocentres for 134 quakes. The Greek seismic stations located on the mainland and on islands recorded just 53 quakes and identified hypocentres for two of them for the same period.

One unexpected result was that 3/4 of the quakes recorded by the ocean bottom seismographs had originated in the Earth's crust and only 1/4 of them in the upper mantle, in the Benioff zone. According to observations made by land-based seismic stations for the previous 80 years and surveyed in the international seismological bulletins, the quakes registered in this region show the opposite relation for the depth of their foci: 1/4 in the crust and 3/4 in the mantle. It was the first time that high microseismicity of the crust had been detected behind the Hellenic arc: it turned out that it had been hard to do so by land based seismic stations.

As far as the peculiarities of the depth distribution of the seismic foci recorded by the ocean bottom seismographs are concerned, apart from the well-known aseismic asthenospheric layer at a depth of 80 to 100 km, another similar layer was traced down immediately beneath the crust.

Studying the attenuation of amplitude of the seismic waves with distance on the ocean bottom, seismograph records showed that the Q-factor of the lithosphere of the Cretan Sea was fairly low (Q_S = 200–300).

The south-eastern part of the Tyrrhenian Sea

In May 1987, five bottom seismographs were installed at depths of 1000–2800 m in the lower part of the submarine slope of the Appenninean peninsula off the coast of Calabria. They were at work for ten days. At the same time, nine temporary digital seismographs were installed on land by Italian seismologists and, along with the permanent stations run by various organizations, these formed a network of 24 land-based observation sites in Calabria. The bottom seismographs recorded about 200 tremors, mostly feeble and with a shallow foci. Judging from the form of the records, the tremors must have been caused by the movements of magma beneath the

sea-mounts which may be thought of as not fully extinguished volcanoes. For instance, a cluster of earthquakes was recorded beneath the Alcione and Diamante Mts. Moreover, the bottom seismographs recorded a score of quakes of tectonic origin. Half of these were found to have originated on the Appenninean peninsula and the other half beneath the bottom of the Tyrrhenian Sea. The land-based stations recorded only 60% of the first group and 22% of the second. Of the quakes recorded by the ocean bottom seismographs in the Tyrrhenian Sea, a little more than 3/4 arose in the crust and less than 1/4 in the mantle, in the seismofocal layer, i. e. the pattern was exactly the same as in the results of the preceding experiment in that the level of microseismicity in the crust behind the Calabrian arc was fairly high (contrary to what had been thought earlier) and land-based stations had been unable to determine this.

The May 24 a tectonic earthquake occurred in the mantle, in the Benioff zone, right beneath the network of bottom seismographs, a fact which allowed the depth of its focus to be ascertained with a high degree of accuracy. The depth was found to be 100 km less than the value determined from observations of land-based stations and reported in the International Seismological Bulletins (216 and 312 km respectively).

For the first time ever, we succeeded in detecting the hypocentres of some very feeble tremors (M_L ~ 0.5-1.5) in the mantle between the crust and the Benioff zone. These hypocentres were found to form a kind of vertical string linking the roots of the Alcione volcano and the assumed asthenospheric layer at a depth of some 100 km.

The Hellenic arc south-east of Crete

In July 1988, five ocean bottom seismographs were installed some 20-40 km apart at depths of 1700-4000 m south-east of Crete, in the Kassos strait and on the slopes of the Pliny trough. They were at work for a week. They recorded nearly a thousand tremors and 150 hypocentres were identified. The concentration of epicentres along the eastern border of the block of Crete, which had been detected in the 1987 experiment, was confirmed — an indication that a violent earthquake anticipated by Greek seismologists in the eastern half of Crete seems likely to be already on the way.

More important, as a result of the more accurate determination of earthquake hypocentres in the Benioff zone by using ocean bottom seismographs, it was ascertained that this zone, just like the deepwater trough bordering the convex side of the Hellenic arc, has en echelon structure. The study area covered the eastern end of the Pliny trough and the beginning of the Strabo trough 50 km to the south (which extended east beyond the area). It was found that each of these two fragments of the Hellenic deepwater trough is accompanied by a thin parallel seismofocal layer beneath the island arc dipping at an inclination of about 60°. These layers were traced to a depth ranging from 0 to 120 km beneath the Pliny trough and from just 30 to 70 km beneath the Strabo trough. Now, the literature claims that the seismofocal layer beneath the Hellenic arc has a 'loose' form in its upper part, dipping below the island arc at a relatively small angle (45°).

The preliminary results of the 1989 experiment around Crete have confirmed the conclusion that the seismofocal layer in the Hellenic arc has en echelon structure.

The Azores-Gibraltar fault

In August 1988, five ocean bottom seismographs were placed at depths from 3400 to 5100 m in the central part of the Azores-Gibraltar fault and were in operation for 13 days. This Atlantic study area was chosen between the foci of the 1941 and 1975 violent tsunamigenic earthquakes of magnitude 8.2 and 8.0 respectively, and it was expected that a large number of microshocks would be recorded. However, the network of ocean bottom seismographs deployed 50 km apart spotted fewer than a hundred tremors, all of which originated beyond the bounds of the study area. The recurrence of weal quakes recorded by OBS's for the range $m_b \leq 3.5$ follows exactly the same line $\lg N = f(mv)$ as the recurrences of more violent ($m_b \geq 4$) quakes in the fault determined from many years of observation by stations set up on the Iberian peninsula and on the Azores with a low b value (0.7). This result is likely to be due to the lithosphere in the Azores-Gibraltar belt being less fragmented than in regions of island arcs. The lithosphere here appears to consist of relatively large and firm blocks. This may be one of the reasons why violent earthquakes are relatively rare.

The 1989 ocean bottom experiment on Gorrindge Bank (in the eastern part of the fault, which many researchers identify with the focal area of the disastrous Lisbon earthquake and tsunami in 1755) has yielded qualitatively the same results as the 1988 experiment.

The North-Aegean Trough

In October 1989, seven ocean bottom seismographs were deployed at depths of 300-1200 m along the North-Aegean trough. During 5 days of operation they recorded 180 quakes and identified 31 hypocentres, with 2/3 of the tremors in the crust and 1/3 in the mantle, at depths to 150 km. The seismic foci have outlined a seismofocal layer, dipping steeply (60°) north-west. This new result is important for a tectonic interpretation of the evolution of the trough and the Aegean Sea as a whole.

Studying the seismicity of Lake Baikal and the first experience in recording ocean bottom seismic oscillations in the low-frequency band

The remaining 1989 observations have not yet been processed and their results are not presented here. Among the other work carried out by the Laboratory mention may be made first of the observations at Lake Baikal in the early 1980s which have shown that short-period (10 Hz) *P*- and *S*-waves in the Baikal zone spread far and that microseismicity in the transverse faults of the lake bottom is higher than in the longitudinal ones, which is contrary to the earlier generally accepted view.

Secondly, the first measurements of ocean bottom seismic oscillations in the low-frequency range are not trivial: no such measurements had been made before in the USSR and very few elsewhere because of the lack of suitable equipment. The Laboratory of Seismology, in conjunction with other agencies, has developed a prototype of an analog-digital seismic station with a passband of 0.01-10 Hz. This station, along with a deepwater hydrophone, was used for observations totalling 18 h each in the Atlantic; at a depth of 1350 m around the Canary upwelling and at a depth of 960 m over the Reykjanes Ridge south of Iceland; and for some longer observations in the North-Aegean trough in the Mediterranean.

Spectra of ocean bottom seismic noise have been plotted and these have been found to be very similar in different study areas. In addition to the well known noise minimum in the 10 Hz region, a minimum in the 0.05–0.1 Hz range has been detected — a discovery which is very promising with regard to the ocean bottom recording of surface waves from strong quakes and the application of their dispersion to studying the depth structure of the ocean lithosphere.

4. Current and temperature measurements in the bottom boundary layer

The pop-up stations described in chapter 2. have a high positive buoyance and, therefore, in addition to the seismograph, their deepwater part can carry some other sensors.

The 'Potok' self-contained digital current-and-temperature meter, now mass-produced by the Oceanological Design Department of the USSR Academy of Sciences, was the first such meter to be used. For the Laboratory, the studying of water currents in the bottom boundary layer is important for two reasons: (1) we wish to know the mechanism by which such currents produce noise in a seismograph, (2) we wish to try to record tsunamis in deep water. But apart from marine seismology, the dynamics of the benthic layer is now a major challenge to oceanographers in general.

'Potok' meters were first put to work in the spring of 1986, but it was not until after the spring of 1988, when the time intervals for averaging current and temperature values had been reduced to 225 s (sometimes even to 112 and 28 s) and the exposure of the sea-bottom instruments extended to 40 days, that valuable scientific results began coming in.

Benthic currents over fields of iron-manganese nodules in the north-eastern Pacific

Two stations were placed over the Clarion and Clipperton Fracture Zones and in the Guatemalan basin in February–March 1988. They were equipped with sediment traps and instruments for measuring (1) two horizontal components of current speed and the water temperature ('Po-

tok'); and (2) salinity, temperature and pressure (STP) and the content of oxygen (O_2) dissolved in water. The stations were at 5000 m and 3600 m, respectively. The study areas are known to abound in iron-manganess nodules (IMN) related to the gently sloping sides of the abyssal hills.

Measurements showed variation both in STP values and O_2 content and in the benthic dynamic characteristics. A benthic storm lasting longer than 48 hours, with the benthic current speed, averaged over intervals of 0.5 h, reaching 13.5 cm/s, was recorded within a 36-day spell. The storm was found to be related to a deep-penetrating synoptic whirl, and the facies conditions of IMN formation were found to be associated with benthic dynamics. The Mn was found to be coming to the Guatemalan basin from the Galapagos rift and not from the central part of the Pacific, as had previously been supposed.

'Warm' benthic storms off Crete

During the July 1988 sea-bottom seismological experiment off Crete, three stations were fitted with 'Potok' meters placed 2.5 m above the sea-bottom. The stations were dropped at a depth of 1780 m on the south-eastern slope of Crete (A), at a depth of 1530 m in the Kassos strait (B) and at a depth of 1745 on the Rodos submarine ridge edged by the Pliny trench on the north (C). Station B recorded 10 benthic storms, whose duration took 15% of the recorded time, within a week. The current speeds during the storms rose sharply from the meter's sensitivity threshold (1 cm/s) to 4.4-8.5 cm/s. During one of the storms, unlike any of the others, the water temperature was found to rise stepwise by 0.4°. Station A recorded a similar storm but at a different time. Station C did not register any thermodynamic processes on the sea-bottom.

Petrological analysis of the suspended sediments from the trap at Station A, among other considerations, has led us to claim that the sea-bottom stations recorded some turbidity currents generated above them, in the upper parts of the submarine slopes. This means that an essentially new mechanism for vertical water motion in the World Ocean and oxygen transfer to sea depths seems to have been discovered. The 'cold' storms recorded by Station B appear to be relics of some complex system of counter-currents in the Kassos strait.

Semi-diurnal migrations of the Canary and Mauretanian currents

A station fitted with a 'Potok' meter was placed in July–August 1988 on the submarine slope of the African continent, 85 km west of Cap Blanc, in the Atlantic. It worked for a week. It happened to lie on the borderline between the warm Mauretanian current flowing along the coast from south to north and the cold Canary current flowing somewhat west of it from north to south. The benthic currents, sometimes as fast as 26 cm/s, were found to change direction steadily twice during 24 hours (with a period of 11–13 hours) from north-north-east to south-west, with a ± 0.2° temperature change invariably accompanying it. This indicates that the two currents are involved in the tidal movement of the ocean and that the borderline between them now advances towards the African coast, now recedes from it. This movement of the borderline, as the sea-bottom station records show, is not a smooth-flowing process but is the result of the penetration of the cold masses of the Canary current into the warm waters of the Mauretanian current (which contributes to the well-known phenomenon of the Canary upwelling).

Change of current speed with depth in the bottom boundary layer

In September 1988, two stations were dropped on the submarine Reykjanes ridge, south of Iceland. They were 100–200 m apart, one — as usual — with a 'Potok' meter, 2.5 m from the sea-bottom, the other with a string of 'Potok' meters deployed 5, 10, 15 and 25 m above sea bottom. The stations were at work for four days. According to their records, the bottom boundary layer was in a very unstable state because at different horizones the times when currents become stronger and weaker did not coincide. But, at the same time, at all horizons a few benthic storms were found to occur synchronously. The speed of water motion grew higher, not as one would expect away from the bottom, but approaching the bottom.

Benthic currents in the Mediterranean deep-water basins

Self-floating sea-bottom stations with 1 to 5 'Potok' meters were placed at 11 sites within the system of the Hellenic trenches and the Crete basin in October–November 1989. A steady mass transfer, with the benthic current up to 8 cm/s, was recorded (up to a depth of 5110 m in the Ionian trench). The water temperature in the bottom boundary layer in the Ionian Sea was found to have increased abnormally. A steady anticyclonic circulation, with the speed of the stream on the periphery of the whirl up to 16 cm/s, was recorded in the Crete basin (at depths of 2000–2200 m).

5. Some considerations regarding further ocean bottom seismological observations and investigations of the bottom boundary layer

The experience accumulated by the Laboratory, particularly the discovery that land-based stations are not sensitive enough to get detailed and reliable information on sea-floor seismicity, has led us to believe that long-term observations using ocean bottom seismographs should be carried out before proceeding to the realization of any costly engineering project connected with seismically active sea-floor regions. This especially applies to projects of bridges or tunnels across the Gibraltar and Messina straits.

It also applies to offshore marine oil and gas platforms which are erected in seismically hazardous sea-floor areas, in particular in the south shelf of Alaska, on the north-eastern shelf of Sakhalin Island, and on some areas of shelf in south-east Asia, the North Sea and elsewhere.

Observations based on ocean bottom seismographs are also useful in epicentral areas where violent earthquakes and tsunamis are most likely.

As far as investigations of currents and temperature in the boundary layer are concerned, they are useful throughout the world's oceans, notably in areas of powerful geostrophic currents such as the Gulf stream and the Kuroshio and in all straits.

BIBLIOGRAPHY

DEMIDOVA T. A., KONTAR E. A. 1989: On benthic current in an area of development of iron-manganese nodules (in Russian). Doklady Akademii Nauk SSSR **308**, 2, pp. 468-472

DOZOROV T. A., SOLOVIEV S. L. 1990: On the registration of ocean bottom seismic noises in the range 0.01-10 Hz (in Russian). Fizika Zemli **8**, pp. 10-20

EL'NIKOV I. N., SOLOVIEV S. L. 1989: New data on the structure of sedimentary cover in the Cretan basin (in Russian). Doklady Akademii Nauk SSSR **309**, 3, pp. 670-675

FERRI M., GUERRA I., KOVACHEV S. A., KUZIN I. P., LUONGO G., SOLOVIEV S. L. 1987: Observazioni seismografiche nel Tirreno meridionale mediante OBS e stazioni temporance a terra. Atti del 6 ° convegno annuale del gruppo nazionale di geofisica della terra solida. Roma, 14-15 Decembre 1987, pp. 235-246

KONTAR E. A. 1990: Measurement of near-bottom currents on the boundary between Canary and Mauritanian currents. Annales Geophysicae, Special Issue (EGS XV General Assembly, Copenhagen, 23-27 April 1990, p. 226

KONTAR E. A., LEVCHENKO D. G., SOLOVIEV S. L. 1990: On bottom boundary currents in the seismically active Azores-Gibraltar region of the Atlantic (in Russian). Doklady Akademii Nauk SSSR **310**, 5, pp. 1231-1235

KONTAR E. A., SOLOVIEV S. L. 1989: Observation of possible small turbidity currents in bottom boundary layer SE of Crete Island. Annales Geophysicae, Special issue (EGS XIV General Assembly, Barcelona, 13-17 March 1989, p. 24

KONTAR E. A., SOLOVIEV S. L. 1989: On near-bottom storms in the Mediterranean (in Russian). Doklady Akademii Nauk SSSR **309**, 5, pp. 1215-1218

KONTAR E. A., SOLOVIEV S. L. 1990: Experimental data on dynamics of bottom boundary layer to the south of Iceland. Annales Geophysicae, Special issue (EGS XV General Assembly, Copenhagen, 23-27 April 1990) p. 226

KONTAR E. A., SOLOVIEV S. L. 1990: Experimental investigation of bottom boundary layer dynamics in the area of the Reykjanes ridge (in Russian). Doklady Akademii Nauk SSSR **312**, 3, pp. 726-730

KONTAR E. A., SOLOVIEV S. L., DEMIDOVA T. A. 1990: Investigation of the bottom boundary layer dynamics with the help of pop-up self-contained stations. Proceedings of the Fourth Pacific Congress on Marine Science and Technology (PACON 90), Tokyo, Japan, July 16-20, 1990, 1, pp. 53-56

KONTAR E. A., SOLOVIEV S. L., GROSUL A. B., SAVOSTIN Y. M. 1989: Measurement of currents in the botom boundary layer in the Mediterranean (in Russian). Okeanologiya XXIX, 6, pp. 928-933

KOVACHEV S. A., KUZIN I. P., SOLOVIEV S. L. 1989: Space distribution of microseismicity in the frontal part of the Hellenic arc according to OBS observation. The 25th General Assembly of International Association of Seismology and Physics of the Earth Interior (IASPEI). Abtracts, August 21-September 1, 1989, Istambul, Turkey, p. 25

KOVACHEV S. A., KUZIN I. P., SOLOVIEV S. L. 1990: Experience of bottom seismological observations in the central part of the Azores-Gibraltar belt (in Russian). Fizika Zemli **7**, pp. 28-37

KOVACHEV S. A., KUZIN I. P., SOLOVIEV S. L., CRUZ J., MOREIRA V. S., NUNES J. C., SENAS M. L. 1989: Microseismicity in the central part of the Azores-Gibraltar fault according to OBS observations. The 25th General Assembly of International Association of Seismology and Physics of the Earth Interior (IASPEI). Abstracts, August 21-September 1, 1989, Istambul, Turkey, p. 386

KOVACHEV S. A., SHODA O. Y., SOLOVIEV S. L. 1990: Microseismicity of North Aegean trough according to OBS observations. XXII General Assembly, European Seismological Commission, Barcelona, 17-20 September, 1990, Program and Abstracts p. 100

KOVACHEV S. A., SOLOVIEV S. L., TIMOSHUK E. P. 1990: Influence of hydrometeorological conditions on sea bottom microseisms in the range 0.1-0.25 Hz. XXII. General Assembly, European Seismological Commission, Barcelona, 17-22 September 1990, Program and Abstracts p. 99

KUZIN I. P., KOVACHEV S. A., SOLOVIEV S. L. 1989: Attenuation of *S*- and *P*-waves on the bottom of the Cretan Sea observed by array of OBS. The 25th General Assembly of International Association of Seismology and Physics of the Earth Interior (IASPEI), August 21 — September 1, 1989, Istambul, Turkey. Abstracts p. 524

KRIVOSHEYA V. G., SOLOVIEV S. L. 1989: 45th cruise of RV 'Dmitrij Mendeleev' (October 4 — December 20, 1989) (in Russian). Okeanologiya **30**, 3, pp. 525-527

SOLOVIEV S. L. 1985: History and perspectives of development of marine seismology (in Russian). Nauka, Moscow 1985, 152 p.

SOLOVIEV S. L. 1986: Seismological bottom observations in the USSR and abroad (in Russian). Nauka, Moscow 1986, 118 p.

SOLOVIEV S. L. 1990: Restless life of the sea floor (in Russian). Priroda 4, pp. 27-31

SOLOVIEV S. L., BUKINA K. I., KOVACHEV S. A., VILLEMSON L. K. 1987: Long-range propagation of short-period transversal and longitudinal seismic waves in the Baikal zone. Geophys. J. R. Astr. Soc. **88**, 1, pp. 125-136

SOLOVIEV S. L., DOZOROV T. A., FEDORIN V. A. 1988: Some results of tests of molecular-electronic sensors incorporated in bottom stations (in Russian). Seism. pribori, 20, Nauka, Moscow pp. 47-52

SOLOVIEV S. L., FERRI M., KUZIN I. P. KOVACHEV S. A. 1989: Seismicity of the Earth's crust in the south-eastern part of the Tyrrhenian Sea (from results of joint bottom and land seismological observations) (in Russian). Doklady Akademii Nauk SSSR, **305**, pp. 1339-1343

SOLOVIEV S. L., KONTAR E. A. 1988: Use of pop-up deep-water carriers for bottom geophysical observations (extended abstract). Proceedings, Pacific Congress on Marine Science and Technology PACON-90. Honolulu, Hawaii, May 16-20, 1988, p. OST1/29-OST1/30

SOLOVIEV S. L., KONTAR E. A., BROVKO V. P. 1983: On the development of deepwater pop-up carriers of seismological equipment (in Russian). Vulkanologia i seismologiya **4**, pp. 100-105

SOLOVIEV S. L., KONTAR E. A., DOZOROV T. A., KOVACHEV S. A. 1988: Deepwater bottom pop-up seismological station ADS-8 (in Russian). Fizika Zemli **9**, pp. 75 - 85

SOLOVIEV S. L., KOROVIN Y. M., KONTAR E. A., LEDENEV A. M., SHCHERBAK N. V. 1988: Integrated corrosion-biological invesatigations based on self-contained bottom stations (in Russian). Okeanologiya **28**, 3, p. 511

SOLOVIEV S. L., KOVACHEV S. A., KUZIN I. P., TASSOS S. 1989: Seismicity of the Earth's crust in the southern part of the Aegean Sea (from the results of bottom seismological observations) (in Russian). Doklady Akademii Nauk SSSR **305**, 5, pp. 1085-1089

SOLOVIEV S. L., KOVACHEV S. A., MISHARINA L. A., UFIMTSEV G. F. 1989: Seismic activity in transverse faults in the Olkhon-Svyatonoskaya zone of Lake Baikal (in Russian). Doklady Akademii Nauk SSSR **309**, 1, pp. 61-64

SOLOVIEV S. L., KUZIN I. P., KOVACHEV C. A., FERRI M., GUERRA I., LUONGO G. 1990: Microearthquakes in the Tyrrhenian Sea as revealed by joint land and sea-bottom seismographs. Marine Geology **94**, 1-2, pp. 131-146

ZHDANOV M. A., LEVCHENKO D. G., SOLOVIEV S. L. 1990: Sea-floor seismic noise in the range 0.01-10 sec in the north of Aegean Sea. XXII General Assembly, European Seismological Commission, Barcelona, 17-22 September 1990, Programme and Abstracts p. 99

A TENGERFENÉK-SZEIZMICITÁS ÉS A MÉLYTENGERI ÁRAMLATOK RÉSZLETES VIZSGÁLTA

S. L. SOLOVIEV

A tenger alatti földrengések méréséhez szükséges műszerek és alapvető módszerek csoportosítása után a dolgozat sorra veszi a Szeizmológiai Laboratórium által végrehajtott tengerfenéki szeizmológiai méréseket és a Laboratórium saját fejlesztésű műszereit. Megállapítja, hogy a szárazföldi mérések nem regisztrálják a tengerfenék rengéseinek jelentős hányadát. Mivel a tenger alatti mérőállomások egy csoportja a szeizmográfokon kívül más szenzorokkal, többek között áramlás- és hőmérsékletmérővel is felszerelhető, a Laboratórium tanulmányozta a tengeri áramlatokat és a határréteg hőmérsékletét is, és a kutatások eredményeit a jelen dolgozatban ismertetik a szerzők.

ДЕТАЛЬНЫЕ ИССЛЕДОВАНИЯ СЕЙСМИЧНОСТИ МОРСКОГО ДНА И ГЛУБОКОВОДНЫХ ТЕЧЕНИЙ

С. Л. СОЛОВЬЕВ

После классификации приборов и основных методов регистрации морских землетрясений ва работе рассматриваются измерения сейсмичности морского дна, выполненные Лабораторией Сейсмологии, а также разработанная в Лаборатории аппаратура. Делается вывод о том, что значительная доля морских землетрясений не фиксируется на суше. Поскольку некоторые из подводных сейсмических станций могут быть оборудованы не только сейсмографами, но также и другими датчиками, в том числе и приборами по измерению подводных течений и температур, Лабораторией изучены также и морские течения и температуры пограничного слоя, причем результаты исследований излагаются в настоящей работе.

ERRATUM

The acknowledgment that the authors should have included at the end of their paper

'PRE-TERTIARY BASEMENT CONTOUR MAP OF THE CARPATHIAN BASIN BENEATH AUSTRIA, CZECHOSLOVASKIA AND HUNGARY'

published in Geophysical Transactions Vol. **36**. Nos. 1-2 was omitted, the editor has therefore been asked to publish the following:

Acknowledgment

During their work the compilers of the map utilized all geological-geophysical data available. Thus the map could not have been realized without the efforts of all institutions and scientists who took part in the field work, data processing and interpretation as well as in the construction of local basement contour maps during the last decades. It would be impossible to mention them all by name especially since the area concerned belongs to three different countries. Therefore the authors acknowledge their collective merit and wish to emphasize that the whole community of geologists and geophysicists of Austria, Czechoslovakia and Hungary deserves credit for the creation of the map.

The proven technology to help you reduce risk and increase your success rate – worldwide.

HGS

Halliburton Geophysical Services

6909 Southwest Freeway Houston, TX 77074 Ph: (713) 774-7561 FAX: (713) 778-3487/Telex: 76-2781

A Halliburton Company

DON'T BUY EQUIPMENT OR SERVICES UNTIL YOU KNOW THE FACTS

ELGI's Well Logging Divison has put its 25 years of experience to work again in the new line of well logging technology in

water,

coal,

mineral,

geotechnical

prospecting

HERE'S WHAT WE OFFER

- Complete series of surface instruments from portable models to the PC controlled data logger
- Sondes for all methods: electrical, nuclear, acoustic, magnetic, mechanical, etc.
- Depth capacity down to 5000 m
- On-site or office computer evaluation
- International Metrological Base for calibration to true petrophysical parameters
- Training and in-house courses
- Design laboratory for custom-tailored assemblies

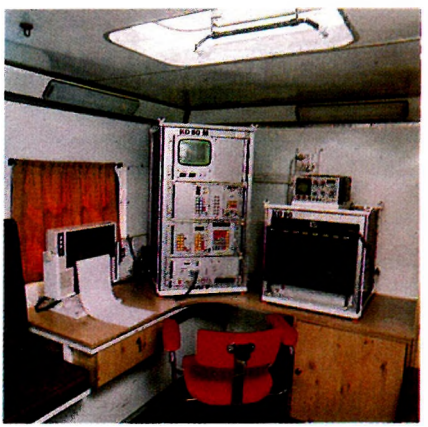

Just think of us as the scientific source of borehole geophysics you may never have heard of

SALES ✣ ✣ ✣ ✣ RENTALS ✣ ✣ ✣ ✣ SERVICES

Well Logging Division of ELGI
POB 35, Budapest, H-1440 Hungary
Phone: (361) 252-4999, Telex: 22-6194,
Fax: (361) 183-7316

INVITATION

The Association of Hungarian Geophysicists decided at its annual meeting to establish the "Foundation for Hungarian Geophysicists" and elected its first Advisory Board for 3 years. The foundation has been started with a moderate initial capital of 300 000 HUF, which has by now increased to more than 3 million and it is open for everybody.

The aim of the foundation is to help Hungarian geophysicists. There are two main target groups whose application for grants will be accepted with preference: young geophysicists needing assistance (travels, participation at conferences, publications,post-graduate education etc.) at the beginning of their professional life as well as retired and unemployed colleagues whose economic and social position became especially unfavourable.

The nine members of the Advisory Board invite everybody to join this foundation; donations should be communicated with the Board. Organisations and persons donating sums exceeding the initial capital will have the opportunity to delegate representatives into the Board. Detailed information is available at the following address:

Advisory Board of the
"Foundation for Hungarian Geophysicists"
H–1371 Budapest, P.O.B. 431
Budapest, I., Fő u. 68.
Telephone 201-2011/590
Telex 22-4343
Telefax 156-1215